



The Journal of Gemmology

Volume 36 / No. 5 / 2019



Inclusions in Burmese Spinel

Peridot from China and N. Korea

Gem Faceting in Sri Lanka

Connemara Marble

Examination of 'Coconut Pearls'

SSEF

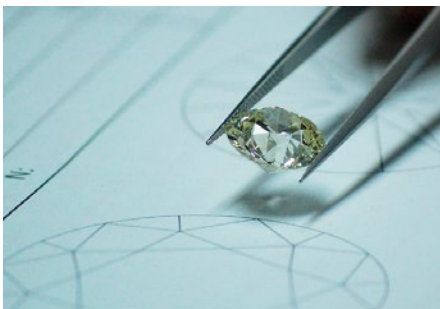
SCHWEIZERISCHES GEMMOLOGISCHES INSTITUT
SWISS GEMMOLOGICAL INSTITUTE
INSTITUT SUISSE DE GEMMOLOGIE



ORIGIN DETERMINATION · TREATMENT DETECTION

DIAMOND GRADING · PEARL TESTING

EDUCATION · RESEARCH



THE SCIENCE OF GEMSTONE TESTING™



COLUMNS

What's New

393

GemPen | J-Certain Synthetic Diamond Detector | Sherlock Holmes 2.0 Synthetic Diamond Detector | ABN-AMRO Diamond Reports | AGTA GemFair Tucson Seminars | Gem Abstracts from the 16th Swiss Geoscience Meeting | Gem Abstracts from the 2018 GSA Annual Meeting | Gem Identification Pamphlet and Poster | GIT Reports on Colour-Change Grossular and Musgravite | Global Diamond Industry 2018 | Gold Demand Trends 2018 | Jewelry Development Impact Index Studies | *The Journal's* Cumulative Index Updated, Plus Subject Bibliographies | LMHC Information Sheet Updates | MVI Marketing Research on Millennials and Synthetic Diamonds | Assume Program for Testing Diamond Verification Instruments | Raman Spectroscopy of Jade and Its Imitations | Responsible Sourcing CIBJO Blue Book | Santa Fe Symposium Proceedings | Sapphires Heated with Pressure | Small-Scale Mining in Kenya | SSEF Facette | Synthetic Periclase Identified by GRS | ColorCodex Update | GemePrice Update | Museum of Whitby Jet Opens

Gem Notes

402

'Black Anorthoclase' from Antarctica | Blödite | Purple Fluorite in Opal from Utah, USA | Garnets from Eastern Democratic Republic of the Congo | Obsidian from Slovakia | Spessartine Crystals from Nigeria | A Faceted Sulphur | Chidliak Diamond Mine in Canada | Synthetic Periclase | Myanma Gems Enterprise 2018 Rough Stone Sale and Opening of Mandalay Yatanar Mall | Educational Aspects of Myanmar Gem Fairs

Cover photo: Burmese spinel is available as attractive crystals and colourful gemstones, and a detailed study of the inclusions in this material appears on pp. 418–435 of this issue. The Burmese spinels shown here include the 6.30 ct centre stone in a gold and carbon-fiber ring that was designed and manufactured by Marc Höllmüller for Carley Jewels (Chattanooga, Tennessee, USA), as well as three larger and nine smaller crystals (courtesy of Federico Barlocher, Como, Italy, and Kathryn Bonanno, New York, New York, USA, respectively) and numerous cut gemstones that weigh up to 10.48 ct (courtesy of RareSource, Chattanooga Tennessee, USA). Photo by Jeff Scovil.

ARTICLES

- Spinel from Mogok, Myanmar—A Detailed Inclusion Study by Raman Microspectroscopy and Scanning Electron Microscopy** 418
By Myint Myat Phyo, Eva Bieler, Leander Franz, Walter Balmer and Michael S. Krzemnicki
- Characterisation of Peridot from China's Jilin Province and from North Korea** 436
By Zhiqing Zhang, Min Ye and Andy H. Shen
- The Modern History of Gemstone Faceting in Sri Lanka** 448
By Justin K Prim
- Mineral Liberation Analysis and Scanning Electron Microscopy of Connemara Marble: New Mineral Distribution Maps of an Iconic Irish Gem Material** 456
By Martin Feely, Derek H. Wilton, Alessandra Costanzo, Albert D. Kollar, Dylan J. Goudie and Ambrose Joyce



GEMMOLOGICAL BRIEF

468

- A Brief Study of Three Reported 'Coconut Pearls' from Southeast Asia**
By Henry A. Hänni and Chiara Parenzan

Conferences

472

AGA Tucson Conference | 21st FEEG Symposium and CIBJO Seminar on Responsible Sourcing

Gem-A Notices

475

New Media

481

Learning Opportunities

478

Literature of Interest

486

The Journal is published by Gem-A in collaboration with SSEF and with the support of AGL.



The Journal of Gemmology

EDITOR-IN-CHIEF

Brendan M. Laurs
brendan.laurs@gem-a.com

EXECUTIVE EDITOR

Alan D. Hart

EDITORIAL ASSISTANT

Carol M. Stockton

EDITOR EMERITUS

Roger R. Harding

ASSOCIATE EDITORS

Ahmadjan Abduriyim, *Tokyo, Japan*; Raquel Alonso-Perez, *Harvard University, Cambridge, Massachusetts, USA*; Edward Boehm, *RareSource, Chattanooga, Tennessee, USA*; Maggie Campbell Pedersen, *Organic Gems, London*; Alan T. Collins, *King's College London*; John L. Emmett, *Crystal Chemistry, Brush Prairie, Washington, USA*; Emmanuel Fritsch, *University of Nantes, France*; Rui Galopin de Carvalho, *PortugalGemas Academy, Lisbon, Portugal*; Lee A. Groat, *University of British Columbia, Vancouver, Canada*; Thomas Hainschwang, *GGTL Laboratories, Balzers, Liechtenstein*; Henry A. Hänni, *GemExpert, Basel, Switzerland*; Jeff W. Harris, *University of Glasgow*; Alan D. Hart, *Gem-A, London*; Ulrich Henn, *German Gemmological Association, Idar-Oberstein*; Jaroslav Hyršl, *Prague, Czech Republic*; Brian Jackson, *National Museums Scotland, Edinburgh*; Mary L. Johnson, *Mary Johnson Consulting, San Diego, California, USA*; Stefanos Karampelas, *Bahrain Institute for Pearls & Gemstones (DANAT), Manama*; Lore Kiefert, *Gübelin Gem Lab Ltd, Lucerne, Switzerland*; Hiroshi Kitawaki, *Central Gem Laboratory, Tokyo, Japan*; Michael S. Krzemnicki, *Swiss Gemmological Institute SSEF, Basel*; Shane F. McClure, *Gemmological Institute of America, Carlsbad, California*; Jack M. Ogden, *Striptwist Ltd, London*; Federico Pezzotta, *Natural History Museum of Milan, Italy*; Jeffrey E. Post, *Smithsonian Institution, Washington DC, USA*; Andrew H. Rankin, *Kingston University, Surrey*; Benjamin Rondeau, *University of Nantes, France*; George R. Rossman, *California Institute of Technology, Pasadena, USA*; Karl Schmetzer, *Petershausen, Germany*; Dietmar Schwarz, *Federated International GemLab, Bangkok, Thailand*; Menahem Sevdemish, *Gemewizard Ltd, Ramat Gan, Israel*; Andy H. Shen, *China University of Geosciences, Wuhan*; Guanghai Shi, *China University of Geosciences, Beijing*; James E. Shigley, *Gemmological Institute of America, Carlsbad, California*; Christopher P. Smith, *American Gemmological Laboratories Inc., New York, New York*; Evelyne Stern, *London*; Elisabeth Strack, *Gemmologisches Institut Hamburg, Germany*; Tay Thy Sun, *Far East Gemological Laboratory, Singapore*; Pornsawat Wathanakul, *Kasetsart University, Bangkok*; Chris M. Welbourn, *Reading, Berkshire*; Bert Willems, *Leica Microsystems, Wetzlar, Germany*; Bear Williams, *Stone Group Laboratories LLC, Jefferson City, Missouri, USA*; J. C. (Hanco) Zwaan, *National Museum of Natural History 'Naturalis', Leiden, The Netherlands*.

CONTENT SUBMISSION

The Editor-in-Chief is glad to consider original articles, news items, conference/excursion reports, announcements and calendar entries on subjects of gemmological interest for publication in *The Journal of Gemmology*. A guide to the various sections and the preparation of manuscripts is given at <https://gem-a.com/index.php/news-publications/journal-of-gemmology/submissions>, or contact the Editor-in-Chief.

SUBSCRIPTIONS

Gem-A members receive *The Journal* as part of their membership package, full details of which are given at <https://gem-a.com/membership>. Laboratories, libraries, museums and similar institutions may become direct subscribers to *The Journal*.

ADVERTISING

Enquiries about advertising in *The Journal* should be directed to advertising@gem-a.com. For more information, see <https://gem-a.com/news-publications/media-pack-2019>.

DATABASE COVERAGE

The Journal of Gemmology is covered by the following abstracting and indexing services: Australian Research Council academic journal list, British Library Document Supply Service, Chemical Abstracts (CA Plus), Copyright Clearance Center's RightFind application, CrossRef, EBSCO Academic Search Ultimate, Gale/Cengage Learning Academic OneFile, GeoRef, Index Copernicus ICI Journals Master List, Mineralogical Abstracts, Cambridge Scientific Abstracts (ProQuest), Scopus and the Clarivate Analytics (formerly Thomson Reuters/ISI) Emerging Sources Citation Index (in the Web of Science).



COPYRIGHT AND REPRINT PERMISSION

For full details of copyright and reprint permission contact the Editor-in-Chief. *The Journal of Gemmology* is published quarterly by Gem-A, The Gemmological Association of Great Britain. Any opinions expressed in *The Journal* are understood to be the views of the contributors and not necessarily of the publisher.

Design & production by Zest Design, www.zest-uk.com

Printed by DG3 Group (Holdings) Ltd

© 2019 Gem-A (The Gemmological Association of Great Britain)

ISSN 1355-4565 (Print), ISSN 2632-1718 (Online)



Gem-A
THE GEMMOLOGICAL ASSOCIATION
OF GREAT BRITAIN

21 Ely Place
London EC1N 6TD
UK

t: +44 (0)20 7404 3334
f: +44 (0)20 7404 8843
e: information@gem-a.com
w: <https://gem-a.com>

Registered Charity No. 1109555
A company limited by guarantee and registered in England No. 1945780
Registered office: Palladium House,
1-4 Argyll Street, London W1F 7LD

PRESIDENT

Maggie Campbell Pedersen

VICE PRESIDENTS

David J. Callaghan
Alan T. Collins
Noel W. Deeks
E. Alan Jobbins
Andrew H. Rankin

HONORARY FELLOWS

Gaetano Cavalieri
Andrew Cody
Terrence S. Coldham
Emmanuel Fritsch

HONORARY DIAMOND MEMBER

Martin Rapaport

CHIEF EXECUTIVE OFFICER

Alan D. Hart

COUNCIL

Justine L. Carmody – Chair
Kathryn L. Bonanno
Joanna Hardy
Philip Sadler
Christopher P. Smith

BRANCH CHAIRMEN

Midlands – Louise Ludlam-Snook
North East – Mark W. Houghton
South East – Veronica Wetten
South West – Richard M. Slater

What's New

INSTRUMENTATION

GemPen

Sweden-based Gemometrics AB released its GemPen in 2018. The rechargeable handheld tool utilises different combinations of UV wavelengths and filters to induce various fluorescence reactions that provide indications for screening natural from synthetic diamond (both HPHT and CVD grown), as well as some treatments such as HPHT + irradiation, glass fillings, and oiling or fracture filling. The instrument's case can be used to provide a darkened space for testing. Owners of the instrument can join the GemPen Academy to learn more about how to use the device. Visit <https://gemometrics.com/product/gempen>.



J-Certain Synthetic Diamond Detector

The J-Certain from Massive Tech Labs (Gujarat, India) is a diamond screening instrument with a large (20 × 11 cm) scanning platform that can handle samples 0.002–10 ct of all shapes, whether loose or mounted in jewellery. It offers rapid testing capable of scanning up to 300,000 melee-sized (1 mm) samples per hour to distinguish natural from synthetic diamonds (CVD and HPHT). Issued in July 2018, the J-Certain evolved from the company's 2017-release G-Certain, which is essentially a smaller version suitable primarily for loose diamonds. Visit www.massivetechlab.com/j-certain-a-synthetic-diamond-detector-for-studded-jewellery.




Sherlock Holmes 2.0 Synthetic Diamond Detector

In January 2019, Yehuda Diamond Co. released version 2.0 of its Sherlock Holmes diamond tester. The instrument is designed for use with colourless to near-colourless (D–K) diamonds ranging from melee to any size that will fit in the instrument's drawer, whether loose or mounted, single stone or assorted parcel. It can distinguish CVD and HPHT synthetic diamonds from natural ones, even if the latter have been colour-enhanced through an HPHT process. The user manual, available for download, provides details of how the mobile-phone-based instrument operates, along with exceptions to its capabilities.

The portable instrument includes a mobile phone interface, international charger, two trays, ring holders and a lab-grown diamond. To learn more, visit www.yehuda.com/shop/hphtmachine.



NEWS AND PUBLICATIONS



ABN-AMRO
Group Economics
Macro & Financial Markets
Research

Diamond Sector Outlook

ABN-AMRO Diamond Reports

Economists at the Amsterdam-based bank recently delved into diamond industry concerns with two reports: 'Diamond Sector Watch – De Beers Launch Lightbox: Disruption' (June 2018) and 'Diamond Sector Outlook – Entering a Growth and Disruption Phase' (January 2019). The first report focuses on the launch of De Beers' synthetic diamond jewellery line. The second describes an industry move from a 'relatively stable environment to a highly uncertain environment', which seems to have been associated with the Lightbox launch, threatening to reduce demand for natural diamonds and forcing diamond miners to 'rethink their strategies' as diamond prices decline. To read or download the two reports, visit <https://insights.abnamro.nl/en/2018/06/diamond-sector-watch-de-beers-launch-lightbox-disruption> and <https://insights.abnamro.nl/en/2019/01/diamond-sector-outlook-entering-a-growth-and-disruption-phase>.

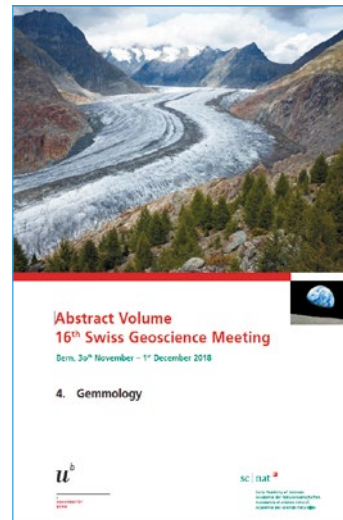
AGTA GemFair Tucson Seminars

From 5 through 10 February 2019, the American Gem Trade Association hosted an array of educational lectures and presentations during the gem shows in Tucson, Arizona, USA. Presenters from around the world discussed gem treatments, cultured pearls, marketing strategies and more. Audio recordings and slides of 25 presentations are available on flash drive for USD50.00. To order, visit <https://agta.org/resources>.



Gem Abstracts from the 16th Swiss Geoscience Meeting

The 16th Swiss Geoscience Meeting was held 30 November to 1 December 2018 in Bern, Switzerland. A half-day session on gemmology included four talks that covered ruby deposits in the Morogoro region of Tanzania, colour instability of padparadscha-like sapphires, inclusions in spinels from Mogok (Myanmar) and age determination of zircon inclusions in Kashmir sapphires. Download the proceedings volume at https://geoscience-meeting.ch/sgm2018/wp-content/uploads/SGM_2018_Symposium_04.pdf.



Gem Abstracts from the 2018 GSA Annual Meeting

The 130th annual meeting of the Geological Society of America took place 4–7 November 2018 in Indianapolis, Indiana, USA.



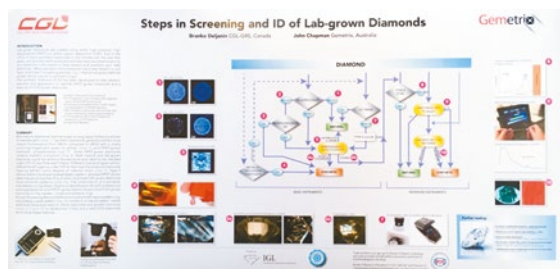
Fourteen abstracts from the session titled 'Gemological Research in the Twenty-First Century—Characterization, Exploration, and Geological Significance of Diamonds and Other Gem Minerals' can be viewed at <https://gsa.confex.com/gsa/2018AM/webprogram/Session45040.html>. Topics include natural diamond colouration, photoluminescence of pink diamond, naturally irradiated black diamonds, chemical imaging of diamonds, inclusions in diamond and sapphire, ruby and sapphire origin determination, rutiled quartz formation, origin of tourmaline-sapphire-phlogopite rocks in Afghanistan and oxygen-isotope ratios in freshwater cultured pearls from Tennessee, USA.

Gem Identification Pamphlet and Poster

Branko Gems/
Gemmological Research
Industries Inc.
(Vancouver,
British Columbia,
Canada) recently released two



products focused on practical gemmology. A pamphlet titled 'ID of Transparent Red, Pink and Purple Gems with Portable Instruments' describes how to separate natural from synthetic gem materials within this colour range using four instruments: 10× loupe, polariscope, spectroscope and the PL-Inspector/Jewellery Inspector. A poster (82.5 × 40.0 cm) titled 'Steps in Screening and ID of Lab-Grown Diamonds' provides a convenient reference for the process of identifying synthetic diamonds using both basic and advanced instrumentation. To order these and other publications, visit www.brankogems.com/shop/product-category/books.



Global Diamond Industry 2018

The eighth annual report on the global diamond industry from the Antwerp World Diamond Centre and Bain & Co. was released in December 2018, titled 'The Global Diamond Industry 2018: A Resilient Industry Shines Through'. The report covers 2017 and the first half of 2018, and includes a forecast of the diamond industry through 2030. The industry experienced approximately 2% growth overall despite 'volatility' in 2017, and diamond production increased almost 20% by volume. In the same period, diamond jewellery sales increased slightly. Factors predicted to affect the industry's future are the influence of digital technologies, lab-grown diamonds and a gradual long-term growth of the diamond market. Visit www.bain.com/insights/global-diamond-industry-report-2018 to read or download the full report.


GIT Reports on Colour-Change Grossular and Musgravite

In December 2018, the Gem and Jewelry Institute of Thailand (GIT) reported on two unusual colour-change garnets that proved to be grossular-rich rather than the pyrope-spessartine, Cr-bearing pyrope

or Cr-bearing grossular-andradite varieties typically associated with this colour phenomenon in garnet. They exhibited a distinct change from green in daylight to brownish red in incandescent illumination. Raman spectroscopy and EDXRF chemical analysis confirmed their grossular-rich composition, and visible absorption spectroscopy showed that $\text{Cr}^{3+} \pm \text{Fe}^{3+}$ are responsible for the colour change. Download the report at www.git.or.th/eng/testing_center_en/lab_notes_en/glab_en/2018/11/Article-2711201801.pdf.

In January 2019, GIT described two faceted specimens of exceptional-quality musgravite recently examined in their laboratory: a 5.95 ct dark green stone and a 1.79 ct light purple gem. The report includes details of microscopic features, semi-quantitative chemical analyses, and Raman, infrared and UV-Vis spectra. Visit www.git.or.th/eng/testing_center_en/lab_notes_en/glab_en/2019/01/Article-1501201901.pdf





31 January 2019 | www.gold.org

Gold Demand Trends

Full year and Q4 2018

Highlights

Central banks added 663.6t to official gold reserves in 2018, the second highest yearly total on record. Net purchases jumped to their highest since the end of US dollar convertibility into gold in 1971, as a greater pool of central banks turned to gold as a diversifier.

Annual jewellery demand was virtually unchanged, down just 1t from 2017. Gems in China, the US and Russia broadly offset sharp losses in the Middle East, where demand was stable at 598t (+1.4t).

ETFs and similar products saw annual inflows of 84.5t, down from 206.4t in 2017. Stock market volatility and signs of falling economic growth in key markets fuelled a global Co recovery, but Europe was the only region to see net growth over the year.

Retail investment in gold bars and coins posted annual growth of 4%. Coin demand surged to reach a five-year high of 226.4t, the second highest on record. Demand for gold bars had steady at 70.5t, the fifth year in succession of holding in a firm 70-80t range.

2018 saw marginal gains in the volume of gold used in technology, crimped by Q4 slowdowns. Other healthy gains during Q1-Q3, a combination of slowing smartphone sales, the trade war and mounting uncertainty over global economic growth, contributed to a 6% decline in Q4.

For more information please contact media@wgc.org

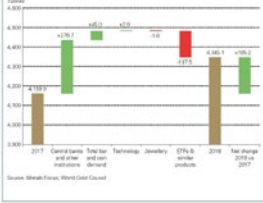
Gold Demand Trends | Full Year and Q4 2018

Annual gold demand gained 4% on highest central bank buying in 50 years

Gold demand in 2018 reached 4,345.1 tonnes (t), up from 4,159.9t in 2017 and in line with the five-year average of 4,347.5t.

A multi-decade high in central bank buying (663.5t) drove annual growth. Demand was bumped up in Q4 by 112.4t of ETF inflows, but annual inflows into these products of 84.5t were 67% lower than 2017. Investment in bars and coins accelerated in the second half of the year, up 4% to 1,080.2t in 2018. Full year jewellery demand was steady at 2,200t. Gold used in technology declined marginally to 334.6t in 2018, although growth ran out of steam in Q4. Annual gold supply firmed slightly to 4,490.2t, with mine production inching up to a new high of 3,364.9t.

4% growth in annual gold demand driven by highest central bank buying in 50 years



Source: World Gold Council, World Gold Council

Gold Demand Trends 2018

The World Gold Council released a combined report in January 2019 that covers the full year and the fourth quarter of 2018. Overall demand for gold during 2018 was higher than in 2017 but consistent with a five-year average of 4,347.5 tonnes. Gold jewellery demand remained steady. Gold supply for the year reached 4,490.2 tonnes, aided by a new high in mine production of 3,364.9 tonnes. To obtain the full report, infographics, data and statistics, go to <http://tinyurl.com/y7oguc7y>.

Jewelry Development Impact Index Studies

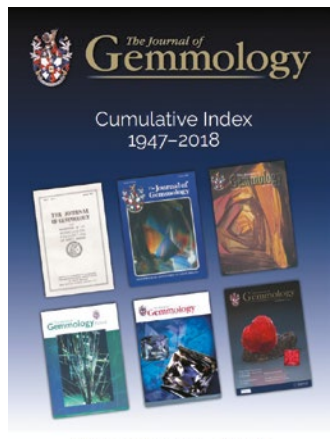
The online Gemstones and Sustainable Development Knowledge Hub offers reports and presentations from various case studies undertaken as part of the Jewelry Development Impact Index. Research results from 2018 cover gems and precious metals in South Africa (platinum), Madagascar (sapphires), Afghanistan (lapis lazuli) and Myanmar (rubies). The studies examine the impact of mining on governance, economy, environment, and health and human rights, and offer suggestions for improvement. Download presentations or full reports at www.sustainablegemstones.org/jewelry-development-index-jdi.



The Journal's Cumulative Index Updated, Plus Subject Bibliographies


The Journal of Gemmology's cumulative index has been updated to cover all issues from 1947 through 2018. Because the index is provided in electronic (PDF) format, it can be searched for specific authors as well as topics.

In addition, bibliographies of articles and notes published in *The Journal* are now available that cover several different gem materials, including biogenic gems, chrysoberyl and alexandrite, diamond, emerald and other beryls, ruby and sapphire, garnet, opal, pearl, quartz and tourmaline. Bibliographies on additional gem materials will be added in the future. The index and bibliographies are freely available to download at <https://gem-a.com/news-publications/journal-of-gemmology#the-journal-index-and-bibliography-lists>.



LMHC Information Sheet Updates

In November 2018, the Laboratory Manual Harmonisation Committee updated four of its Information Sheets: 'Gemmological Laboratory Reports', 'Padparadscha Sapphire', 'Corundum – No Indications of Heating and Indications of Heating', and 'Alexandrite and Other Colour-Change Gemstones'. In addition, new Information Sheets were issued on 'Organic Fillers (Oil, Resin, Wax) in Gemstones' and 'Hydrophane Opal'. Download the sheets at www.lmhc-gemmology.org/gemstones.



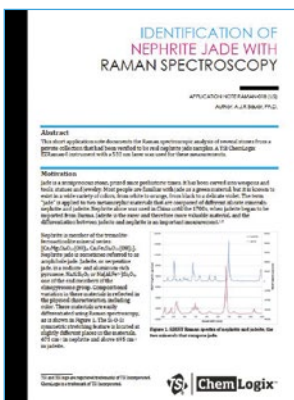
MVI Marketing Research on Millennials and Synthetic Diamonds

MVI Marketing, a USA-based company focused on market research on luxury goods (primarily jewellery), released a report titled 'Millennial Consumer Research: Lab Grown Diamonds' in May 2018. It summarises the results of an online research study involving 1,010 respondents in the USA, aged 21–40 years, from a range of incomes. More than 75% of men and nearly 65% of women reported they would consider a lab-grown diamond for the centre stone in an engagement ring, on average a 13% increase from the previous year. Reasons included obtaining a larger stone for their money, the ability to save money on an engagement ring, and both environmental and social concerns about diamond mining. Key findings break down the information to help trade members explore ways of marketing lab-grown diamonds to millennials. To receive a presentation of this research (PDF format) via email, submit the form at www.mvimarketing.com/download-report.php?report=34.



Assure Program for Testing Diamond Verification Instruments

The Diamond Producers Association hosts the Assure Program, a collaborative venture designed to evaluate the performance of 'diamond verification instruments' (DVI). The project has developed the DVI Standard that includes test protocols and methods used to determine the performance of DVIs. In collaboration with DVI manufacturers, the Assure Program oversees the testing through UL, an independent testing organisation that guides the development of and sets internationally recognised standards in a variety of technical fields. Manufacturers submitted their instruments under one of three categories: those that separate natural from synthetic diamonds; those that distinguish natural diamonds from synthetic diamonds and diamond simulants; and those that separate natural diamonds, synthetic diamonds and diamonds simulants. The first phase of testing started in 2018 and on 5 March 2019 results were posted for 11 instruments at <https://diamondproducers.com/assure>, which also contains advice for how to read the test results, select an appropriate instrument and maintain diamond pipeline integrity.



Raman Spectroscopy of Jade and Its Imitations

TSI Incorporated, an instrument manufacturer based in Minnesota, USA, published two application notes in September 2018 titled 'Identification of Nephrite Jade with Raman Spectroscopy' and 'Detection of Imitation Jade with Raman Spectroscopy'. The first report compares the Raman spectra of greenish blue and white nephrite samples, as well as various amphiboles from the RRUFF database. The second report provides the results of Raman analysis of four 'jade' samples purchased from three different online vendors. Two of the stones were identified as chrysotile and aventurine quartz, and the other two samples (obtained from a single vendor) consisted of chrysotile that was coated with a material that fluoresced when exposed to the instrument's 532 nm laser. Download the reports from www.tsi.com/system/search-results/?searchtext=jade.

Responsible Sourcing CIBJO Blue Book

Released in January 2019, *The Responsible Sourcing Book* is a 14-page guide to CIBJO's responsible sourcing policy. The report covers aspects such as supply chain due diligence, risk assessment, product integrity and certification, and concludes with a series of appendices that include lists of various supply chain guidance and standards organisations, a list of audit agencies and a checklist for responsible sourcing. Download the document at www.cibjo.org/downloads/19-01-06%20Responsible%20Sourcing%20Book%20.pdf.



Santa Fe Symposium Proceedings

Papers from 23 presentations delivered at the 32nd Santa Fe Symposium (held 20–23 May 2018 in Albuquerque, New Mexico, USA) are available for download, on topics such as precious metals, history of metallurgy, jewellery manufacturing methods, long-term predictions for the jewellery industry and more. Visit www.santafesymposium.org/papers to download PDF files of these papers, as well as those from earlier symposia dating back to 2000.



Sapphires Heated with Pressure

Blue sapphires that have undergone high-temperature heat treatment under pressure (sometimes called 'HPHT-treated' sapphires) have recently become the subject of various investigations. GRS Lab researchers in Switzerland, Thailand, Sri Lanka and Hong Kong contributed to a November 2018 report on how GRS identifies these sapphires and describes them on identification reports. The research covers 159 treated samples seen in GRS labs during 2015–2018 and 128 samples examined at various stages of treatment. Analytical methods included FTIR, UV-Vis-NIR, LIBS, EDXRF and Raman spectroscopy, and DiamondView fluorescence imaging. A unique set of inclusion features can help distinguish these treated sapphires from untreated and conventionally heat-treated samples, and the researchers also noted durability issues (e.g. increased brittleness) attributed to the treatment. GRS distinguishes these sapphires on its identification reports with the code 'PHT' to separate them from conventionally heat-treated sapphires. Download the report at <http://gemresearch.ch/wp/wp-content/>

uploads/2018/11/GRS_HPHT_Update_2018_11_12_Sm.pdf. Also available on the GRS website (<http://gemresearch.ch/retake-gilc-2019>) is a video presentation by Dr Adolf Peretti on these treated sapphires from research that was originally presented at the February 2019 Gemstone Industry & Laboratory Conference (GILC) conference in Tucson.

During the GILC conference, a presentation on these treated sapphires was also given by the LMHC group of gemmological laboratories, and a PDF file containing the slides can be downloaded at www.lmhc-gemmology.org/s/Heat-with-pressure-LMHC-final-for-web-Feb2019.pdf. Based on this research, on 27 February 2019, Lotus Gemology posted an article titled 'Squeezing Sapphire: Corundums treated with high temperatures and low pressure (HT + P)'. It provides a compendium of information from numerous labs worldwide, including a history of the heat treatment of corundum (which puts the relatively new method into context), a description of the treatment methodology (from visits to a heating facility in South Korea) and characteristics of inclusions, UV fluorescence, trace-element composition and various spectral features in sapphires treated by this method. The article concludes with the results of various durability tests, which revealed no particular problems associated with this treatment. Read the article at www.lotusgemology.com/index.php/library/articles/346-sapphires-treated-with-high-temperature-and-low-pressure or download it from <http://gtljaipur.info/publications.aspx>.

Version 17 November 2018

Identification and characteristics of PHT ('HPHT') - treated sapphires - An update of the GRS research progress

Adolf Peretti^{1,2,3,4*}, Maya Meesa¹, Willy Bari¹, Edward Cleveland¹, Ishtiyaq Ahmad¹, Matthias Alessandro¹, Lawrence Haka⁴

¹GRS Gemmerh Suisah AG, Bannachring 13, 6045 Meggen, Switzerland (* corresponding author, e-mail: adolp@peretti.ch)
²GRS (Thailand) Co., Ltd., 10th Fl. 506, Siam P/Bldg., Soi 19, Silom, Bangkok, Bangkok 10500, Thailand
³GRS Lanka (PVT) Ltd, 471, 211 Galle Road, Colombo 3, Sri Lanka
⁴GRS Lab (Hong Kong) Limited, 19/F, Man Hing Commercial Building, 79-83 Queen's Road Central, Hong Kong, China

Fig. 1. A series of faceted HPHT-treated sapphires in a color range from pastel, vivid (vivid blue) to deep blue in different shape and sizes (4–54 ct).

Introduction
 A series of peculiar events that commenced in 2015 brought a degree of uncertainty to the Sri Lankan gemstone industry. Sri Lanka is known as the world's foremost producer of 'natural' corundum. So far only corundum of higher clarity has been used to produce clean sapphires. It was noticed that a few buyers began purchasing previously 'untreated' rough at uncommonly high prices. A rumor spread that a new treatment was developed and from emerged that a new type of diffusion treatment could be responsible. Shortly afterwards some sapphire vendors were selling 'heated' sapphires below the already decreasing market prices of heated sapphires, and rumors were confirmed that a new type of sapphire treatment had been discovered. While speculation that HPHT-treated sapphires being responsible for the price decrease of heated sapphires are unsubstantiated, it can not be ignored (see Fig. 29) due to the coincidental occurrence of event. The appearance of this new treatment came at a critical time of political and economic changes in Asia. If it did not negatively affect the market, it surely did not help.

In 2009, a Korean company called HBI Laboratory Co. Ltd first successfully treated corundum with a new HPHT technique. The new heat treatment executed at elevated pressures is similar to low diamonds are being HPHT-treated, although the applied pressure is significantly lower. The applied pressure during the HPHT-treatment for diamonds is larger than 50 Kbar (Dobrinets, Vlas and Zaitsev, 2012) whereas the

categories of sapphires: untreated rough and already conventionally heat treated sapphires (multi-step treatment). The treated product has been commercially available since 2013. An influx at GRS lab was seen in 2015.

The advantages of this new technique are significant when compared to traditional heat treating methods. The traditional heat treatment methods require high temperature-soaking times between 1500-1800°C for many hours or even several days. The new elevated pressure method reduces the soaking time to less than 30 minutes at similar temperatures.

Another key competitive advantage is the heating effect on fractures and surface reaching features. The process of crack-healing and improvement of clarity has also been reported by Choi et al., 2018.

The Korean HBI Gemological Institute Laboratory (GILG) first reported in November 2011 on blue sapphires having unusual infrared spectroscopic characteristics. The HPHT-processed gemstones show a strong absorption band centered around the 3047cm⁻¹ in the infrared

LOTUS new directions in GEM-ology

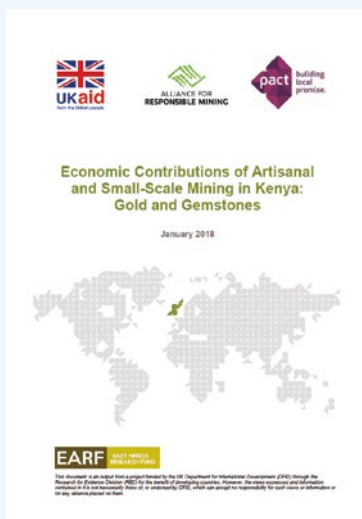
01 HOME 02 ABOUT 03 LAB 04 LIBRARY 05 CONTACT

REPORT VERIFICATION SEARCH

Squeezing Sapphire • Corundums treated with high temperatures and low pressure (HT+P)

by Adolf Peretti (author)

27 February 2019: Sapphires heated with high temperatures and low pressures (=HPHT) first entered the market in 2009, becoming more common since 2015. This article examines the process in detail and looks at the question of whether a separate disclosure is needed for the treatment.



Small-Scale Mining in Kenya

Released in January 2018, ‘Economic Contributions of Artisanal and Small-Scale Mining in Kenya: Gold and Gemstones’ is a collaborative report from Pact Global and the Alliance for Responsible Mining that describes recent revisions to mining regulations and policies in Kenya, and includes recommendations intended to further develop gold and gem mining in that country. Case studies that form the foundation of the report include gold mining in Migori and gem mining in Taita Taveta. Recommendations include improvement of the mine permitting and granting process, training in extraction methods, encouragement of gender inclusion, and the development of gem cutting and marketing centres. Download the report at www.pactworld.org/sites/default/files/Pact%20-%20DFID%20EARF-%20Kenya%20case%20study%20-Jan%202018VF.pdf.

SSEF Facette

Facette Magazine

No. 25 was

released by the Swiss Gemmological Institute SSEF in February 2019.

The issue covers: gem traceability and blockchain; low-temperature heated rubies from Mozambique; damage to emeralds;

repair-related laser damage to sapphires; recently encountered examples of synthetic ruby, sapphire and spinel; DNA fingerprinting of pearls, coral and ivory; colour-change phenomena in various gem materials; lead-glass-filled pink sapphire; gem deposits of Luc Yen, northern Vietnam; age dating of ruby in a Harry Winston necklace; a historic sapphire that belonged to Catherine the Great of Russia; spinel from Mogok; pink cobalt-calcite from Switzerland; V-rich ruby from Mogok; a cultured pearl with a bead containing organic matter; artificial aging of cultured pearls; cultured pearls with natural pearl beads; chemical analysis of Paraíba tourmaline; a review of diamond HPHT treatment research at SSEF; auction highlights of gems and jewellery accompanied by SSEF reports, including Marie Antoinette’s pearl pendant; several conference and travel reports; and information on various SSEF news and services. Download this and previous issues of *Facette Magazine* at www.ssef.ch/ssef-facette.



Synthetic Periclase Identified by GRS

The GemResearch Swisslab released a Special Alert on synthetic periclase in December 2018. The report describes research on numerous rough and cut samples showing various colours (brownish orange, yellow, green and colourless) that were offered as garnet from Turkey. The gemmological properties were consistent with periclase, and by destructively targeting selected areas of rough samples for inclusion investigation the researchers conclusively identified the material as synthetic periclase by the presence of an artificial dicalcium silicate compound. The material was further characterised by DiamondView fluorescence, SEM-EDS and LA-ICP-MS analyses, and by Raman, photoluminescence, FTIR and UV-Vis-NIR spectroscopy. An abstract and a link to the full article are available at <http://gemresearch.ch/synthetic-periclase>. See also the Gem Note on synthetic periclase in the Gem Notes section of this issue (pp. 414–416).



OTHER RESOURCES

ColorCodex Update

An updated version of the ColorCodex colour referencing system was launched at the February 2019 AGTA show in Tucson. Originally released in a slightly different format in early 2017 (see What's New section, Vol. 35, No. 5, 2017, p. 376), the system has been expanded into a more practical and innovative tool for industry professionals to compare and reference the colour of gemstones.

The ColorCodex system consists of coloured windows that have a shiny, reflective and textured surface which mimics the appearance of colour in transparent faceted gemstones. There are 65 columns representing different hues (labelled with even numbers 10 through 138) that are distributed on 13 ColorCodex sheets. Each column has eight rows of coloured windows (labelled with odd numbers 03 through 17) that depict varying saturations of that colour. (Tonal values are brought in through the addition of grey overlays.) Combining the two numeric values (e.g. 22-07) defines not only a specific colour (column 22), but also its saturation (level 07). The numbering convention used by the system



allows for the situation of a colour falling between two windows. The system references a particular colour using a precise numeric code without the introduction of colour descriptions. Numeric codes are not influenced by how individuals learn to describe colour, nor by cultural or geographical considerations. By eliminating the ambiguity inherent in colour terminology, the system's colour designations are useful toward a wide range of applications from gemmological education and appraisals to laboratory terminology. Because it is intuitive, one is able to master the use of the system with little instruction. For more information, visit www.color-codex.com.

*Dr Çiğdem Liüle (info@kybelellc.com)
Kybele LLC, Buffalo Grove, Illinois, USA*



Announcing GemPrice
Version Update



GemPrice Update

The GemPrice online wholesale pricing system for diamonds, coloured stones and jewellery from GemWizzard Inc. (Ramat Gan, Israel) was updated in late 2018 with new pricing, gem colour borders, gem type information, tutorials and support. The changes are also reflected in the GemPrice app, available for both iOS and Android mobile devices. Access is by annual subscription. For detailed information, video demonstrations and a trial version (limited to amethyst), visit www.gemewizard.com/products-services/gemtrade/buyers/gemprice/index.html.

MISCELLANEOUS

Museum of Whitby Jet Opens

W. Hamond jewellers, the oldest manufacturer and retailer of Whitby jet (founded in 1860), recently opened the Museum of Whitby Jet to house its collection of antique jet specimens along with displays of the history and manufacturing of this Yorkshire gem material. The museum is located in restored Wesley Hall in the heart of old Whitby, and offers periodic educational courses focusing on jet and jewellery. For more on the museum's background, displays and access, visit www.museumofwhitbyjet.com.

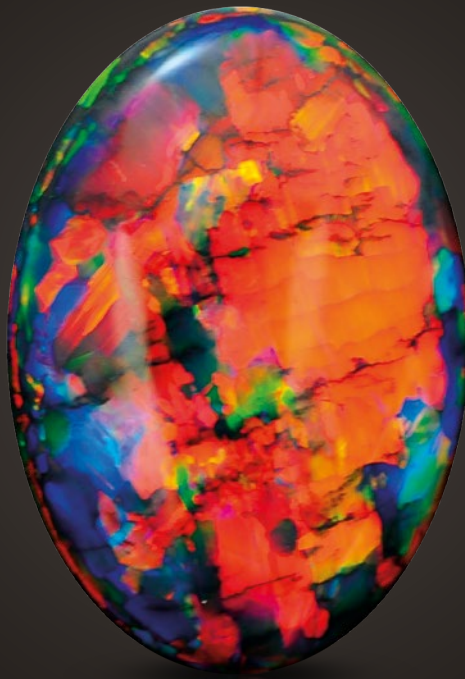


What's New provides announcements of new instruments/technology, publications, online resources and more. Inclusion in What's New does not imply recommendation or endorsement by Gem-A. Entries were prepared by Carol M. Stockton unless otherwise noted.

The Fire Within

“For in them you shall see the living fire of the ruby, the glorious purple of the amethyst, the sea-green of the emerald, all glittering together in an incredible mixture of light.”

- Roman Elder Pliny, 1st Century AD



BLACK OPAL 15.7 CARATS

Suppliers of Australia's finest opals to the world's gem trade.

CODY  OPAL

LEVEL 1 - 119 SWANSTON STREET MELBOURNE AUSTRALIA

T. +61 3 9654 5533 E. INFO@CODYOPAL.COM

WWW.CODYOPAL.COM


INTERNATIONAL
COLORED GEMSTONE
ASSOCIATION
MEMBER

Gem Notes

COLOURED STONES



Figure 1: Anorthoclase from Antarctica (here, 2.29 and 1.61 ct) has a dark appearance due to the presence of abundant melt inclusions. Photo by Mauro Pantò.

‘Black Anorthoclase’ from Antarctica

Mount Erebus is an active volcano on Ross Island in Antarctica, and is known as a source of large ‘anorthoclase’ feldspar crystals (i.e. phenocrysts) that occur in lava flows and volcanic bombs on the mountain’s flanks (Dunbar *et al.* 1994). (*Editor’s note:* Although mining on Antarctica is prohibited, samples may be collected for scientific research. The mineral name *anorthoclase* has been discredited by the International Mineralogical Association, but the term remains widely used—especially by geologists studying Mount Erebus—and therefore this term will continue to be used here, without quotes for simplicity. It refers to an intermediate member of the solid-solution series constituted by high albite–sanidine alkali feldspar.) The crystals are hosted by phonolite, which is an uncommon volcanic rock of intermediate chemical composition (i.e. between felsic and mafic). The phonolite contains abundant (up to 30% by volume) anorthoclase megacrysts up to 10 cm long, and physical weathering of the lavas and bombs has resulted in lag deposits containing abundant anorthoclase crystals that are locally present on the summit cone of the volcano (Dunbar *et al.* 1994; Kelly *et al.* 2008).

The anorthoclase is chemically zoned with a compositional range of $An_{10.3-22.9}Ab_{62.8-68.1}Or_{11.4-27.2}$ (expressed as mol. % anorthite, albite and orthoclase, respectively; Kelly *et al.* 2008). Besides their large size, the anorthoclase crystals are notable for containing abundant melt inclusions that may give them a dark greyish brown to nearly black appearance.

At the 2018 gem shows in Tucson, Arizona, USA, Mauro Pantò (The Beauty in the Rocks, Sassari, Italy) had a few anorthoclase gemstones from Mount Erebus. They were cut from a single piece of rough that was presented to him as a gift from a geologist who had also received it as a gift. The rough piece measured about 30 mm long and 8 mm wide, and yielded six stones ranging from approximately 1 to 3 ct (e.g. Figure 1). Pantò kindly donated one of the stones to Gem-A, and it was characterised by authors CE and PD.

The stone had RIs of 1.531–1.538 (birefringence 0.007) and a hydrostatic SG of 2.66. These values are both somewhat high for anorthoclase, which may be due to the abundant melt inclusions (Figure 2). Chemical analysis with a Thermo Scientific ARL Quant’X energy-dispersive X-ray fluorescence (EDXRF) spectrometer showed major amounts of Si, Al, Na, Ca and K, consistent with

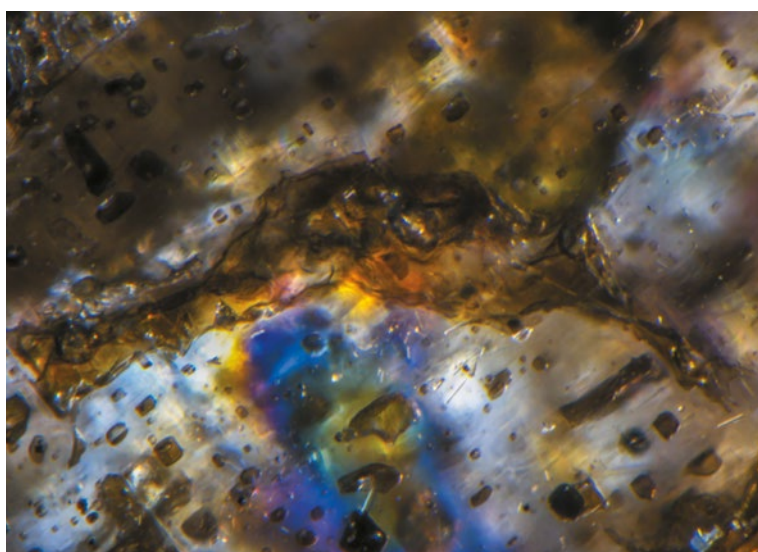


Figure 2: Melt inclusions in the anorthoclase form relatively large irregular masses or smaller rectangular bodies, both of which contain contraction bubbles. Photomicrograph by N. D. Renfro, © GIA; image width 0.96 mm.

anorthoclase. In addition, the analyses showed traces of Fe and Ti (probably due to the melt inclusions), as well as Sr and Ba (which are common impurities in the feldspar).

Microscopic examination of the stone by author NDR showed that two types of melt inclusions were present: those that were large and irregular, and those that were small and rectangular (again, see Figure 2), as previously reported by Dunbar and Kyle (1990). Raman analysis of the inclusions yielded spectra that would be expected for a glass, which is consistent with the presence of contraction bubbles that formed in the melt as it cooled into glass. Also common were iridescent cleavage fractures (Figure 3).

Moussallam *et al.* (2015) determined that the anorthoclase megacrysts at Mount Erebus formed in a vigorously convecting magmatic system involving perhaps 1–3 complete journeys between the magma chamber (at a depth of several kilometres) and the lava lake at the earth's surface, and that a typical crystal of 1 cm across may have formed over a period of at least 14 years.

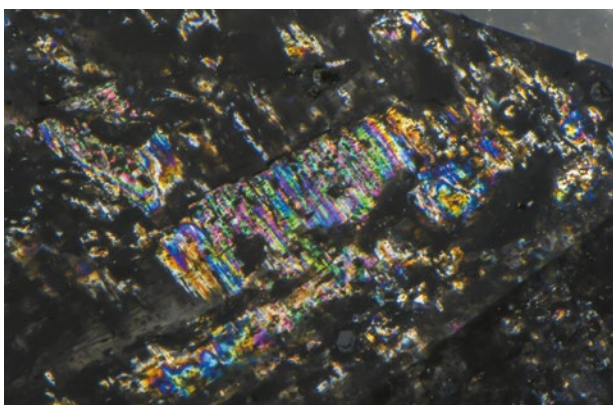


Figure 3: Iridescent cleavages are commonly seen in the anorthoclase. Photomicrograph by N. D. Renfro, © GIA; image width 4.10 mm.

Considering the recent age of some of the lava flows (several years to decades in some cases), these may be the youngest feldspars that have been cut into gemstones.

Brendan M. Laurs FGA

Charles Evans FGA DGA and Pat Daly FGA
Gem-A, London

Nathan D. Renfro FGA
Gemological Institute of America (GIA)
Carlsbad, California, USA

References

- Dunbar, N.W. & Kyle, P.R. 1990. Volatile contents of melt inclusions in anorthoclase phenocrysts from Mount Erebus: Implications for magmatic crystallization. *Antarctic Journal of the United States*, **25**, 9–11.
- Dunbar, N.W., Cashman, K.V. & Dupré, R. 1994. Crystallization processes of anorthoclase phenocrysts in the Mount Erebus magmatic system: Evidence from crystal composition, crystal size distributions, and volatile contents of melt inclusions. In: Kyle, P.R. (ed) *Volcanological and Environmental Studies of Mount Erebus, Antarctica*. American Geophysical Union, Washington DC, USA, 129–146, <http://doi.org/10.1029/ar066p0129>.
- Kelly, P.J., Kyle P.R., Dunbar, N.W. & Sims, K.W.W. 2008. Geochemistry and mineralogy of the phonolite lava lake, Erebus volcano, Antarctica: 1972–2004 and comparison with older lavas. *Journal of Volcanology and Geothermal Research*, **177**(3), 589–605, <http://doi.org/10.1016/j.jvolgeores.2007.11.025>.
- Moussallam, Y., Oppenheimer, C., Scaillet, B., Buisman, I., Kimball, C., Dunbar, N., Burgisser, A., Schipper, C.I., Andújar, J. & Kyle, P. 2015. Megacrystals track magma convection between reservoir and surface. *Earth and Planetary Science Letters*, **413**, 1–12, <http://doi.org/10.1016/j.epsl.2014.12.022>.

Blödite—A Rare Collector's Stone

Blödite is a rare, hydrated Na-Mg sulphate with the chemical formula $\text{Na}_2\text{Mg}(\text{SO}_4)_2 \cdot 4\text{H}_2\text{O}$. It is monoclinic and typically forms short prismatic crystals with glass-like lustre, or it may occur in granular to massive aggregates; it is usually colourless, pale red or dark grey (Bernard & Hyršl 2004). Blödite was discovered in 1821 in a salt deposit at Ischler Salzberg in Bad Ischl, Gmunden, Austria, and was first described by Johann Friedrich John, who named it in honour of German chemist Karl August Blöde (John 1821). Decades later, Austrian mineralogist Gustav Tschermak named a new mineral *simonyite* (after

the geographer Friedrich Simony; Tschermak 1869), but it turned out to be the same mineral as blödite (Groth & Hintze 1871). Today the name *simonyite* is discredited, but sometimes it is used synonymously with blödite.

Blödite is found mainly in marine evaporite deposits (Bernard & Hyršl 2004). The mineral is easily soluble in various liquids, even in cold water (www.mindat.org/min-695.html). It will dehydrate in air, resulting in a white crust forming on its surfaces. Due to these qualities, as well as its low hardness (Mohs 2½–3), blödite is rarely faceted and certainly qualifies as a collector's stone.



Figure 4: This faceted blödite (1.26 ct), reportedly from California, USA, was examined for this report. Photo by Samantha Laddin, DSEF German Gem Lab.

The author recently had the opportunity to investigate a faceted blödite of 1.26 ct, which reportedly came from California, USA (Figure 4). The mineral has RIs of $n_x = 1.483$, $n_y = 1.486$ and $n_z = 1.487$, and its SG is 2.25 (Schaller 1932; Madsen 1966; Bernard & Hyršl 2004), so it can be identified by standard gemmological testing (though not by hydrostatic weighing to determine SG due to its solubility). Nevertheless, because of its fragility, the identity of the stone shown in Figure 4 was confirmed using Raman spectroscopy, with the spectra compared to the RRUFF database as well as to the reference collection of the German Gemmological Association. Observation with the gemmological microscope revealed growth structures, partially healed fractures and minute two-phase inclusions (Figure 5).

Specimens of blödite should be stored in an airtight container to prevent them from dehydrating.

Acknowledgements: The author thanks Michael Wild of Werner Wild e.K., Idar-Oberstein, Germany, for loaning this faceted blödite.

Tom Stephan (t.stephan@dgemg.com)
German Gemmological Association
Idar-Oberstein, Germany



Figure 5: Examination with a gemmological microscope revealed this two-phase inclusion in the faceted blödite in Figure 4, which is seen here among prominent polishing lines. Because of the low hardness and the solubility of blödite, it is difficult to achieve a good polish. Photomicrograph by T. Stephan in transmitted light; image width 1.5 mm.

References

- Bernard, J.H. & Hyršl, J. 2004. *Minerals and Their Localities*. Granit, Prague, Czech Republic, 808 pp.
- Groth, P. & Hintze, C. 1871. Über krystallisirten Blödit von Stassfurt. *Zeitschrift der Deutschen Geologischen Gesellschaft*, **23**(4), 670–678.
- John, J.F. 1821. Chemische Zerlegung eines neuen fossilen Salzes des Blödits und des Polyhaliths. *Chemische Untersuchungen mineralischer, vegetabilischer und animalischer Substanzen*. Maurerschen Buchhandlung, Berlin, Germany, **6**, 240–247.
- Madsen, B.M. 1966. Loeweite, vanthoffite, bloedite, and leonite from southeastern New Mexico. *U.S. Geological Survey Professional Paper 550-B*, Washington DC, USA, B125–B129.
- Schaller, W.T. 1932. The refractive indices of bloedite. *American Mineralogist*, **17**(11), 530–533.
- Tschermak, G. 1869. Ueber den Simonyit, ein neues Salz von Hallstatt. *Sitzungsberichte der Kaiserlichen Akademie der Wissenschaften in Wien*, **60**(1), 718–724.

Purple Fluorite in Opal from Utah, USA

The Tucson gem shows are an ideal place to find new and exotic gem materials (some of which might not be accurately labelled), as well as those that are familiar with only a new name or new origin. During the 2018 Kino ‘Electric Park’ show, one dealer had dozens of

opaque mottled purple cabochons and beads—some of which had a brecciated appearance with white to light brown areas—which he represented as ‘opalized fluorite’ from Utah, USA. However, the material did not have the typical look of an opalised product, and it had a greater



Figure 6: These cabochons (up to 31.5 × 16.5 mm) are representative of the more uniformly purple material from Utah, USA that is sold as 'opalized fluorite'. Characterisation of two similar samples showed they consisted of opal-A with abundant purple fluorite inclusions. Photo by Brendan M. Laurs.

heft than opal. Similar material (e.g. Figure 6) was seen at the 2018 and 2019 AGTA shows in Tucson with gem dealer Bill Gangi (Gangi Gems, Franklin Square, New York, USA). Two mottled purple cabochons obtained from Gangi were characterised for this report. Standard gemmological properties were determined separately by authors EF and CW, and advanced testing by authors EF and BW included EDXRF and Raman spectroscopy, scanning electron microscopy and visible-range reflectance spectroscopy.

The colour of the material was somewhat patchy and ranged from light to dark purple, with irregular colour patterns. There were also some veins that were semi-transparent and slightly milky with chevron-like shapes. The samples exhibited the moderate-to-low vitreous lustre typical of common opal. The RI value, measured by EF using the spot method on different areas of the samples, ranged from 1.45 to 1.50 (a slightly lower value of 1.44 was obtained by CW). The SG was measured hydrostatically by author EF to be between 2.24 and 2.66, and author CW obtained a value of 2.31. The range of RI and SG measurements relates to the inhomogeneous and also possibly porous nature of this material.

Ultraviolet luminescence was observed with a Vilber Lourmat VL-215.LC UV lamp using both long-wave (365 nm) and short-wave (254 nm) radiation, with a power of 6 W for each lamp, at a distance of 7 cm from the sample, in total darkness. The stones luminesced a whitish blue to long-wave UV, with the whiter areas emitting a moderate green. In short-wave UV, the whitish blue was somewhat weaker but the green component was much stronger. This is reminiscent of the short-wave UV luminescence of many common opals due to traces of uranium (Gaillou *et al.* 2012).

Microscopic observation revealed the inhomogeneous nature of the material, with purple spots in an otherwise grey to white matrix. The purple inclusions showed at

least two size ranges (Figure 7). This is reminiscent of purple fluorite mixed with opal from various localities, including so-called Tiffany Stone from Utah and Morado opal from central Mexico (<https://geology.com/gemstones/opal/morado-opal.shtml>).

With an Amptek X123-SDD EDXRF spectrometer we detected significant Ca, minor amounts of Zn, Fe and Pb, and traces of U. A Geiger counter revealed radioactivity emitted at 180–210 counts per minute, which is approximately three times background levels. This amount of emission is not considered dangerous or of health consequence.

Raman spectroscopy using a Fourier-transform spectrometer provided no useful spectra, even though this is usually the preferred instrument to identify opal (Ostrooumov *et al.* 1999; Fritsch *et al.* 2012). Using a typical dispersive Horiba Scientific T64000 Raman spectrometer with 514 nm excitation (argon-ion laser), we obtained a weak signal with a main broad band centred at $\sim 400\text{ cm}^{-1}$. This is consistent with opal-A

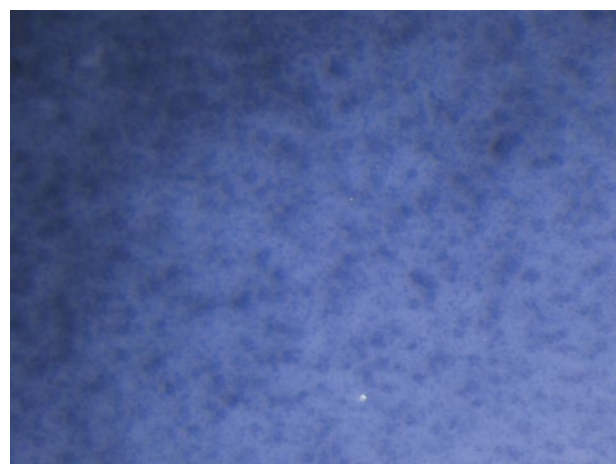
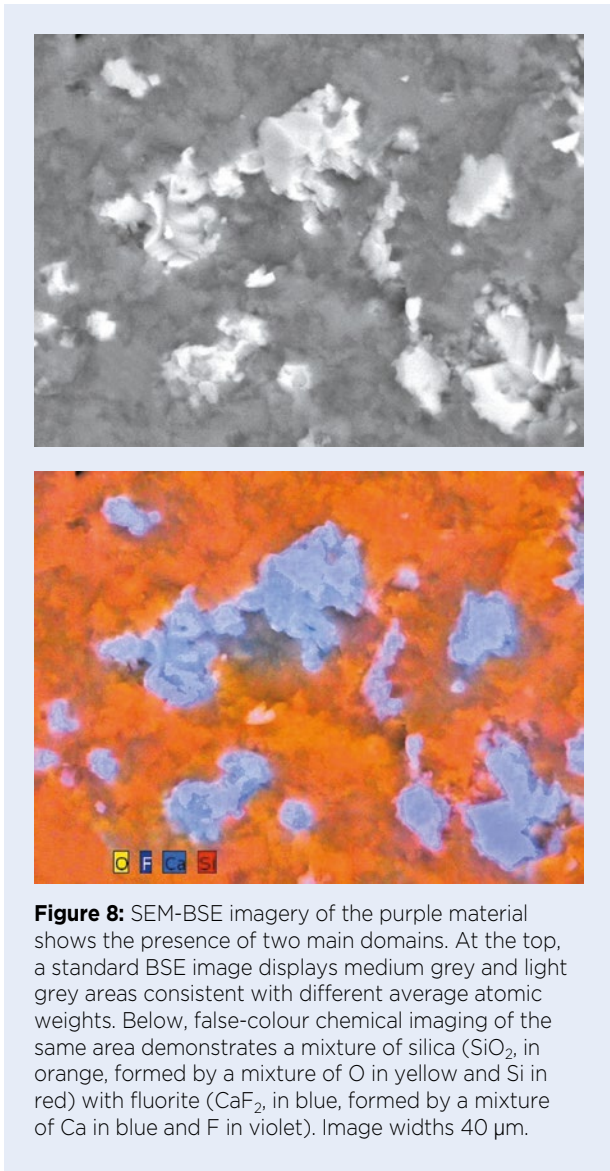


Figure 7: Magnification of the purple gem material from Utah reveals an inhomogeneous mixture of purple spots of various sizes in a light-coloured matrix. Photomicrograph by E. Fritsch; image width 2.0 mm.



(amorphous), which also commonly displays weaker opal-related Raman bands at 780, 970 and 1068 cm^{-1} . Using an Enwave 785 nm laser Raman spectrometer, we detected fluorite in the purple areas. The Gemmo-Raman-532SG identified some grains as quartz.

Examination of a freshly broken sample with a JEOL 5800 scanning electron microscope (SEM) at 2,000 \times magnification in backscattered electron (BSE) mode revealed a mixture of two components with different fracture types and contrasting chemical compositions (Figure 8). The matrix material appeared medium grey in the BSE images (thus, composed of relatively lighter elements) and showed a rather smooth, curved, probably conchoidal fracture. The much lighter grey-appearing inclusions (thus composed of relatively heavier elements) had a blocky appearance, with flat surfaces (possibly cleavages) measuring a few micrometres across and sharp edges that sometimes showed 90° angles. Veins and occasional inclusions measuring several hundred micrometres were observed in some areas. Energy-dispersive spectroscopy with the SEM revealed that the matrix was composed essentially of Si and O, whereas the inclusions contained Ca and F. This confirms the presence of fluorite (CaF_2) inclusions in a matrix of opal ($\text{SiO}_2 \cdot n\text{H}_2\text{O}$).

The colour of this gem is due to the purple fluorite inclusions, as initially suggested by microscopic observations. A visible-range reflectance spectrum obtained with a PerkinElmer Lambda 1050 spectrophotometer with an integrating sphere showed that the colour is induced by a broad band centred at around 580 nm (Figure 9a). This is a classic absorption feature of purple fluorite, due to nano-precipitates of colloidal Ca (Braithwaite *et al.* 1973).

Finally, the green short-wave UV emission is typical

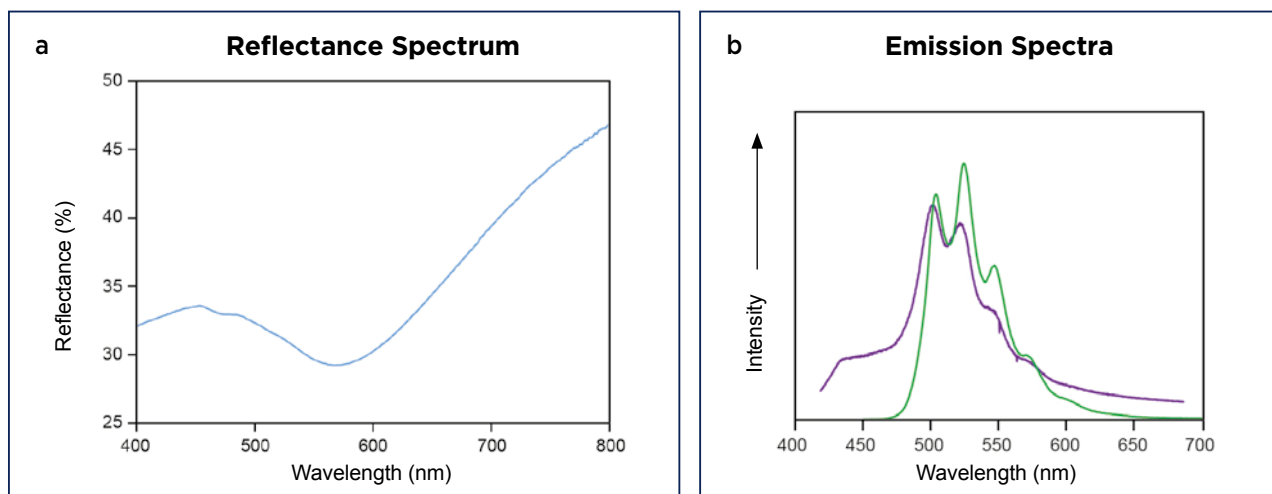


Figure 9: (a) The visible-range reflectance spectrum of this gem material is typical of purple fluorite, with a broad band centred at ~580 nm. (b) Comparison of the short-wave UV emission of the purple gem material with hyalite opal from Mexico (green spectrum) shows closely matching positions of the emission maxima and troughs, as well as similar band widths and shapes. This emission is typical of opal containing traces of U.

of various opals. Figure 9b compares the emission spectrum of this purple material with that of hyalite opal from Mexico (see also Fritsch *et al.* 2015). The emissions are very close in position, width and perceived colour, confirming that the luminescing matrix is indeed opal containing traces of U.

This gem material from Utah is constituted by common opal (i.e. opal-A) containing myriad of minute purple fluorite inclusions that cause its colour. It is similar to Morado opal from Mexico, which also consists of common opal coloured by purple fluorite (e.g. Renfro 2012). Most purple opals coloured by fluorite inclusions tend to be mixed with quartz and a whitish host rock and have a mottled, uneven colouration. Although Tiffany Stone from Utah reportedly contains bertrandite $[\text{Be}_4(\text{Si}_2\text{O}_7)(\text{OH})_2]$ as a common constituent (e.g.

Serras-Herman 2012), this mineral was not detected by Raman spectroscopy in the relatively homogeneous purple samples that were tested for this report.

Dr Emmanuel Fritsch FGA
(emmanuel.fritsch@cncrs-imn.fr)

University of Nantes and CNRS Nantes, France

Blanca Mocquet
Nantes, France

Bear Williams FGA and Cara Williams FGA
Stone Group Laboratories
Jefferson City, Missouri, USA

Starla Turner FGA
Lang Antiques, San Francisco, California, USA

References

- Braithwaite, R.S.W., Flowers, W.T., Haszeldine, R.N. & Russell, M. 1973. The cause of the colour of Blue John and other purple fluorites. *Mineralogical Magazine*, **39**(304), 401–411, <http://doi.org/10.1180/minmag.1973.039.304.03>.
- Fritsch, E., Rondeau, B., Hainschwang, T. & Karampelas, S. 2012. Raman spectroscopy applied to gemmology. In: Dubessy, J., Caumon, M.-C. & Rull, F. (eds) *Raman Spectroscopy Applied to Earth Sciences and Cultural Heritage*. Mineralogical Society of Great Britain and Ireland, Twickenham, 455–489, <http://doi.org/10.1180/EMU-notes.12.13>.
- Fritsch, E., Megaw, P.K.M., Spano, T.L., Chauviré, B., Rondeau, B., Gray, M., Hainschwang, T. & Renfro, N. 2015. Green-luminescing hyalite opal from Zacatecas, Mexico. *Journal of Gemmology*, **34**(6), 490–508, <http://doi.org/10.15506/JoG.2015.34.6.490>.
- Gaillou, E., Fritsch, E. & Massuyeau, F. 2012. Luminescence of gem opals: A review of intrinsic and extrinsic emission. *Australian Gemmologist*, **24**(8), 200–201.
- Ostrooumov, M., Fritsch, E., Lasnier, B. & Lefrant, S. 1999. Spectres Raman des opales: Aspect diagnostique et aide à la classification. *European Journal of Mineralogy*, **11**(5), 899–908, <http://doi.org/10.1127/ejm/11/5/0899>.
- Renfro, N. 2012. Gem News International: New production of purple common opal from Mexico. *Gems & Gemology*, **48**(1), 56–57.
- Serras-Herman, H. 2012. Exotic common opals. *Rock & Gem*, **42**(10), 26–30.

Garnets from Eastern Democratic Republic of the Congo

While on a June 2016 buying trip in Rwanda, rough stone dealer Farooq Hashmi (Intimate Gems, Glen Cove, New York, USA) encountered some new garnets that reportedly came from Caminola, which is located in eastern Democratic Republic of the Congo (DRC) at the northern end of Lake Tanganyika near the border with Burundi. He purchased approximately 1 kg of rough material, which consisted mostly of small waterworn pebbles that weighed up to approximately 0.5 g each. The garnets ranged from yellowish orange to dark red to pinkish purple (Figure 10).

Four round brilliants were faceted for this report: three were cut by Todd Wacks (Tucson Todd's Gems,



Figure 10: The garnets from eastern DRC show a variety of colours. The largest samples shown here weigh approximately 0.5 g. Photo by Farooq Hashmi.

Tucson, Arizona, USA) that weighed 0.85, 1.10 and 2.14 ct, and one was faceted by Mary van der Aa (Mary van der Aa, Port Huron, Michigan, USA) that was 3.48 ct (Figure 11). The physical and chemical properties of the samples are summarised in Table I. In general, the most prominent internal features were rounded colourless crystals (Figure 12), which were surrounded by tension fractures in one of the samples. In addition, cross-hatched anomalous double refraction (ADR) was commonly seen, and one of the samples also displayed angular graining patterns (Figure 13).

The chemical composition of the garnets was

obtained by authors AUF and WBS, who performed standard-based scanning electron microscopy–energy-dispersive spectroscopy (SEM-EDS) using a JEOL JSM-6400 instrument with the Iridium Ultra software package by IXRF Systems Inc. The data showed widely variable spessartine, almandine, pyrope and grossular components (again, see Table I), as well as traces of V and Cr. The 2.14 ct garnet had a much higher pyrope content than the other samples and also showed different internal features (i.e. parallel needles rather than rounded colourless crystals and no ADR), making it distinctive from the rest of the garnets.

Table I: Physical and chemical (by SEM-EDS) properties of four garnets from eastern DRC.

Property	3.48 ct	2.14 ct	1.10 ct	0.85 ct
Colour	Red	Dark red	Orangey red	Yellowish orange
RI	1.790	1.780	1.801	>1.81
SG	4.12	4.03	4.14	4.21
Internal features	Colourless crystals, cross-hatched ADR	Parallel-orientated short needles in one direction (not birefringent), fine particles	Colourless crystals surrounded by tension fractures, few birefringent short needles, cross-hatched ADR	Clouds of white particles, irregular-shaped dark planar film, prominent cross-hatched ADR with angular graining
Oxides (wt.%)				
SiO ₂	37.39	38.93	37.11	37.12
TiO ₂	0.10	0.09	0.36	0.07
Al ₂ O ₃	20.99	21.71	21.11	20.94
FeO	13.82	21.08	4.11	17.93
MnO	21.61	6.61	32.96	20.35
MgO	2.10	7.53	1.63	1.83
CaO	3.97	4.02	2.70	1.73
Total	99.99	99.98	99.99	99.97
Ions per 12 oxygens				
Si	3.006	3.012	2.994	3.006
Al	1.988	1.979	2.007	1.998
Ti	0.006	0.005	0.022	0.004
Mg	0.252	0.868	0.196	0.221
Fe	0.929	1.364	0.277	1.215
Mn	1.471	0.433	2.252	1.395
Ca	0.341	0.333	0.233	0.150
Mol.% end-members				
Spessartine	49.1	14.4	75.2	46.6
Pyrope	8.4	29.0	6.5	7.4
Almandine	31.0	45.5	9.3	40.5
Grossular	11.0	10.1	7.8	5.0
Others	0.5	1.0	1.2	0.5



Figure 11: The DRC garnets studied for this report range from red to yellowish orange and weigh 1.10, 2.14, 3.48 and 0.85 ct (from left to right). Photo by Robison McMurtry, © GIA.

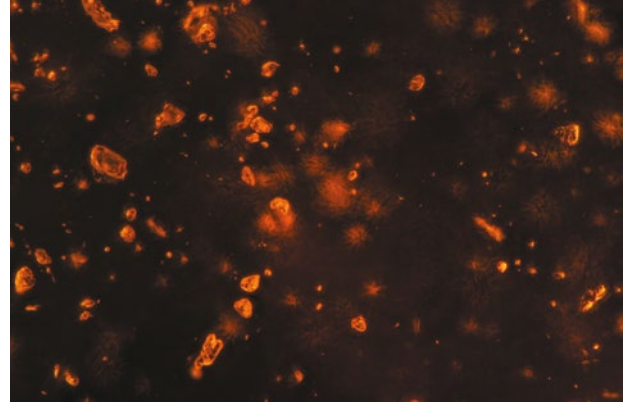


Figure 12: Numerous rounded, colourless crystals form inclusions in the 3.48 ct garnet. Photomicrograph by N. D. Renfro, © GIA; image width 3.20 mm.

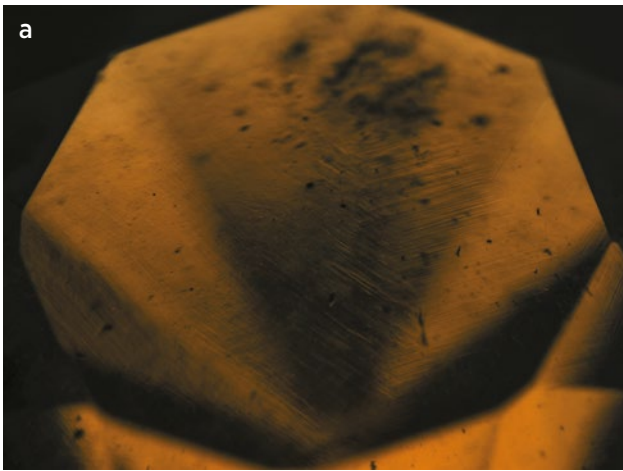


Figure 13: Microscopic examination of the 0.85 ct garnet reveals (a) angular graining patterns in shadowed transmitted light and (b) anomalous double refraction in cross-polarised light. Photomicrographs by N. D. Renfro, © GIA; image widths 3.57 mm.

The rough parcel obtained by Hashmi also contained three dark-coloured stones that appeared different from the rest of the garnets. These were identified by SEM-EDS as two pieces of dark brownish green dravite–uvite tourmaline and a black to dark purple spinel. It is not clear if this mineral assemblage together with the garnets of varying composition resulted from mixing different parcels or if the stones were derived from the

weathering of a variety of geological environments that formed this alluvial deposit in eastern DRC.

Brendan M. Laurs FGA and Nathan D. Renfro FGA

*Alexander U. Falster and
Dr William ‘Skip’ B. Simmons
Maine Mineral & Gem Museum
Bethel, Maine, USA*

Obsidian from Slovakia

Obsidian is a natural glass of volcanic origin. It was often used by prehistoric man to make tools because it is easily knapped. Several obsidian occurrences are known in Europe, and most are in the eastern Mediterranean. In the Tokaj Mountains of Slovakia and Hungary, obsidian is associated with Late Tertiary volcanic activity. The stones appear quite dark, in mostly blackish to greyish

tints, although in some cases deep greenish or brownish hues are found. The obsidian is most abundant between the villages of Viničky and Veľká Bara in the Košice region of eastern Slovakia (Illášová & Turnovec 2003). Tribes initially settled in this area as early as the Paleolithic, and archaeological aspects of obsidian in the Tokaj Mountains have been covered in various articles (e.g. Soják & Wawrzczak 2017).

In present-day Slovakia, prospecting for gem deposits



Figure 14: These faceted obsidians (0.40–3.20 ct) are from the Tokaj Mountains in the Košice region of eastern Slovakia. Photo by J. Štubňa.

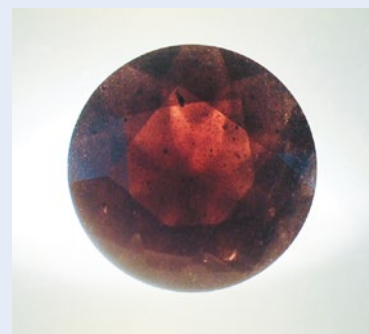


Figure 15: The transparency of this relatively large Slovakian obsidian (24.06 ct or 20.42 × 20.45 × 13.81 mm) is shown here in transmitted light. Photo by J. Štubňa.

has resulted in the discovery of various siliceous materials, including obsidian, which were not previously identified for gem use (Illášová & Spišiak 2010). In recent years, a traditional obsidian craft industry has produced small ornamental hangings and various objects such as arrowheads, hair and clothing accessories, and jewellery such as necklaces, pendants and earrings. The gems are fashioned into cabochons as well as faceted stones.

For this study, we examined 100 rough and 10 faceted samples of obsidian from the Tokaj Mountains. The rough pieces varied from 1 to 20 cm in maximum dimension and the cut stones weighed 0.40–24.06 ct (e.g. Figures 14 and 15). They ranged from black to dark grey; thin areas along their edges appeared grey to pale grey or brownish. Their hydrostatic SG ranged from 2.33 to 2.36 and their RIs were around 1.489–1.491. Microscopic examination of the cut stones revealed micro-phenocrysts of plagioclase, biotite, ilmenite and, rarely, orthopyroxene

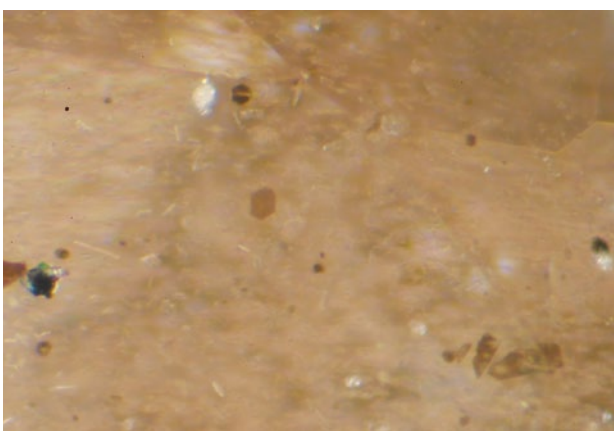


Figure 16: A closer look at the 0.40 ct Slovakian obsidian in Figure 14 shows minute crystallites of plagioclase (white), biotite (brown), ilmenite (black) and pyroxene (colourless) that are locally flow-aligned. Photomicrograph by J. Štubňa; magnified 30×.

(Figure 16). The inclusions were identified by optical microscopy and by comparing them to photomicrographs in Bačo *et al.* (2017) and in Gübelin and Koivula (2008). The samples commonly showed a banded texture with alternating dark and light streaks caused by flow-oriented minute crystals. This internal fabric is the probable cause of sculpturing into fluted shapes that occurs when the glass is exposed to weathering (Bačo *et al.* 2017).

Obsidian from Slovakia has been used for millennia and could experience a renaissance in present times as a non-traditional gemstone.

Dr Ján Štubňa (janstubna@gmail.com)
and Dr Eudmila Illášová
Gemmological Institute, Constantine the Philosopher
University, Nitra, Slovakia

Dr Jana Fridrichová and Dr Peter Bačík
Comenius University, Bratislava, Slovakia

References

- Bačo, P., Kaminská, L., Lexa, J., Pécskay, Z., Bačová, Z. & Konečný, V. 2017. Occurrences of Neogene volcanic glass in the eastern Slovakia – Raw material source for the stone industry. *Anthropologie*, **55**(1–2), 207–230.
- Gübelin, E.J. & Koivula, J.I. 2008. *Photoatlas of Inclusions in Gemstones*, Vol. 3. Opinio Publishers, Basel, Switzerland, 672 pp.
- Illášová, E. & Spišiak, J. 2010. Slovak gemstones. *Geologica Balcanica*, **39**(1–2), 164–165.
- Illášová, E. & Turnovec, I. 2003. Obsidians of eastern Slovakia and their utilization. *Bulletin Mineralogie Petrologie*, **11**, 150–152.
- Soják, M. & Wawrzczak, M. 2017. The study of stone materials from the collection of the Mining Museum in Rožňava. *Študijné Zvesti Archeologického Ústavu SAV*, **62**, 7–36.

Spessartine Crystals from Oyo State, Nigeria

Nigeria is a well-known source of gem-quality spessartine (e.g. Lind & Henn 2000), which has mostly been produced from secondary deposits. In 2017, a small amount of well-formed spessartine crystals was found at a granitic pegmatite in the Oyo State of western Nigeria. According to rough stone dealer Farooq Hashmi, most of the production consisted of loose single crystals and clusters, although a few matrix specimens were available. Prized by mineral collectors for their deep orange colour, high lustre and euhedral crystal form, the material soon became scarce in the market.

During the February 2019 Tucson gem shows, this author was surprised to see a full layout of these spessartine crystals that was assembled together for mounting in jewellery. Displayed at the booth of Valerio Zancanella (Cavalese, Italy), it consisted of 38 pieces for mounting in a necklace, a matched pair of crystals for earrings and a larger crystal cluster for a pendant or brooch (Figure 17). A parure featuring these attractive garnets would clearly be unique.

[*Editor's note:* Reports on additional items seen at the 2019 Tucson shows will appear in the Gem Notes section of upcoming issues of *The Journal*.]

Brendan M. Laurs FGA

Reference

Lind, T. & Henn, U. 2000. A new find of spessartine garnets in Nigeria. *Journal of Gemmology*, **27**(3), 129–132, <http://doi.org/10.15506/jog.2000.27.3.129>.



Figure 17: This spessartine layout, displayed at the 2019 Tucson gem shows, features well-formed crystals from Oyo, Nigeria. The entire set weighs ~31 g and the largest crystal cluster is ~2 cm tall. Photo by B. M. Laurs.

A Faceted Sulphur

Sulphur is a commonly occurring native element, but it is rarely transparent enough to facet. It is nearly always bright yellow, sometimes tending towards green or orange. Sulphur ranges from only 1½ to 2½ on the Mohs scale, roughly equivalent to the hardness of a fingernail. It is also quite frail, so even a slight physical shock can break it. The softness, combined with its fragility and extreme heat sensitivity (if placed in the hand it could shatter due to the thermal shock), all conspire to make it very difficult to cut. Recently this author concave-faceted a large (29.25 ct; Figure 18) sulphur gemstone from Vodinskoye, Samara Oblast, Russia, and this report describes some of the challenges with cutting this delicate material.

The first step involved attaching the rough stone to a dop stick for insertion into the faceting machine. Selecting

the appropriate glue was not easy because it must hold fast during cutting and then be released from the stone after faceting is complete. In addition, the substance used to dissolve the glue must not also attack the sulphur. In this case, five-minute epoxy was used. The epoxy can be released by soaking in vinegar for two weeks, but since vinegar is corrosive to the metal normally used for dops it was necessary to custom-make a glass dop stick.

Preforming was done on a special lap created by gluing a piece of sandpaper to a worn-out lap. Then, grinding was done on a wax lap that was fabricated from a dimensionally stable wood material with molten casting wax poured over it and machined flat. The wax was coated with 1,200 grit diamond paste for fine grinding, and 3,000 grit diamond paste was used on a separate wax lap for pre-polishing. Polishing was done with aluminium oxide on yet another wax lap.

In concave cutting, most (if not all) of the stone is initially cut with flat facets, and then selected facets are ground into concave shapes. Cutting this stone was no different. However, the curved facets posed a considerable challenge because the intersection of two curved surfaces produces a sharp ridge. For a delicate material like sulphur, such edges would be very fragile and could lead to cracking and chipping. Special tooling and techniques had to be developed through trial and error, and the facet pattern itself had to be designed so that these intersections were minimised. This was done by placing flat facets between each of the eight curved pavilion facets.

The sequence of cutting the facets was also out of the ordinary. Most stones are cut pavilion first and then crown second. However, this requires attaching the dop to the pointed culet in order to cut the crown. This is problematic for sulphur, since it is likely that the fragile culet would be damaged when releasing the stone from the glue. Therefore, cutting the crown first meant that the dop could then be attached to the flat table facet, a far less risky approach. Since there was still no guarantee that the table facet would be unharmed when releasing the epoxy, the crown was step cut so that any damage could be removed by hand-holding the stone during grinding and polishing without affecting facet meets and symmetry.

Several additional considerations for faceting this sulphur were taken into account. To protect it from exposure to heat, a small piece of chamois leather was used to handle the stone and oil was used as a lubricant to help dissipate heat while grinding and polishing. The oil was also used to remove swarf (the powdered sulphur

created from the grinding process). To minimise exposing the stone to shear forces (which can create sub-surface damage or cracking) as it was rubbed across the lap, only slow rotation speeds were used (i.e. during grinding) or the lap was held stationary (i.e. during polishing). Additional considerations were involved with the complex interactions between the sulphur, grit, lubricant and lap, as well as the crystallographic orientation of the stone.

Faceted sulphur is quite rare, but the result of proper cutting is a beautiful and unusual stone that is prized by collectors.

Scott Sucher (scott@museumdiamonds.com)
The Stonecutter, Tijeras, New Mexico, USA

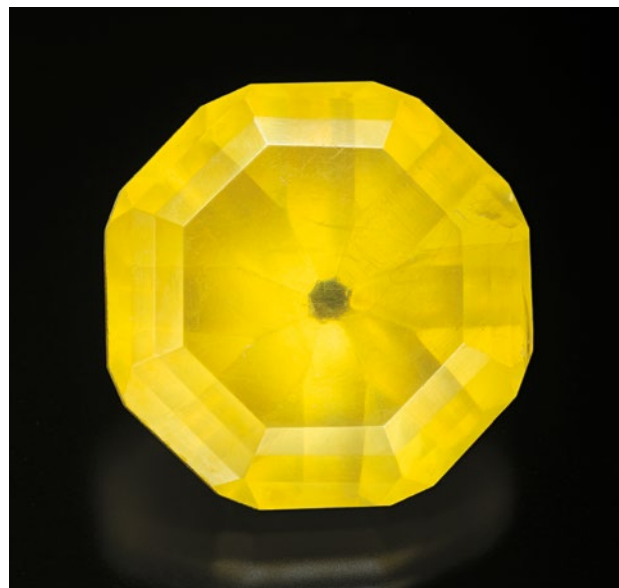


Figure 18: Special techniques were developed by the author to facet this 29.25 ct concave-cut sulphur. Photo by Jeff Scovil.

DIAMONDS

Chidliak: A Sustainable Future Diamond Mine in Canada?

In July 2018, news broke that De Beers Canada purchased the Chidliak diamond resource from Peregrine Diamonds Ltd (Jamasmie 2018). The purchase closed in September 2018 for a cost of CAD107 million. Both BHP Billiton and De Beers had walked away from previous joint ventures in 2012 and 2013, respectively. This time, De Beers jumped back into the resource and bought it outright. This may be because there are no new tier-one diamond mine assets coming online in the next 10 years, and as we look to the future of slowly declining inventories with slightly

increasing demand for diamonds (Linde *et al.* 2018), any new viable mine would make sense. History shows us, however, that for Chidliak it has always been the cost-to-benefit analysis that had suitors backing off. Even though the diamonds are of high quality, the costs associated with mining the diamonds were deemed too high.

Chidliak is located on Baffin Island, about 120 km from Iqaluit, the capital of Nunavut, Canada (Figure 19). The asset hosts at least 74 kimberlites, eight of which are potentially economic, and has an inferred resource of 22 million carats (Jamasmie 2018). Since the area is very remote, access to transportation and logistics support for any mining operation is expensive. The average

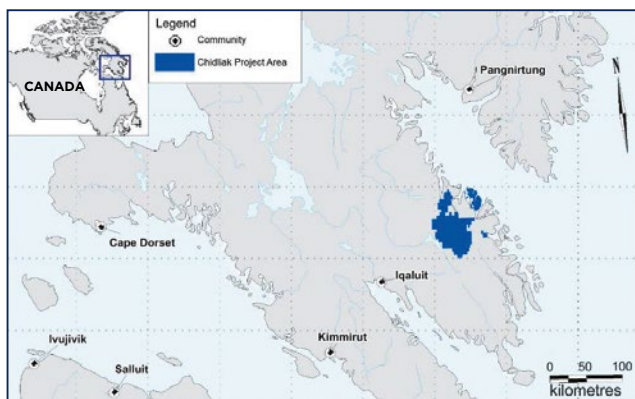


Figure 19: The Chidliak diamond property (shown in blue) is located in a remote part of Baffin Island. Courtesy of Peregrine Diamonds Ltd.

temperature in February is -27°C and there is just $4\frac{1}{2}$ hours of daylight in December (<https://en.climate-data.org/north-america/canada/nunavut/iqaluit-1251>). Chidliak does not have a winter ice road for bringing in supplies and diesel fuel like the diamond mines at Ekati, Gahcho Kué and Diavik in Canada's Northwest Territories. Therefore, everything must be taken in or out either by plane or, in the summer months, by boat to Iqalaut.

In December 2018, during the 6th annual meeting of the Energy and Mines World Congress in Toronto, the CEO of De Beers Canada, Kim Truter, announced their goal to make the mine 100% 'renewable'. To accomplish this, they will look at 'radical solutions' like dramatically reducing the footprint of the mine, including eliminating the need for haul trucks and not building a road from Iqaluit (which would be a major contributor to overall carbon emissions of the project), and making the site fly-in only by helicopter (Rolfe 2018). There is actually a precedent for sustainability at a Canadian diamond mine: Rio Tinto built a windfarm at Diavik in 2012, which resulted in a diesel offset of 3.8 million litres in its first year. The windfarm has since achieved peak power generation of 52% of the mine's energy needs. Before the windfarm, Diavik relied on diesel for all its energy usage. The windfarm reduces greenhouse gas emissions by approximately 12,000 tonnes (or 6% of emissions), and by diversifying the energy mix, Diavik offsets some of the risks associated with reliance on diesel (National Resources Canada 2018). Elsewhere in Canada, De Beers' Victor mine in Ontario (which is closing this year) draws a mix of nuclear and hydroelectric power from Nunavut's grid, while its joint-venture Gahcho Kué property in the Northwest Territories relies on diesel.

If a diamond mine at Chidliak proves economic, it will be a perfect opportunity for De Beers to put into action their new FutureSmart Mining approach being developed

by Anglo American, De Beers' parent company. This initiative aims to adopt new processes and technology to enable precision mining with minimal energy, water and capital intensity with an aim of carbon neutrality (see <http://tinyurl.com/y7k7o65s>).

De Beers' approach to Chidliak is admirable, and would make a fantastic case study, but we will have to wait and see the outcome. The motivation for change is more than just doing the 'right thing' and the potential profits from high-quality diamonds (e.g. Figure 20). New Canadian government regulations to fight carbon emissions, and increasing investor and consumer demands for more sustainably mined goods, especially in the diamond market, have motivated many major companies to look more closely at their mining processes.

*Jon C. Phillips (jonp@coronacompany.com)
Corona Jewellery Co., Toronto,
Ontario, Canada*

References

- Jamasmie, C. 2018. De Beers buys Canada's Peregrine Diamonds for \$81 million. *Mining.com*, 19 July, www.mining.com/de-beers-buys-canadas-peregrine-diamonds-81-million, accessed 21 January 2019.
- Linde, O., Geyle, O. & Epstein, A. 2018. *The Global Diamond Industry 2018*. Bain & Co., Boston, Massachusetts, USA, 43 pp, www.bain.com/insights/global-diamond-industry-report-2018.
- National Resources Canada 2018. Diavik Diamond Mine – Northwest Territories. www.nrcan.gc.ca/mining-materials/publications/aboriginal/bulletin/8816, accessed 21 January 2019.
- Rolfe, K. 2018. Chidliak could be completely powered by renewables, De Beers Canada CEO says. *CIM Magazine*, 11 December, <http://magazine.cim.org/en/news/2018/chidliak-could-be-completely-powered-by-renewables>, accessed 21 January 2019.



Figure 20: This selection of colourless and yellow diamonds is from Chidliak's CH-6 kimberlite. The largest stone weighs 3.54 ct. Photo courtesy of De Beers Canada.

SYNTHETICS AND SIMULANTS



Figure 21: Although represented as being natural stones from a new discovery in Turkey, these samples were identified as synthetic periclase. Photo by Alex Mercado, AGL.

Identifying Synthetic Periclase

In November 2018, American Gemmological Laboratories was asked to identify three rough gems that were bicolored orange-brown (sample 1), yellowish green (sample 2) and bicolored colourless-white (sample 3), as seen in Figure 21. They were represented by the supplier as natural stones from a new discovery in Turkey. We collected standard gemmological properties and also performed Fourier-transform infrared (FTIR), EDXRF and Raman spectroscopy.

The samples showed no birefringence (regardless of their colour) or anomalous double refraction, and were inert to long- and short-wave UV radiation. An RI of 1.735 and hydrostatic SG of 3.58 were measured for all three samples. EDXRF data showed a high Mg concentration, with small amounts of Cr, Ca, Fe and Si. The optical properties and chemical composition pointed us

toward the mineral periclase (MgO), and are similar to the characteristics provided for synthetic periclase by Kitawaki (2004).

Periclase crystals occur naturally in small sizes, and no facetable periclase has been reported so far. However, starting in 1969, synthetic periclase was sold for jewellery purposes as Lavernite, and various techniques have been employed to produce transparent MgO. Abraham *et al.* (1971) refer to a carbon arc-fusion technique for growing high-purity, large single-crystal MgO free of microbubbles. Brown (1993) reported that large facetable crystals of synthetic periclase were produced as a by-product of the fabrication of magnesia (MgO) from magnesite (MgCO₃). The procedure uses nodules of magnesite that are calcined to magnesia which is then electro-fused to form ingots of cryptocrystalline synthetic periclase. Bowles *et al.* (2011) reported that synthetic periclase can be produced from various minerals, including brucite,

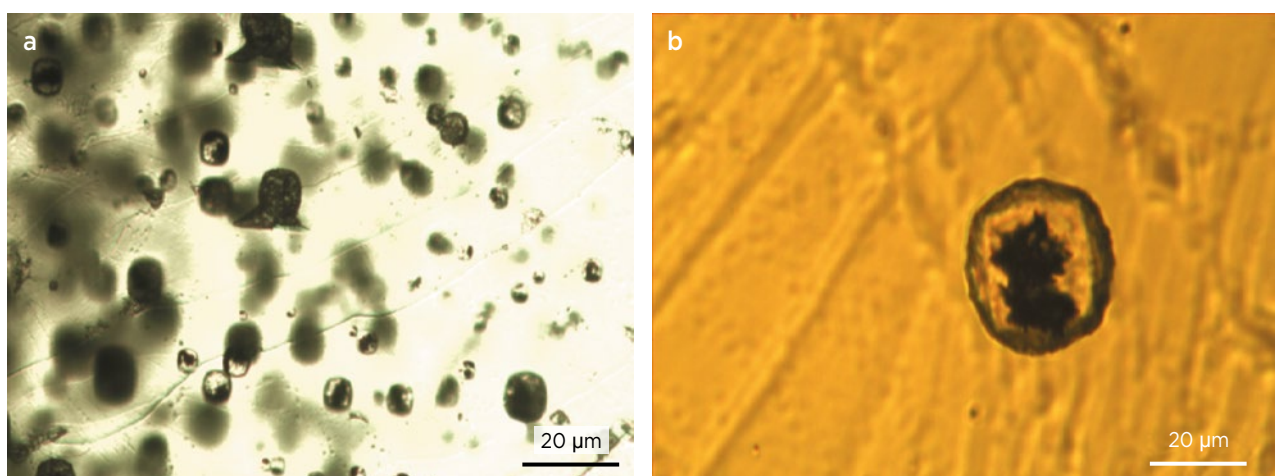


Figure 22: Rounded inclusions in the synthetic periclase consisted of (a) concentrations of many individuals, as seen here in sample 3, and (b) isolated features, as shown here in sample 1. Photomicrographs by R. Zellagui in transmitted light.

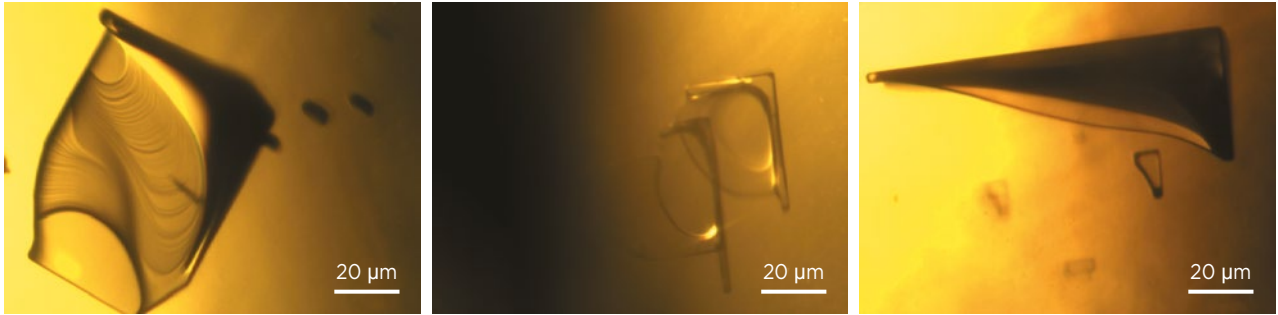


Figure 23: Plate-like negative crystals displaying squarish shapes showed various forms in the synthetic periclase, as seen here in sample 1. Photomicrographs by R. Zellagui in transmitted light.

ankerite, leuchtenbergite, talc, antigorite, vermiculite, forsterite and spinel; white, yellow and brown colours can be produced by the addition of Fe, while green is due to the addition of Cr and Fe to the system.

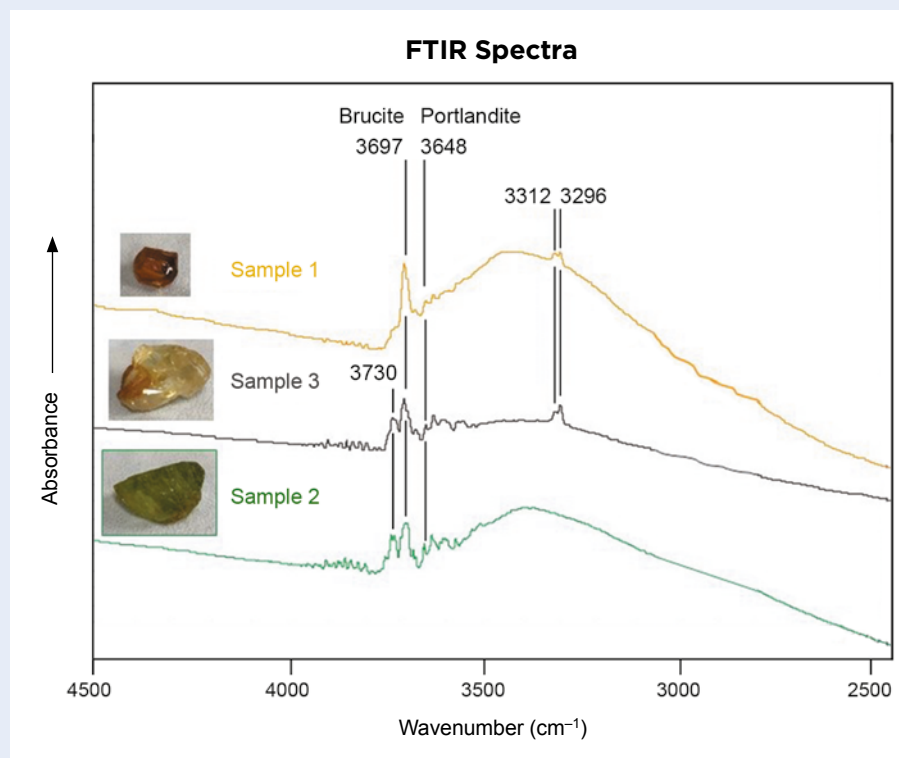
Microscopic observations showed rounded inclusions (Figure 22), as well as some plate-like negative crystals with square shapes (Figure 23), as previously described in synthetic periclase (Brown 1993; DeMaggio & McClure 1997; Peretti *et al.* 2018).

FTIR spectroscopy of samples 1 and 3 showed two narrow bands at 3312 and 3296 cm^{-1} (Figure 24) associated with V_{OH} centres in the MgO structure of a hydrogen-doped synthetic periclase (Joachim *et al.* 2012). Sample 2, however, did not display these bands, indicating it was anhydrous. All samples displayed bands at 3697 and

3648 cm^{-1} corresponding, respectively, to brucite and portlandite OH vibrational modes; these are known as alteration products of periclase, and are indicative of water diffusion that takes place when the material is heated (Joachim *et al.* 2012). A strong band was observed at 3730 cm^{-1} in samples 2 and 3, but its cause has not yet been identified. Other minor unidentified bands were observed at 3672, 3625, 3603, 3595, 3562 and 3548 cm^{-1} .

Raman analysis of the synthetic periclase did not show any relevant bands, which concurs with the fact that MgO has no first-order Raman scattering (Farmer 1974). Raman microspectroscopy of the rounded inclusions revealed the presence of merwinite ($\text{Ca}_3\text{Mg}[\text{SiO}_4]_2$) in sample 3 and monticellite (CaMgSiO_4) in sample 2. By comparison, Raman analysis of synthetic periclase inclusions

Figure 24: FTIR spectra of the synthetic periclase samples reveal bands associated with brucite and portlandite, along with other unidentified features. Samples 1 and 3 display narrow bands at 3312 and 3296 cm^{-1} that are characteristic of OH centres in hydrogen-doped synthetic periclase. The absence of these features from sample 2 suggests it is anhydrous.



by Peretti *et al.* (2018) identified a dicalcium silicate cement hardener as well as forsterite and monticellite. Indeed, depending on the starting material, manufacturing technique and temperature used for calcination and fusing of magnesite, a variety of impurities can be produced, including forsterite, monticellite, merwinite, and dicalcium and tricalcium silicates (Perepelitsyn & Perepelitsyna 1971; Ebrahimi-Nasrabadi *et al.* 2011).

The combination of gemmological properties and advanced testing confirms the identity of this material as synthetic periclase. It has been reported that faceted synthetic periclase tends to alter in contact with the atmosphere and produce a thin layer of brucite on the surface, which diminishes its usefulness as a gem (Brown 1993).

Riadh Zellagui (riadh@aglgemlab.com)
American Gemological Laboratories
New York, New York, USA

References

- Abraham, M.M., Butler, C.T. & Chen, Y. 1971. Growth of high-purity and doped alkaline earth oxides: I. MgO and CaO. *Journal of Chemical Physics*, **55**(8), 3752–3756, <http://doi.org/10.1063/1.1676658>.
- Bowles, J.F.W., Howie, R.A., Vaughan, D.J. & Zussman, J. 2011. *Rock-Forming Minerals—Non-Silicates: Oxides, Hydroxides and Sulphides*, Vol. 5A, 2nd edn. The Geological Society, London, 920 pp.
- Brown, G. 1993. Australian synthetic periclase. *Australian Gemmologist*, **18**(8), 265–269.
- DeMaggio, M. & McClure, S.F. 1997. Lab Notes: Synthetic green periclase. *Gems & Gemology*, **33**(3), 215–216.
- Ebrahimi-Nasrabadi, K., Barati, M. & Lalonde, A.E. 2011. Characterization of high purity hydrothermal magnesite deposits for refractory manufacturing. *Industrial Ceramics*, **31**(3), 1–8.
- Farmer, V.C. (ed) 1974. *The Infrared Spectra of Minerals*. Mineralogical Society of Great Britain and Ireland, London, 539 pp, <http://doi.org/10.1180/mono-4>.
- Joachim, B., Wohlers, A., Norberg, N., Gardés, E., Petrishcheva, E. & Abart, R. 2012. Diffusion and solubility of hydrogen and water in periclase. *Physics and Chemistry of Minerals*, **40**(1), 19–27, <http://doi.org/10.1007/s00269-012-0542-8>.
- Kitawaki, H. 2004. Synthetic periclase. Gemmological Association of All Japan, Tokyo, 28 July.
- Perepelitsyn, V.A. & Perepelitsyna, S.M. 1971. Composition and formation of fusions of metallurgical magnesite powder. *Refractories*, **12**(5–6), 325–331, <http://doi.org/10.1007/bf01282043>.
- Peretti, A., Bieri, W., Cleveland, E., Alessandri, M., Kradolfer, S., Günther, D., Meier, M., Jaramillo, D. & Musa, M. 2018. New types of synthetic periclase identified by C₂S inclusions - dicalcium silicate cement hardener. *Contributions to Gemology*, Special Alert Issue, 19 December, 2–31.

MISCELLANEOUS

Myanmar Gems Enterprise 2018 Rough Stone Sale and Opening of Mandalay Yatanar Mall

On 12–17 November 2018, the Myanmar Gems Emporium held its sixth sale (in kyats) for local merchants of gem and jade rough material in Nay Pyi Taw, Myanmar. There were 1,493 merchants who attended this emporium (1,440 for jade and 53 for gems). A total of 96 gem lots and 3,339 jade lots were offered for sale. The gem lots included 29 for ruby, 18 for sapphire and 15 for peridot, as well as others for topaz, quartz, goshenite and assorted gems. A total of 50 gem lots sold for approximately 795 million kyats and 3,185 jade lots sold for about 48,300 million kyats. The highest price paid for jade was lot no. 305, with 555 pieces weighing a total of 3,470 kg fetching 320,007,777 kyats. Overall, sales were down compared to most previous rough stone emporiums (Table II).



Figure 25: The Mandalay Yatanar Mall hosts numerous gem and jewellery dealers with storefronts, as well as those who are involved with online trading. Photo courtesy of T. Hlaing.

In Mandalay, the Yatanar Mall opened in January 2017. 'Yatanar' means 'gems and jewellery', and the sales area is located on the second floor of a five-storey building (e.g. Figure 25). Of the 385 available rooms, about 200 were reserved for Mogok merchants, but only 120 were occupied as of December 2018. A wide variety

of rough and polished stones from Myanmar are offered at the mall.

Dr U Tin Hlaing (p.tinhlaing@gmail.com)
Dept. of Geology (retired)
Panglong University, Myanmar

Table II: Rough gem and jade sales at various Myanmar Gems Emporiums.

No.	Date	Type	Lots Shown	Lots Sold	Amount (million kyats)
1	December 2012	Jade	1,520	1,342	22,217.74
2	January 2014	Gems and Jade	2,996	2,362	77,839.63
3	October 2014	Gems and Jade	7,142	6,110	128,763.74
4	December 2015	Gems and Jade	6,978	5,606	80,841.85
5	March 2017	Gems and Jade	4,649	4,267	61,915.21
6	November 2018	Gems and Jade	3,435	3,235	49,093.39

Educational Aspects of Myanmar Gem Fairs Held in January 2018

The 2nd Yangon International Gems & Jewelry Fair took place at the Lotte Hotel in Yangon 9–13 January 2019, and was organised by the Gems and Jewellery Entrepreneurs Association in Yangon. In addition to a show catalogue, attendees received a book titled *Alphabetical Summary of Myanmar Gem Species* (Figure 26), which contains a list of gem varieties available from Myanmar (with their basic gemmological properties), as well as photos of the fair's organising committee and foreign delegation, information on Nawarat rings and birthstones, and the story of Albert Ramsay (an Englishman who pioneered the cutting of Burmese star rubies). A Myanmar Gems Forum included talks from Dr Kyaw Thu titled 'Gem Mining and Sustainability in Myanmar' and Daw Mai Mu Mu Win on the 'Role of Ethics in Gem Trading World', as well as two panel discussions moderated by Dr Yin Yin Nwe: (1) 'Sustainable Sourcing Gems with Full Awareness of Environmental and Social Impacts'

featuring Dr Ye Myint Swe, Min Thu, Ye Minn Htun and Maung Maung, and (2) 'Ethical Value Chain from Mine to Market' with Hla Aung, Hpone-Phyo Kan-Nyunt, Aye Myo Naing and Aung Kyaw Zin.

The 1st Mandalay Yatanar Mall International Gems & Jewellery Fair took place 15–19 January 2019 at the Mandalay Yatanar Mall. The show was held under the guidance of the Myanmar Gems Enterprise with the support of the Myanmar Gems & Jewellery Entrepreneurs Association in collaboration with the Gems & Jewellery Entrepreneurs of Mandalay Yatanar Mall. Attendees received a fair booklet containing a message from the Minister, a list of committee members and vendors, insights on Buddhist culture and information on various aspects of jade, gold, amber, and gems and jewellery from Myanmar. The show included a lecture programme that featured Dr Thet Tin Nyunt, Aung San Win, Maung Maung, Hpone-Phyo Kan-Nyunt, Tay Thye Sun, Richard Li, Kyaw Win and Tin Kyaw Than.

The total sales of gems and jewellery at the two January 2019 Myanmar gem fairs are shown in Table III.

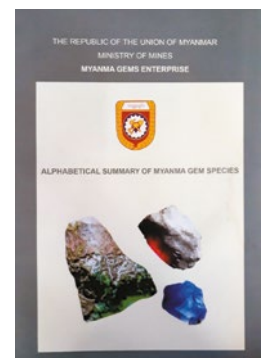


Figure 26: Attendees of the 2nd Yangon International Gems & Jewelry Fair received an informative book published by Myanmar Gems Enterprise. Photo courtesy of T. Hlaing.

Table III: Gem and jewellery sales at January 2019 Myanmar gem fairs.*

Show location	Amount sold (in currencies received)		Total (GBP)
	Kyats	USD	
Yangon	15,627,690	4,863	11,847
Mandalay	665,480,150	20	342,477
Total	681,107,840	4,883	354,324

* Source: Myanmar Gems Enterprise.

Dr U Tin Hlaing

Spinel from Mogok, Myanmar—A Detailed Inclusion Study by Raman Microspectroscopy and Scanning Electron Microscopy

Myint Myat Phyo, Eva Bieler, Leander Franz, Walter Balmer and Michael S. Krzemnicki

ABSTRACT: Mineral inclusions within 100 gem-quality spinels from both primary marble and secondary alluvial mining sites within Myanmar's Mogok Valley were analysed using Raman microspectroscopy and scanning electron microscopy (including backscattered-electron imaging and energy-dispersive spectroscopy). The samples ranged from pink to red, orangey pink to orangey red, and grey to purplish grey. We identified a number of inclusions that are reported here for the first time in Mogok spinel: amphibole (presumably pargasite), anatase, baddeleyite, boehmite, brucite, chlorite, clinohumite, clinopyroxene, diaspore, geikielite, goethite, halite, marcasite, molybdenite, periclase and pyrrhotite. We also found several minerals that were previously known as inclusions in Mogok spinel, including anhydrite, apatite, carbonates (calcite, dolomite and magnesite), chondrodite, elemental sulphur, graphite, iron oxides or iron hydroxides, phlogopite and zircon. We further differentiated the occurrence of inclusions in spinel from different mining sites in Mogok to assess whether these mineral assemblages can enhance our understanding of the geological origin of these gems and whether the inclusions can help separate Mogok spinels from those of other marble-related deposits worldwide.

The Journal of Gemmology, 36(5), 2019, pp. 418–435, <http://doi.org/10.15506/JoG.2019.36.5.418>

© 2019 Gem-A (The Gemmological Association of Great Britain)

Since ancient times, gem-quality spinel (ideally MgAl_2O_4) has been appreciated for its range of colour and often exceptional clarity, and today spinel is the second most important and popular red gemstone after ruby (Cesbron *et al.* 2002; Pardieu *et al.* 2008). Spinel's significance is well illustrated by the famed 'Balas rubies'—which are actually spinels from historic mines in Badakhshan (i.e. Kuh-i-Lal, in what is today Tajikistan)—that were described and praised by the Persian scholar Al-Biruni (973–1048 AD). Exceptional pinkish red spinels were part of the Moghul

imperial jewels, two of which were later integrated into British royal jewels (the Black Prince's 'Ruby' and the Timur 'Ruby'; see also Pardieu & Hughes 2008; Yavorsky & Hughes 2010; Truong 2017).

Spinel may form by high-grade metamorphism in calc-silicate rocks and marbles (Balmer *et al.* 2017) or in skarns (contact zones between Ca-rocks and magmatic intrusions; Gorghinian *et al.* 2013), and is also found in secondary deposits (Thein 2008). It shows a wide variety of colours, mainly pink to red and purple, orange, violet to blue, green and even black. Although sometimes

showing greyish or brownish hues, it may also display strong colour saturation, especially in the pink to red range. Moreover, the demand for and value of spinel have increased sharply in recent years. Although known from deposits throughout the world (Myanmar, Sri Lanka, Tanzania, Madagascar and Vietnam, to name a few), some of the finest spinels are found in the Mogok area of Myanmar (e.g. Figure 1). Mogok is one of the world's most eminent gem sources, renowned for producing exceptional rubies, sapphires and other popular stones, as well as rarities such as hibonite, jeremejevite, johachidolite, poudretteite and painite (Iyer 1953; Hughes 1997, 2017b; Themelis 2008).

Although the literature contains some information on inclusions in Burmese spinel (see, e.g., Gübelin & Koivula 1986; Hughes 1997; Themelis 2008; Malsy & Klemm 2010; Zhu & Yu 2018), most publications to date describe Burmese spinel in general (Themelis 2008; Peretti *et al.* 2015), or focus on specific gemmological features (Pardieu 2014; Vertriest & Raynaud 2017) or the oxygen isotope composition of these spinels (Giuliani *et al.* 2017). Several publications deal with inclusions in spinel from worldwide localities (Gübelin & Koivula 1986, 2005; Cooper & Ziyin 2014; Hughes 2017a).

In this study, we describe in detail the solid inclusions found in pink to red, orangey pink to orangey red and grey to purplish grey gem-quality spinels collected from various sites (and local gem markets) in the Mogok area. We found systematic variations in the inclusions related

to the different mining sites, suggesting that such inclusion research may be applied to the origin determination of spinels and to separating them from their synthetic flux-grown counterparts (Krzemnicki 2008).

GEOLOGICAL SETTING AND MINING METHODS

Since the 15th century, the Mogok area of Myanmar has been known as a major source of rubies and other gems (Iyer 1953). Often referred to as the 'Mogok Stone Tract' (La Touche 1913; Fermor 1931; Chhibber 1934; Iyer 1953), this gem-rich area is located within the central part of the Mogok Metamorphic Belt. This assemblage is composed of Palaeozoic and Mesozoic high-grade metasediments and intrusive rocks (Searle & Haq 1964; Barley *et al.* 2003; Searle *et al.* 2007; Thu *et al.* 2016; Phyo *et al.* 2017) and forms part of the Mogok-Mandalay-Mergui belt (Figure 2), which extends for more than 2,000 km, north to south, along the western margin of the Shan-Thai (or Sibumasu) terrane, from the Himalayan syntaxis to the Andaman Sea (Bender 1983; Zaw 1990, 2017; Zaw *et al.* 2015). The Mogok Stone Tract is mainly composed of gneiss, marble, calc-silicate rocks and quartzite, which were intruded by various felsic to mafic igneous rocks (Iyer 1953).

Ruby, sapphire, spinel and other gems are mined from primary deposits (calc-silicate rocks and marbles, with spinel only forming in the latter) and from secondary



Figure 1: The spinels in this photo are all from Mogok, Myanmar. The faceted stones range from approximately 7 to 35 ct (not shown to scale). Composite photo by V. Lanzafame, © SSEF.

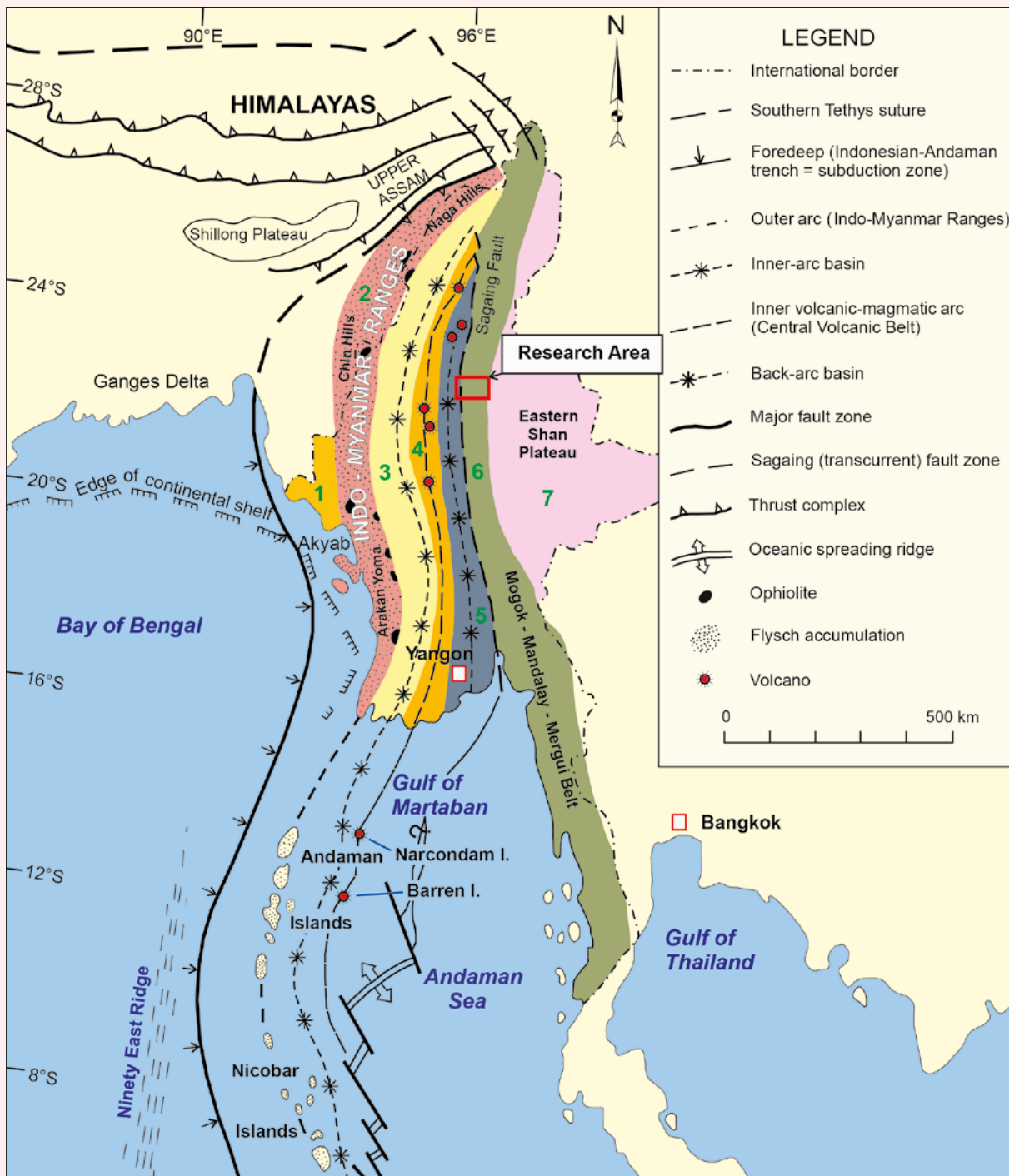


Figure 2: The Mogok research area is indicated on this regional map of Myanmar, which shows the main tectonic domains (numbered 1-7 from west to east) and fault structures (after Bender 1983; Zaw *et al.* 1989, 2015; Zaw 1990). The domains are: (1) Arakan (Rakhine) Coastal Strip, (2) Indo-Myanmar Ranges, (3) Western Inner-Burman Tertiary Basin, (4) Central Volcanic Belt (or Central Volcanic Line), (5) Eastern Inner-Burman Tertiary Basin, (6) Mogok-Mandalay-Mergui Belt and (7) Eastern Shan Highlands.



Figure 3: The main tunnel at the Kyauksaung mine in central Mogok provides an example of spinel extraction from primary (marble) host rocks. Photo © S. Hänsel, 2016.

deposits such as alluvial and eluvial placers, as well as karstic sinkholes and caverns (Thein 2008). To extract the gems from the primary rocks and associated karstic deposits, an extensive network of tunnels (e.g. Figure 3) has been excavated by drilling and blasting. For the secondary deposits, traditional mining methods are used such as *twinlon* (digging shafts in the soil/gravel with a maximum depth of ~30 m), *myawdwin* (hydraulic mining along hillsides; Figure 4) and *ludwin* (mainly used in sinkhole and cavern excavations). In the alluvial plains of the Mogok area, the gem-bearing gravel is usually reached at approximately 6–7 m below the surface (Iyer 1953). Detailed descriptions of the traditional mining methods used in the Mogok area are given in numerous reports (e.g. Gordon 1888; Halford-Watkins 1932a, b, c; Ehrmann 1957; Gübelin 1965; Keller 1983).



Figure 4: Hydraulic mining of gem-bearing gravels at Mansin in north-eastern Mogok demonstrates how spinels are obtained from secondary deposits. Photo © M. M. Phyo, 2016.

MATERIALS AND METHODS

For this study, we collected and analysed 87 pink to red, orangey pink to orangey red and grey to purplish grey gem-quality spinel samples from six mining sites in the Mogok area (Yadanar Kaday Kadar, Bawlongyi, Kyauksin, Kyauksaung, Pyaungpyin and Mansin; see Figure 5) and 13 samples bought in local gem markets. A list of the samples is shown in Table I.

We polished the surface of each spinel to provide a clear view of the interior and then used a standard gemmological microscope (Cambridge Instruments) at $10\times$ – $70\times$ magnification to observe mineral inclusions in the samples. Photomicrographs of the inclusions were taken with a Nikon D7000 digital camera attached to a System Eickhorst GemMaster microscope using $16\times$ – $80\times$ magnification.

Raman microspectroscopy was performed on the inclusions in each sample using one of two different setups: a Renishaw inVia Raman system coupled with a Leica DM2500 M microscope, using an argon-ion laser at 514.5 nm wavelength; and a Bruker Senterra Raman spectrometer coupled with an Olympus microscope, using a solid-state Nd-YAG laser at 532 nm or a direct diode laser at 785 nm. Raman spectra were mostly collected in the range of 1400 – 100 cm^{-1} , except for graphite (1600 – 100 cm^{-1}) and apatite (4000 – 100 cm^{-1} , to detect water peaks). Maximum exposure time per scan was 10 seconds and 10–50 scan accumulations were collected. Remarkably, there was only minor interference with the fluorescence of spinel. However, we were not able to identify very tiny inclusions with Raman

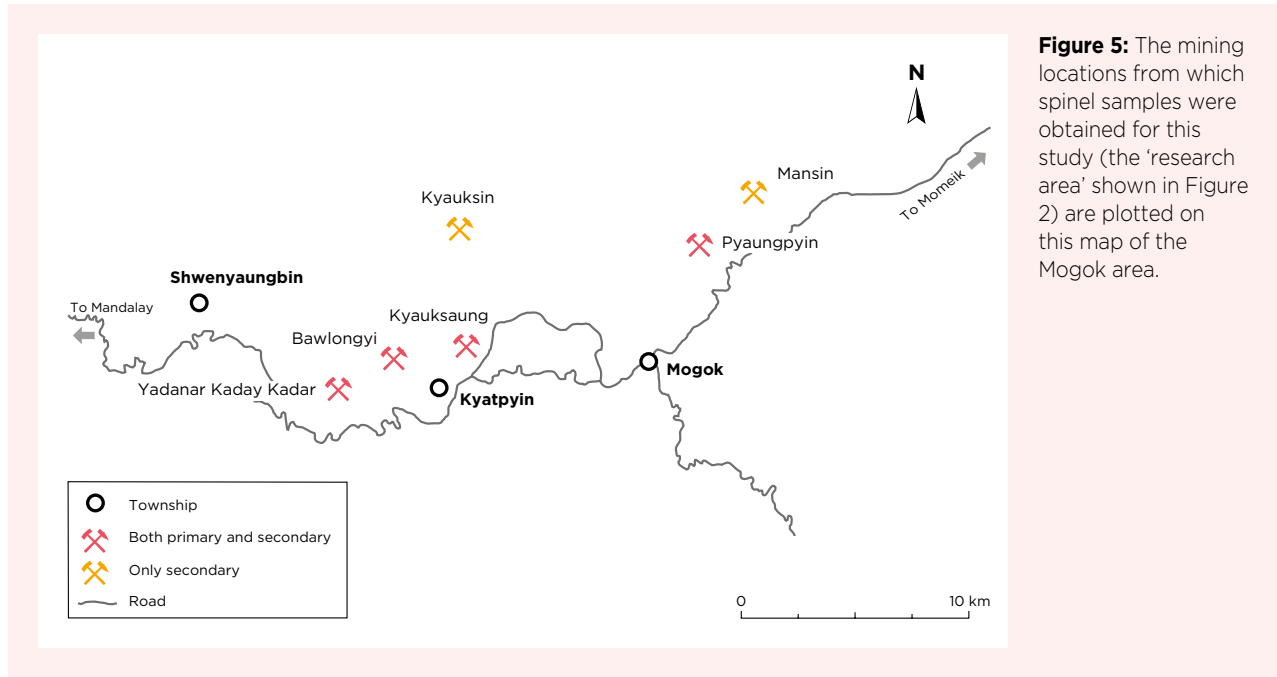


Figure 5: The mining locations from which spinel samples were obtained for this study (the ‘research area’ shown in Figure 2) are plotted on this map of the Mogok area.

Table 1: Mogok spinel samples investigated for this study.

Location*	Coordinates	No. samples	Weight range	Colour	Photo
Yadananar Kaday Kadar	22°54'18.54"N 96°22'38.18"E	5	0.18–0.35 ct	Orangey pink, light pink to red	
Bawlongyi	22°54'53.59"N 96°23'53.09"E	19	0.16–2.21 ct	Light pink to red, dark red, orange to orangey red, grey, purplish grey	
Kyauksin	22°57'26.51"N 96°25'31.63"E	17	0.45–1.24 ct	Light orange to orange, purplish grey	
Kyauksaung	22°55'20.08"N 96°25'55.44"E	10	0.10–0.62 ct	Light orange to orange, grey to purplish grey	
Pyaungpyin	22°57'13.53"N 96°31'10.63"E	6	0.45–0.67 ct	Intense red	
Mansin	22°58'28.64"N 96°32'23.57"E	30	0.05–2.59 ct	Light pink to strong pink, red to dark red	
Market	–	13	0.54–8.65 ct	Light pink to dark red, grey	

* Sample locations (top to bottom) are arranged from west to east. Photos by M. M. Phy.

microspectroscopy due to their small size. In addition, some inclusions produced Raman spectra of superposed combinations of two or more minerals, while others did not reveal a conclusive spectrum (probably because their weak Raman signal was dominated by the signal from the host spinel).

Scanning electron microscopy (SEM) was used to gain more information about selected mineral inclusions by visualising their shape and paragenetic intergrowths. In addition, SEM with energy-dispersive X-ray spectroscopy (EDS) was used to analyse their chemical composition. To accomplish this, the samples were carefully polished to expose the inclusions at the surface, and were then analysed at the Nano Imaging Lab of the University of Basel using a REM-FEI Nova NanoSEM 230 unit

equipped with an energy-dispersive spectrometer and both secondary-electron (SE) and backscattered-electron (BSE) imaging modes. This system employed an in-lens detector for producing secondary-electron images and an Octane Elite detector for EDS analysis. With this setup, we were able (in principle) to detect elements ranging from carbon to uranium as long as they were above the instrumental detection limit. We used an accelerating voltage of 15 kV, with magnifications of 50×–2,500× and a working distance of 4.0–12.5 mm.

RESULTS

The solid inclusions that we identified in the Mogok spinels are listed in Table II, along with those identified

Table II: Alphabetical list and abundance of solid inclusions in Mogok spinels documented in the present study and compared with previously published work and other localities.

Mineral	Mogok area		Other localities				
	Present study ¹	Previous studies ²	Vietnam	Tajikistan	Tanzania	Madagascar	Sri Lanka
Amphibole (presumably pargasite)	xxx	—	—	—	—	—	—
Anatase	x	—	—	—	—	—	—
Anhydrite	x	3	—	—	—	—	—
Apatite	xxx	1, 2, 3, 6, 7	1, 3	—	1	1	1, 7
Baddeleyite	x	—	—	—	—	—	—
Boehmite	x	—	—	—	—	—	1
Brucite	x	—	—	—	—	—	—
Calcite	xxxxx	3, 6, 7	3	—	—	—	1
Chlorite	x	—	—	—	—	—	—
Chondrodite	xxxxx	3	—	—	—	—	—
Clinohumite	x	—	—	—	—	—	—
Clinopyroxene	xxx	—	—	—	—	1	—
Diaspore	x	—	—	—	—	—	1
Dolomite	xxxxx	1, 3, 6	3	—	—	—	1
Geikielite	xxx	—	—	—	—	—	—
Goethite	x	—	1	—	—	—	—
Graphite	x	1, 3	3	—	—	—	1
Halite	x	—	—	—	—	—	—
Ilmenite	—	1	—	—	1	—	—
Magnesite	xxx	3	3	—	—	—	—
Marcasite	x	—	—	—	—	—	—
Molybdenite	x	—	—	—	—	—	—
Olivine (forsterite)	x	1	—	—	1	—	1
Periclase	x	—	—	—	—	—	—
Phlogopite	xxx	1	—	—	1	—	1
Potassium feldspar	—	3	3	—	—	—	1
Pyrite	—	1	—	—	—	—	1
Pyrrhotite	x	—	—	—	—	—	1
Quartz	—	1	—	—	—	—	1
Rutile	—	1	—	—	1	1	1
Sulfur	xxxxx	4, 5, 7	—	—	—	—	—
Titanite	—	1	3	—	—	—	1
Uraninite	—	1	—	—	1	—	1
Zircon	x	2	3	3	—	—	1

¹ Abbreviations: xxxxx = frequently seen; xxx = sometimes encountered; x = rarely found; — = not found.

² References: 1 = Gübelin & Koivula (1986, 2005); 2 = Themelis (2008); 3 = Malsy & Klemm (2010); 4 = Pardieu *et al.* (2016); 5 = Peretti *et al.* (2017); 6 = Zhu & Yu (2018); 7 = www.lotusgemology.com (accessed June 2018).

by other researchers in the published literature for spinels from Mogok and various deposits worldwide. The Raman spectra of representative inclusions that we identified are available in the Appendix at the end of this article, and photomicrographs and BSE images of the inclusions are shown below. Mineral abbreviations in these images are from Whitney & Evans (2010).

In general, most of the inclusions formed anhedral grains, although some of them (such as amphibole and phlogopite) showed subhedral to euhedral shapes. Inclusion sizes commonly ranged from 1 μm to several millimetres. Their wide range of composition is reflected in the presence of several mineral groups (silicate, oxide, hydroxide, carbonate, phosphate, sulphate, sulphide and native element).

Optical Microscopy and Raman Analysis

Since Mogok spinels formed in marbles, it was not surprising to find abundant carbonates (i.e. calcite, dolomite and magnesite; e.g. Figure 6) in most of the samples. They were typically present as colourless, irregularly shaped (partially resorbed) inclusions. Raman microspectrometry further revealed that carbonates sometimes also occurred as filling substances in octahedral negative crystals (similar to calcite and dolomite found by Zhu & Yu 2018).

A range of Ca- and Mg-bearing silicates was found in the investigated spinels. The humite-group minerals chondrodite $[(\text{Mg}, \text{Fe}^{2+})_5(\text{SiO}_4)_2(\text{F}, \text{OH})_2]$ and clinohumite $[\text{Mg}_9(\text{SiO}_4)_4\text{F}_2]$ were the most abundant Mg-silicates in our samples (Figure 7). A colourless, short-prismatic Ca-Mg amphibole (presumably pargasite; Figure 8a) and clinopyroxenes (diopside and augite) were found in spinels from both Kyauksin and Mansin. Figure 8b reveals a colourless clinopyroxene inclusion with distinct cleavage that is associated with minute yellow elemental sulphur

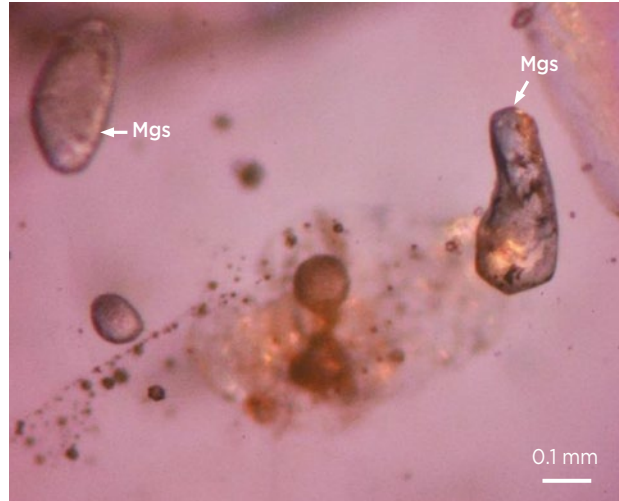


Figure 6: An example of carbonate inclusions observed in the Mogok spinel samples is shown here by magnesite (Mgs). Photomicrograph by M. M. Phyto.

and black marcasite grains in a spinel from Mansin. In accordance with Gübelin & Koivula (2005), we also found forsterite, the Mg end member of the olivine group, as colourless rounded crystals (Figure 8c) in a few Mogok spinels. However, we did not find titanite and feldspar in our samples, both of which were mentioned by Gübelin & Koivula (2005) in spinel from Mogok. Zircon, although a common inclusion in sapphires and rubies from Mogok, was found only as tiny accessory inclusions in a few spinels from Kyauksin and Kyauksaung.

Oxides were commonly present as accessory phases in the studied spinels. We found yellow, rounded anatase (TiO_2) and yellow, prismatic baddeleyite (ZrO_2) inclusions, both surrounded by tension cracks (Figure 9a, b). Interestingly, using SEM-EDS we identified geikielite (MgTiO_3) as tiny needles/lamellae in spinel from Yadanar Kaday Kadar (western Mogok; Figure 9c). They were oriented along $\{111\}$ lattice planes and

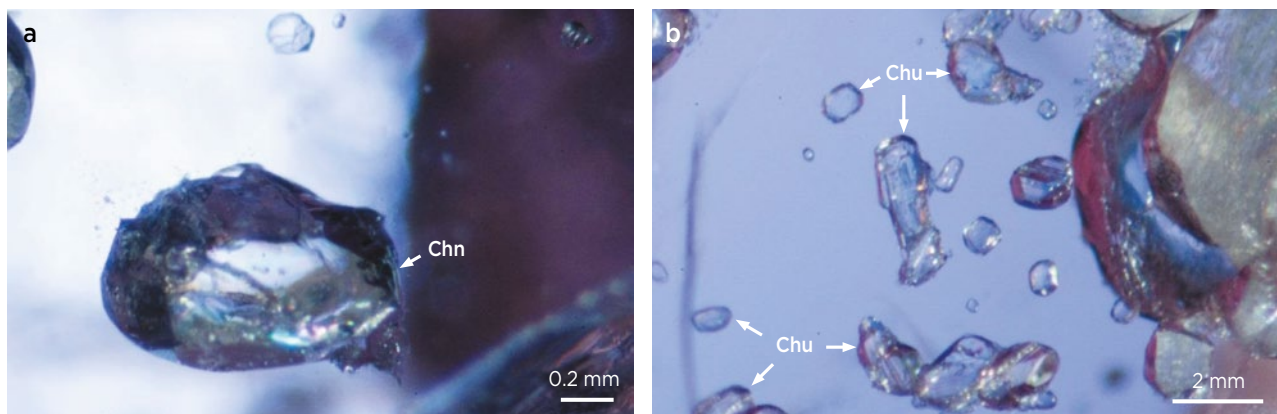


Figure 7: Among the silicate inclusions that were identified, humite-group minerals were common in some of the spinels: (a) anhedral chondrodite (Chn) and (b) a cluster of subhedral clinohumite (Chu) crystals. Photomicrographs by M. M. Phyto.

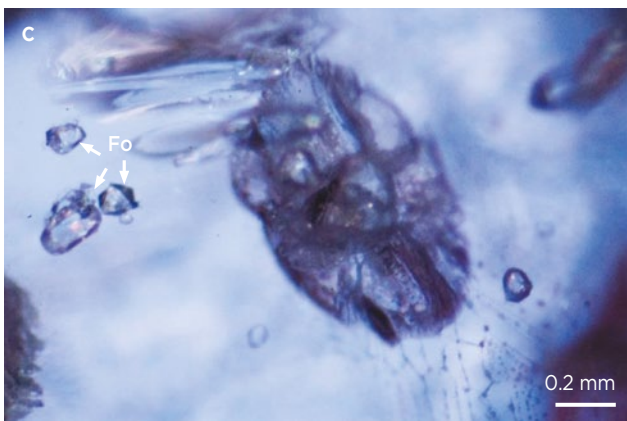
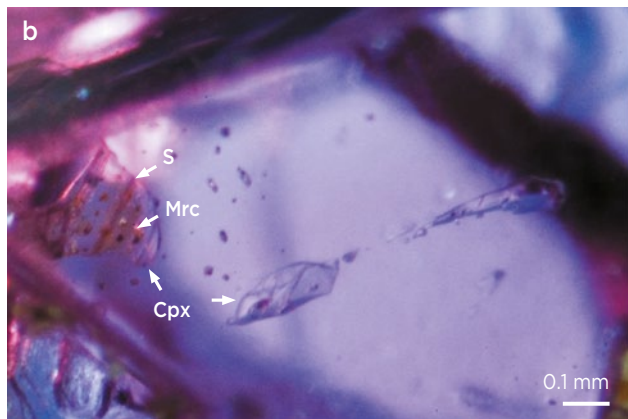
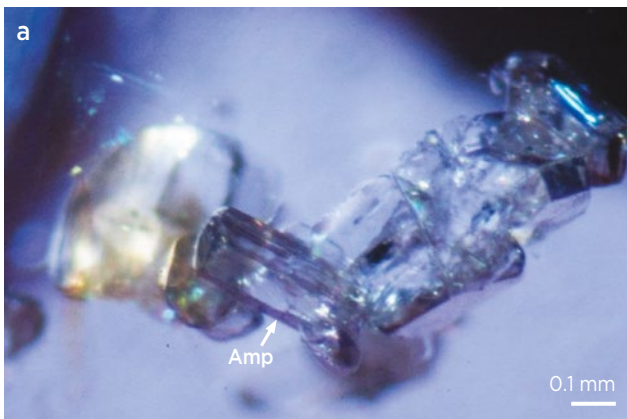


Figure 8: Other Ca- and Mg-bearing silicate inclusions were also present in the spinels. (a) Euhedral colourless amphibole (Amp; presumably pargasite) crystals form clusters in Kyauksin spinel. (b) Anhedral clinopyroxene (Cpx) showing a distinct set of cleavage planes is associated with tiny yellow sulphur (S) and black marcasite (Mrc) spots in a spinel from Mansin. (c) Anhedral olivine (forsterite; Fo) crystals are seen here next to a larger clinohumite inclusion. Photomicrographs by M. M. Phyo.

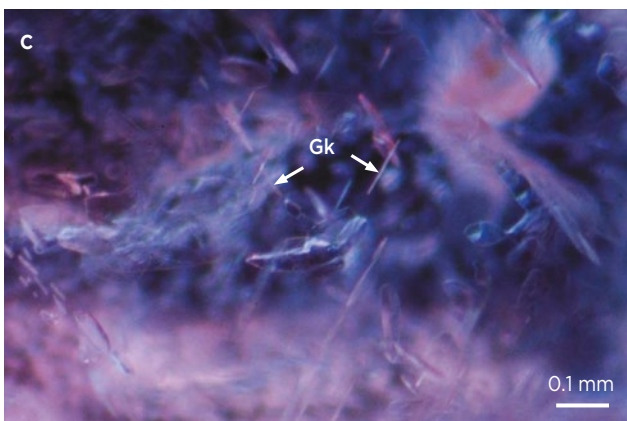
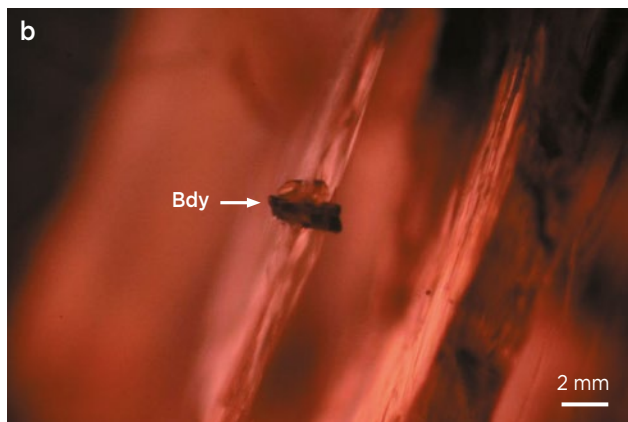


Figure 9: Oxide minerals identified in the spinels include (a) yellow anatase (Ant) that is surrounded here by negative crystals and tension cracks, (b) baddeleyite (Bdy) crystals that are also often associated with tension cracks and (c) tiny flake-like colourless geikielite (Gk) lamellae along {111} lattice planes in a spinel from Yadanar Kaday Kadar. Photomicrographs by M. M. Phyo.

presumably formed by epigenetic exsolution, similar to geikielite-rich ilmenite exsolution lamellae seen in chromite-chrome spinel from metacarbonates in Austria (Mogessie *et al.* 1988). To our knowledge, this is the first time such geikielite exsolution lamellae have been reported in gem-quality spinel.

We also found several hydroxides in our spinels, including diaspore [$\alpha\text{-AlO}(\text{OH})$], boehmite [$\gamma\text{-AlO}(\text{OH})$], brucite [$\text{Mg}(\text{OH})_2$] and goethite [$\alpha\text{-Fe}^{3+}\text{O}(\text{OH})$]. They probably formed as retrograde phases, and were present in secondary inclusion trails (boehmite) or associated with phlogopite (brucite) or pyrrhotite (goethite).

Additional accessory inclusions in our spinels included anhydrite (CaSO_4 , also known from Mogok rubies; Smith & Dunaigre 2001), apatite [$\text{Ca}_5(\text{PO}_4)_3(\text{F,Cl,OH})$], sulphides (marcasite, molybdenite and pyrrhotite), graphite (C) and elemental sulphur (S_8). Apatite was seen as transparent to semi-transparent, anhedral to subhedral crystals (Figure 10). As for the elemental sulphur, its presence within fluid inclusions and as solid inclusions (Figure 11) seems to be highly characteristic for spinels from Mansin (Pardieu *et al.* 2016; Peretti *et al.* 2017). Less commonly, we also found elemental sulphur in the spinels from Kyauksaung and Pyaungpyin.

SEM Imaging and EDS Analysis

Using SEM-EDS, it was possible to visualise and identify for the first time the complex intergrowth of multiphase inclusions (some containing small fluid cavities) within spinel from Mogok. These assemblages consisted of various minerals such as calcite (CaCO_3), dolomite [$\text{CaMg}(\text{CO}_3)_2$], halite (NaCl), phlogopite [$\text{KMg}_3(\text{AlSi}_3\text{O}_{10}(\text{F,OH})_2$), apatite and/or anhydrite of sugary texture (Figure 12). They were similar to the inclusions

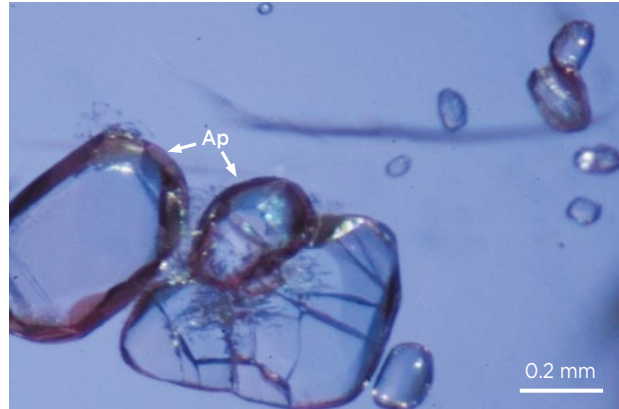


Figure 10: Rounded anhedral apatite (Ap) inclusions are present in this Mogok spinel. Photomicrograph by M. M. Phyo.



Figure 11: Solid inclusions of elemental sulphur (S) are seen here with multiphase fluid inclusions (probably containing liquid and sulphur) in a spinel from Mansin. Photomicrograph by M. M. Phyo.

containing residues of molten salts described by Giuliani *et al.* (2015) in rubies from Mogok.

SEM-EDS also revealed other inclusion features in the spinels. A euhedral amphibole inclusion contained

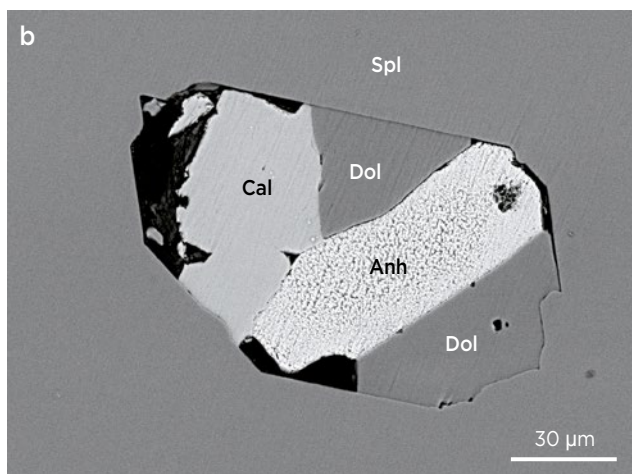
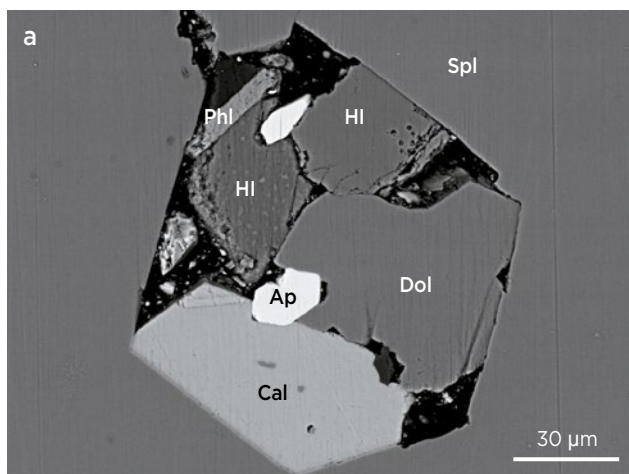


Figure 12: BSE images reveal the contents of multiphase inclusions in Mogok spinel (Spl): (a) calcite (Cal), dolomite (Dol), halite (HI), phlogopite (Phl) and apatite (Ap); and (b) calcite, dolomite and anhydrite (Anh).

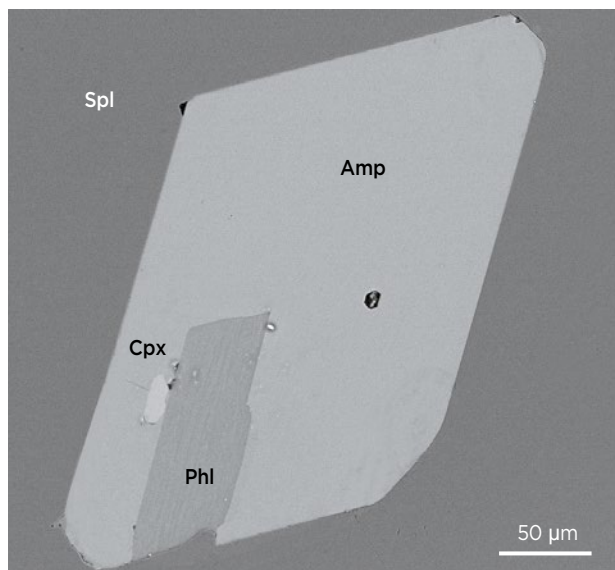


Figure 13: BSE imaging shows that a euhedral amphibole (Amp) inclusion in a spinel from Kyauksin contains inclusions of phlogopite (Phl) and clinopyroxene (Cpx).

clinopyroxene and phlogopite domains in a spinel from Kyauksin (Figure 13). We also imaged some phases that presumably exsolved from their hosts: dolomite blebs in certain calcite inclusions (Figure 14a) and the geikielite lamellae in spinel (Figure 14b) that were mentioned above. Furthermore, rare accessory inclusions of baddeleyite (also mentioned above) were easily visible with the SEM (Figure 15).

Various secondary mineral inclusions were identified with SEM-EDS, such as chlorite and brucite together with a phlogopite inclusion (Figure 16a), and a bright red powder-like substance that proved to be an iron compound (e.g. an Fe oxide or hydroxide, probably goethite) that formed an epigenetic encrustation along the cleavages and boundaries of a phlogopite inclusion (Figure 16b).

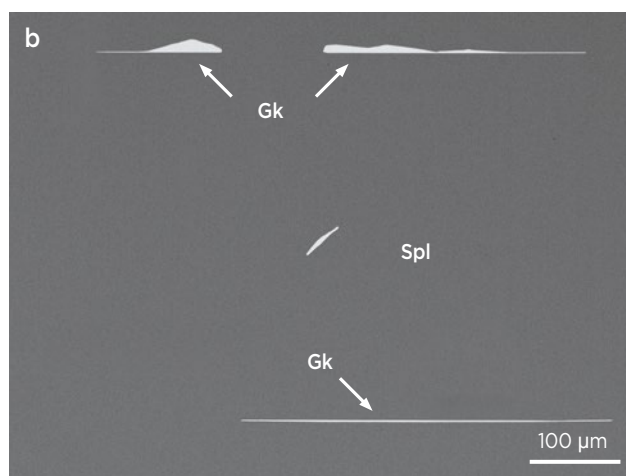
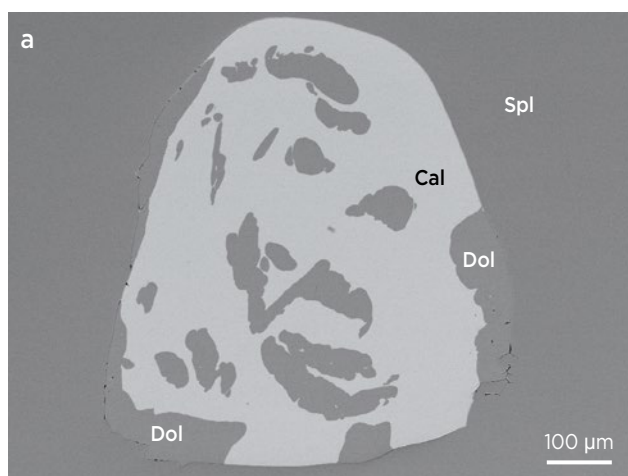


Figure 14: Evidence of exsolved mineral phases in Mogok spinels is seen in these BSE images of (a) dolomite (Dol) blebs in a calcite (Cal) inclusion and (b) oriented geikielite (Gk) lamellae.

DISCUSSION

In the present study, we not only confirmed the presence of most inclusions previously described in the literature for Burmese spinel, but also identified for the first time 16 new solid inclusions in our samples from Mogok: amphibole (presumably pargasite), anatase, baddeleyite, boehmite, brucite, chlorite, clinohumite, clinopyroxene, diaspore, geikielite, goethite, halite, marcasite, molybdenite, periclase and pyrrhotite (see Table II).

Interestingly, we did not observe in our study any 'belly button' apatite inclusions that are considered typical for spinel from Mogok (Gübelin & Koivula 1986, 2005). These inclusions are characterised by a tiny black graphite or ilmenite platelet attached to rounded apatite. As previously described by Malsy & Klemm (2010), we only observed in our samples subhedral to anhedral colourless apatite crystals as individuals or clusters.

We also documented for the first time in gem-quality spinel multiphase inclusions (Figure 12) with small fluid cavities, which may be interpreted as residues of molten salts (Giuliani *et al.* 2003, 2015, 2018; Peretti *et al.* 2017, 2018). Their assemblages are reflective of paragenetic relationships within the host rock (e.g. calcite-dolomite-phlogopite-apatite). Some of the spinel inclusions also demonstrate mineral exsolution (e.g. oriented geikielite lamellae in Figures 9c and 14b) and retrograde transformations after spinel formation (e.g. the breakdown of phlogopite to chlorite, brucite and Fe oxides/hydroxides; see Figure 16; Yau *et al.* 1984).

We observed carbonate inclusions in our spinels from all mining locations sampled in the Mogok area. Some of these carbonate inclusions did not occur as a single mineral phase but were present within multiphase inclusions (Figure 12) and possibly as exsolved assemblages

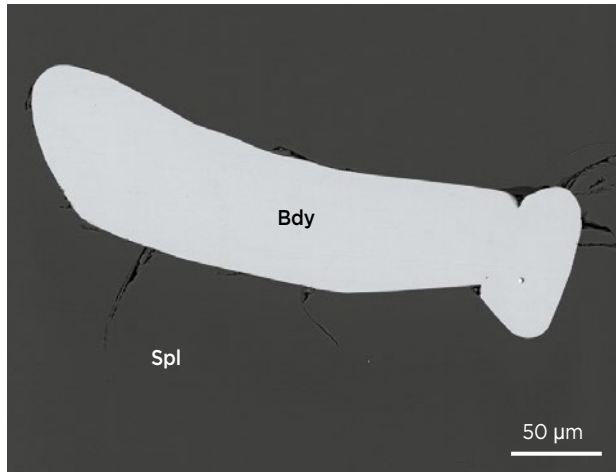


Figure 15: A baddeleyite (Bdy) inclusion with tension cracks shows high contrast against the host spinel in this BSE image.

(Figure 14a). In a few cases, such carbonates were also found in negative-crystal cavities. Moreover, the presence in spinel of various silicates such as amphibole (presumably pargasite), chondrodite, clinohumite and zircon—similar to the carbonate inclusions—reflects the compositional range of the host-rock marbles with interlayered calc-silicates in which these spinels from the Mogok area were formed.

The complex metamorphic evolution of the Mogok Stone Tract during the Himalayan orogeny is connected to and influenced by several magmatic events (Barley *et al.* 2003; Searle *et al.* 2007). Geographically and geologically, all of the spinel localities that were sampled for this study (primary marbles and secondary deposits) were found in close proximity to granite intrusions (Thu 2007). Mineral inclusions such as anatase, olivine, clinopyroxene, periclase and chondrodite could have formed

either during granulite-facies regional metamorphism (Thu 2007; Phyo *et al.* 2017; Thu & Zaw 2017) or by contact metamorphism from the nearby intrusions. Remarkable is the prevalence of elemental sulphur and graphite in spinel from Mansin (Gübelin & Koivula 2005; Pardieu 2014; Vertriest & Raynaud 2017), which points to highly reducing conditions. Moreover, the multiphase inclusions with small fluid cavities that we observed in our Mogok spinels showed similarities to hypersaline fluid inclusions in Mansin spinel (Peretti *et al.* 2017, 2018) and to the residues of molten salts found in Mogok ruby (Giuliani *et al.* 2015).

We also sought to investigate whether it is possible to separate spinels from different locations within the Mogok Stone Tract based on their inclusions (see Figure 17; see also the sample locations in Figures 5 and 18). Although the number of samples (87, not including those obtained from local markets) and inclusions (about 400) that were analysed might not be sufficient, we can still report meaningful results. Similar to Themelis (2008) and Malsy & Klemm (2010), and as expected for marble-related spinels, we observed an abundance of carbonate inclusions in spinels from all of the studied localities. Closely related are impurities in the marble host rock—graphite, apatite and phlogopite—which were present in spinels from nearly all of the localities, although in distinctly smaller quantities. Additional inclusion phases were observed in spinel from a few localities, such as elemental sulphur (most prominently from Mansin but also from Pyaungpyin and Kyauksaung), anatase (Yadanar Kaday Kadar, Kyauksin and Kyauksaung) and chondrodite (Bawlongyi, Kyauksaung and Mansin). In contrast, a number of inclusions were found only in samples from one locality, such

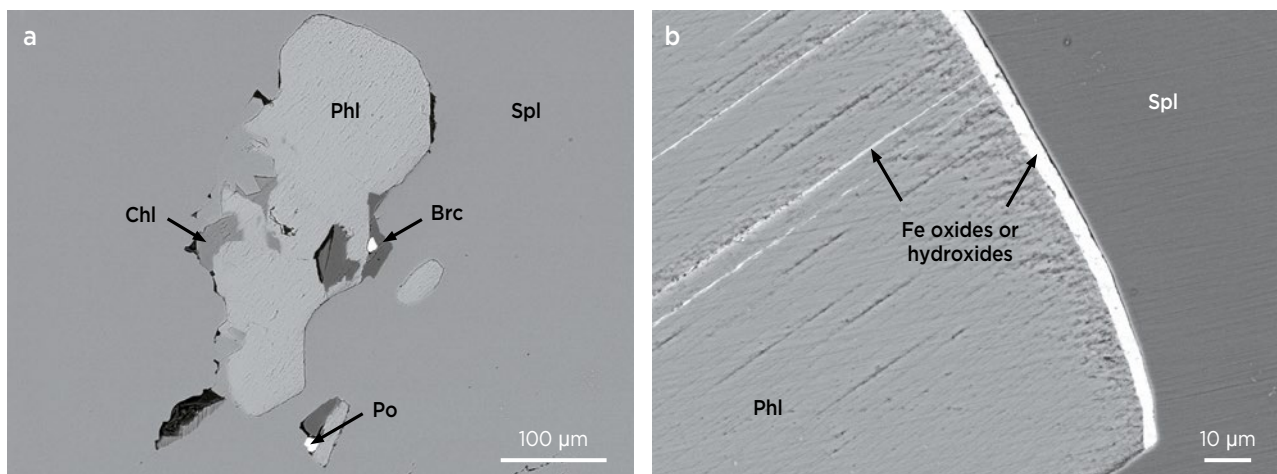


Figure 16: BSE imaging showed various secondary mineral assemblages associated with phlogopite (Phl) in Mogok spinel. (a) Phlogopite inclusions with tiny pyrrhotite (Po) grains are intergrown with the secondary minerals brucite (Brc) and chlorite (Chl). (b) Secondary Fe oxides or hydroxides are seen as bright areas along the rim and within cleavages in this phlogopite inclusion.

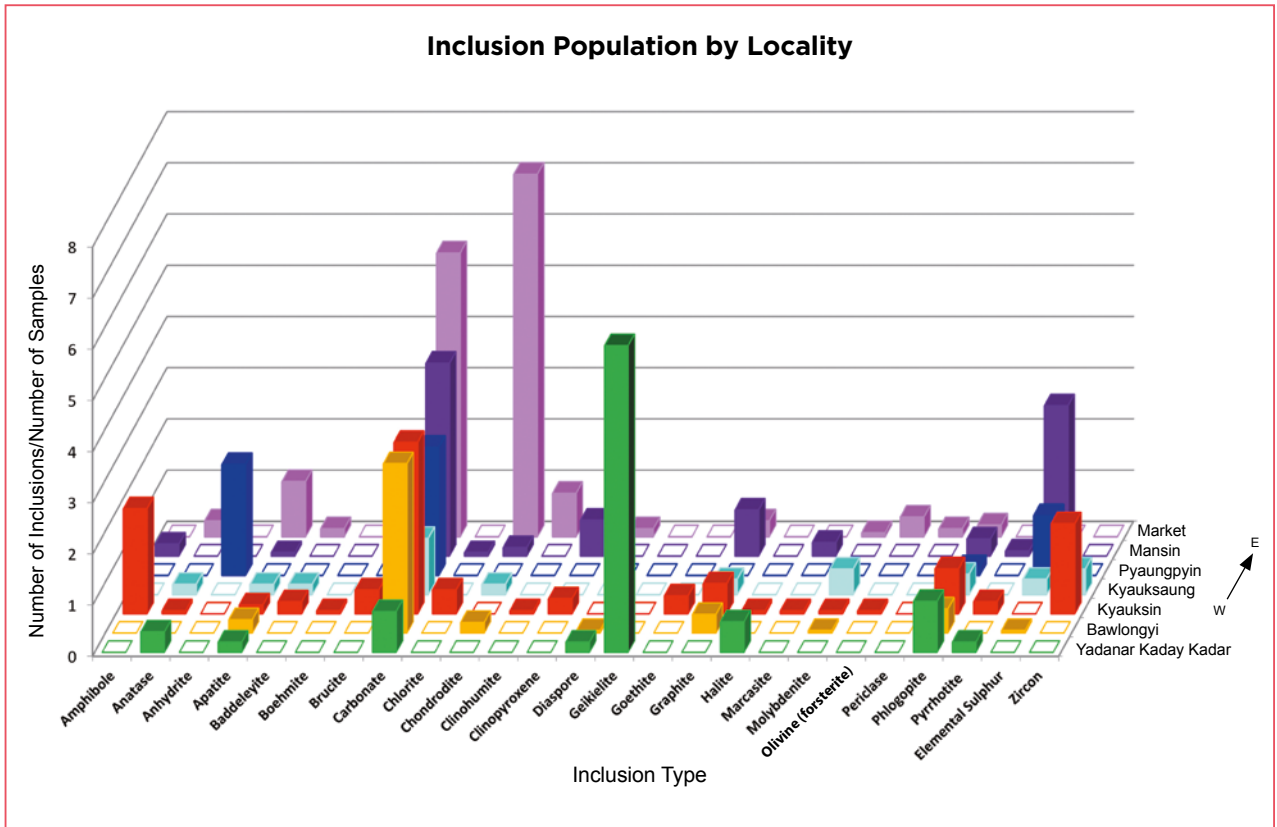


Figure 17: To express the relative amount of inclusions found in spinel from various mining sites (and local markets) in the Mogok region of Myanmar, the total number of observed inclusions was divided by the number of samples from that location. The distribution of the different inclusion types suggests that, with further research, they could be helpful for distinguishing spinels from certain localities.

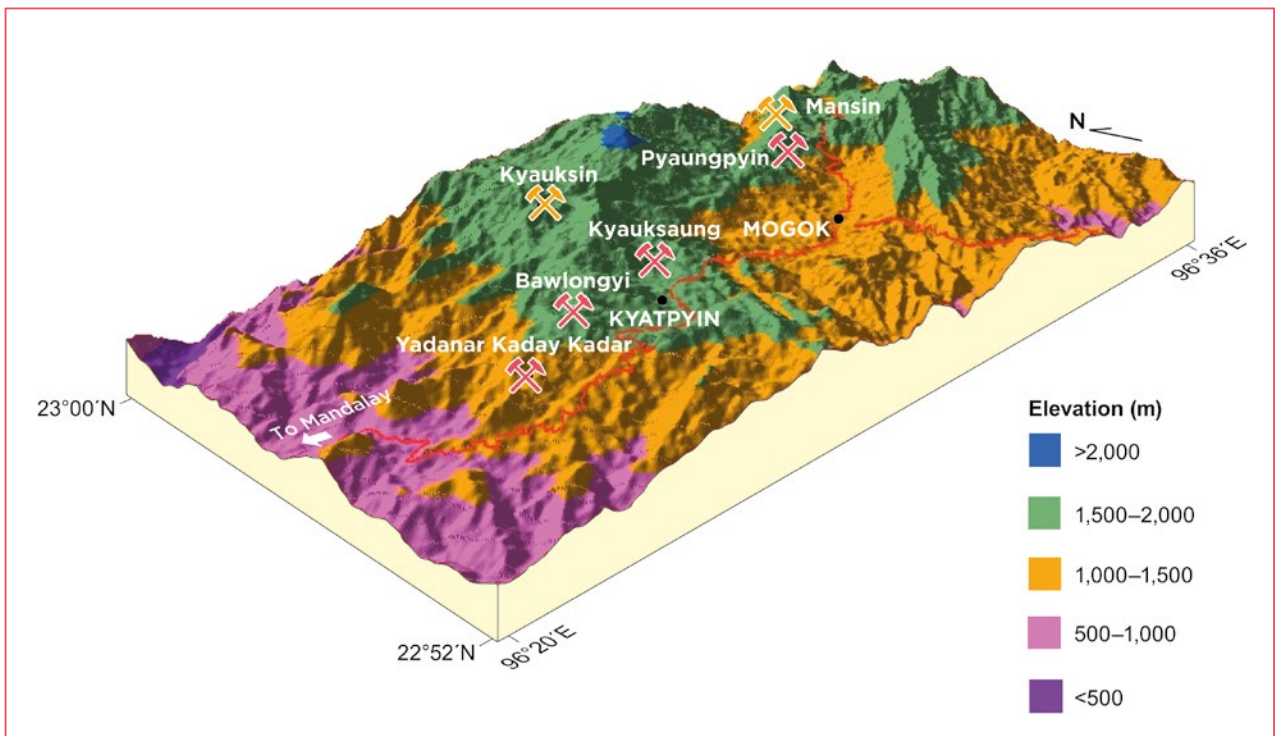


Figure 18: The mine sites sampled for this study are shown on this three-dimensional map of the Mogok area. Most of them are situated at elevations ranging from 1,500 to 2,000 m. The colouration of the mine symbols is explained in Figure 5. Spatial data are based on topographic maps of Northern Shan State and the Katha District (93 B-5 and 93 B-9, scale 1" = 1 mile, 1945).

as goethite (Kyauksin), anhydrite (Pyaungpyin) and geikielite lamellae (Yadanar Kaday Kadar). Whether these findings are truly specific to these locations or just the result of the limited sampling is presently unknown. Nevertheless, the assemblages documented in spinel from Mogok and elsewhere are clearly different from the inclusions seen in synthetic flux-grown spinel (Krzemnicki 2008), and therefore are useful for separating natural spinels from their synthetic counterparts.

CONCLUSION

This study presents the first detailed description of inclusions in spinel from Mogok, Myanmar. It documents several solid inclusions for the first time in these spinels, as well as multiphase assemblages (some containing small fluid cavities) that add to their complexity. All of the mineral inclusions are related to the local geology

and geochemistry of the host rocks in the Mogok area. Spinel and its associated minerals such as ruby, diopside, olivine, chondrodite and clinohumite testify to granulite-facies metamorphic conditions in the Mogok Metamorphic Belt (Thu *et al.* 2016; Phyo *et al.* 2017). Elemental sulphur and graphite inclusions furthermore indicate highly reducing conditions during the formation of these spinels. The generation of gem-quality spinel by skarn-forming processes can be excluded due to the absence of typical skarn mineral inclusions (e.g. vesuvianite, pectolite or nephrite) in our samples.

Based on the data presented in this article, the authors feel that such inclusion studies can help distinguish Mogok spinels from those of other sources worldwide (e.g. Figure 19), and therefore contribute to the origin determination of spinels in gemmological laboratories. We expect that further studies of spinel inclusions in the future will add to this knowledge.



Figure 19: Detailed inclusion studies may be helpful toward geographic origin determinations of spinel from various world localities, such as those shown here. All of the crystals are from Mogok, and the cut stones are from Tanzania (7.31 ct pink oval), Tajikistan (5.90 ct pink cushion), Vietnam (all pear shapes, up to 3.22 ct) and Mogok (4.01 and 2.63 ct red cushions). Photo by Prasit Prachagool, Thai Lanka Trading Ltd Part., Bangkok, Thailand.

REFERENCES

- Balmer, W.A., Hauzenberger, C.A., Fritz, H. & Sutthirat, C. 2017. Marble-hosted ruby deposits of the Morogoro region, Tanzania. *Journal of African Earth Sciences*, **134**, 626–643, <https://doi.org/10.1016/j.jafrearsci.2017.07.026>.
- Barley, M.E., Pickard, A.L., Zaw, K., Rak, P. & Doyle, M.G. 2003. Jurassic to Miocene magmatism and metamorphism in the Mogok Metamorphic Belt and the India-Eurasia collision in Myanmar. *Tectonics*, **22**(3), article no. 1019, 11 pp., <http://doi.org/10.1029/2002tc001398>.
- Bender, F. 1983. *Geology of Burma*. Gebrüder Borntraeger, Berlin, Germany, 295 pp.
- Cesbron, F., Lebrun, P., Le Cléac'h, J.-M., Notari, F., Grobon, C. & Deville, J. 2002. Corindon et spinelles. *Minéraux & Fossiles*, Special Issue No. 15, 105 pp.
- Chhibber, H.L. 1934. *The Geology of Burma*. Macmillan and Co. Ltd, London, 538 pp.
- Cooper, A. & Sun, Z. 2014. Lab Notes: Spinel inclusion in spinel. *Gems & Gemology*, **50**(4), 293–301.
- Ehrmann, M. 1957. Gem mining in Burma. *Gems & Gemology*, **9**(1), 2–30.
- Fermor, L.L. 1931. General report for the Geological Survey of India, 1930. *Records of the Geological Survey India*, **65**, 445–456.
- Giuliani, G., Dubessy, J., Banks, D., Hoàng Quang Vinh, Lhomme, T., Pironon, J., Garnier, V., Phan Trong Trinh, Pham Van Long, Ohnenstetter, D. & Schwarz, D. 2003. CO₂-H₂S-COS-S₈-AlO(OH)-bearing fluid inclusions in ruby from marble-hosted deposits in Luc Yen area, North Vietnam. *Chemical Geology*, **194**(1–3), 167–185, [http://doi.org/10.1016/s0009-2541\(02\)00276-0](http://doi.org/10.1016/s0009-2541(02)00276-0).
- Giuliani, G., Dubessy, J., Banks, D.A., Lhomme, T. & Ohnenstetter, D. 2015. Fluid inclusions in ruby from Asian marble deposits: Genetic implications. *European Journal of Mineralogy*, **27**(3), 393–404, <http://doi.org/10.1127/ejm/2015/0027-2442>.
- Giuliani, G., Fallick, A.E., Boyce, A.J., Pardieu, V. & Pham, V.L. 2017. Pink and red spinels in marble: Trace elements, oxygen isotopes, and sources. *Canadian Mineralogist*, **55**(4), 743–761, <https://doi.org/10.3749/canmin.1700009>.
- Giuliani, G., Dubessy, J., Ohnenstetter, D., Banks, D., Branquet, Y., Feneyrol, J., Fallick, A.E. & Martelat, J.-E. 2018. The role of evaporites in the formation of gems during metamorphism of carbonate platforms: A review. *Mineralium Deposita*, **53**(1), 1–20, <http://doi.org/10.1007/s00126-017-0738-4>.
- Gordon, R. 1888. On the ruby mines near Mogok, Burma. *Proceedings of the Royal Geographical Society and Monthly Record of Geography*, **10**(5), 261–275, <http://doi.org/10.2307/1801309>.
- Gorghinian, A., Mottana, A., Rossi, A., Oltean, F.M., Esposito, A. & Marcelli, A. 2013. Investigating the colour of spinel: 1. Red gem-quality spinels (“balas”) from Ratnapura (Sri Lanka). *Rendiconti Lincei*, **24**, 127–140.
- Gübelin, E. 1965. The ruby mines in Mogok in Burma. *Journal of Gemmology*, **9**(12), 411–425, <http://doi.org/10.15506/JoG.1965.9.12.411>.
- Gübelin, E.J. & Koivula, J.I. 1986. *Photoatlas of Inclusions in Gemstones*. ABC Edition, Zurich, Switzerland, 532 pp.
- Gübelin, E.J. & Koivula, J.I. 2005. *Photoatlas of Inclusions in Gemstones*, Vol. 2. Opinio Publishers, Basel, Switzerland, 829 pp.
- Halford-Watkins, J.F. 1932a. The ruby mines of upper Burma: A short history of their working. *The Gemmologist*, **1**(9), 263–272.
- Halford-Watkins, J.F. 1932b. Methods of ruby mining in Burma. *The Gemmologist*, **1**(11), 335–342.
- Halford-Watkins, J.F. 1932c. Methods of ruby mining in Burma: Washing, grading and selling the stones. *The Gemmologist*, **1**(12), 367–373.
- Hughes, E.B. 2017a. Beyond octahedra: Inclusions in spinel. *Journal of the Gemmological Association of Hong Kong*, **38**, 41–44, www.gahk.org/journal/GAHK_Journal_2017_v5.pdf.
- Hughes, R.W. 1997. *Ruby & Sapphire*. RWH Publishing, Bangkok, Thailand, 511 pp.
- Hughes, R.W. 2017b. *Ruby & Sapphire: A Gemologist's Guide*. RWH Publishing, Bangkok, Thailand, 816 pp.
- Iyer, L.A.N. 1953. The geology and gem-stones of the Mogok Stone Tract, Burma. *Memoirs of the Geological Survey of India*, **82**, 100 pp.
- Keller, P.C. 1983. The rubies of Burma: A review of the Mogok Stone Tract. *Gems & Gemology*, **19**(4), 209–219, <http://doi.org/10.5741/gems.19.4.209>.
- Krzemnicki, M.S. 2008. Trade Alert: Flux-grown synthetic red spinels on the market. *SSEF Newsletter*, No. 14, October, 3 pp, www.ssef.ch/wp-content/uploads/2018/03/2008_Krzemnicki_Trade_Alert_-_Flux_grown_synthetic_red_spinel_again_on_the_market.pdf.
- La Touche, T.H.D. 1913. Geology of the northern Shan States. *Memoirs of the Geological Survey of India*, **39**, Part 2, 379 pp.
- Malsy, A. & Klemm, L. 2010. Distinction of gem spinels from the Himalayan mountain belt. *CHIMIA International Journal for Chemistry*, **64**(10), 741–746, <http://doi.org/10.2533/chimia.2010.741>.
- Mogessie, A., Purtscheller, F. & Tessadri, R. 1988. Chromite and chrome spinel occurrences from metacarbonates of the Oetztal-Stubai complex (northern Tyrol, Austria). *Mineralogical Magazine*, **52**(365), 229–236, <http://doi.org/10.1180/minmag.1988.052.365.09>.

- Pardieu, V. 2014. Hunting for “Jedi” spinels in Mogok. *Gems & Gemology*, **50**(1), 46–57, <http://doi.org/10.5741/gems.50.1.46>.
- Pardieu, V. & Hughes, R.W. 2008. Spinel: Resurrection of a classic. *InColor*, No. 2, 10–18.
- Pardieu, V., Sangsawong, S., Vertriest, W. & Raynaud, V. 2016. Gem News International: “Star of David” spinel twin crystal with multiphase inclusions from Mogok. *Gems & Gemology*, **52**(1), 100–101.
- Peretti, A., Kanpraphai-Peretti, A. & Günther, D. 2015. World of magnificent spinel: Provenance and identification. *Contributions to Gemmology*, **11**, 293 pp.
- Peretti, A., Mullis, J., Franz, L. & Günther, D. 2017. Spinel formation by sulphur-rich saline brines from Mansin (Mogok area, Myanmar). *15th Swiss Geoscience Meeting*, Davos, Switzerland, 17–18 November, 149–150.
- Peretti, A., Mullis, J., Franz, L. & Günther, D. 2018. Spinel formation by sulphur-rich saline brines from Mansin (Mogok area, Myanmar). GRS GemResearch Swisslab AG, Lucerne, Switzerland, <http://gemresearch.ch/spinel-formation-mansin>, accessed 24 December 2018.
- Phyo, M.M., Franz, L., de Capitani, C., Balmer, W. & Krzemnicki, M. 2017. Petrology and PT-conditions of quartz- and nepheline-bearing gneisses from Mogok Stone Tract, Myanmar. *15th Swiss Geoscience Meeting*, Davos, Switzerland, 17–18 November, 88–89.
- Searle, D.L. & Haq, B.T. 1964. The Mogok belt of Burma and its relationship to the Himalayan orogeny. *22nd International Geological Congress*, New Delhi, India, 14–22 December, 132–161.
- Searle, M.P., Noble, S.R., Cottle, J.M., Waters, D.J., Mitchell, A.H.G., Hlaing, T. & Horstwood, M.S.A. 2007. Tectonic evolution of the Mogok Metamorphic Belt, Burma (Myanmar) constrained by U-Th-Pb dating of metamorphic and magmatic rocks. *Tectonics*, **26**(3), article no. TC3014, 24 pp, <https://doi.org/10.1029/2006tc002083>.
- Smith, C.P. & Dunaigre, C. 2001. Gem News: Anhydrite inclusion in a ruby from Myanmar. *Gems & Gemology*, **37**(3), 236.
- Thein, M. 2008. Modes of occurrence and origin of precious gemstone deposits of the Mogok Stone Tract. *Journal of the Myanmar Geosciences Society*, **1**(1), 75–84.
- Themelis, T. 2008. *Gems & Mines of Mogok*. Self-published, 352 pp.
- Thu, K. 2007. *The igneous rocks of the Mogok Stone Tract: Their distributions, petrography, petrochemistry, sequence, geochronology and economic geology*. PhD thesis, Department of Geology, University of Yangon, Myanmar, <http://m.palaminerals.com/mogok>.
- Thu, K. & Zaw, K. 2017. Gem deposits of Myanmar. *Geological Society, London, Memoirs*, **48**(1), 497–529, <http://doi.org/10.1144/m48.23>.
- Thu, Y.K., Win, M.M., Enami, M. & Tsuboi, M. 2016. Ti-rich biotite in spinel and quartz-bearing paragneiss and related rocks from the Mogok Metamorphic Belt, central Myanmar. *Journal of Mineralogical and Petrological Sciences*, **111**(4), 270–282, <http://doi.org/10.2465/jmps.151020>.
- Truong, A.R. 2017. A highly-important imperial Mughal spinel, India, dated 1024 AH/1615 AD and 1070 AH/1659 AD. www.alaintruong.com/archives/2017/03/23/35086977.html, accessed 24 December 2018.
- Vertriest, W. & Reynaud, V. 2017. G&G Micro-World: Complex yellow fluid inclusions in red Burmese spinel. *Gems & Gemology*, **53**(4), 468.
- Whitney, D.L. & Evans, B.W. 2010. Abbreviations for names of rock-forming minerals. *American Mineralogist*, **95**(1), 185–187, <http://doi.org/10.2138/am.2010.3371>.
- Yau, Y.C., Anovitz, L.M., Essene, E.J. & Peacor, D.R. 1984. Phlogopite-chlorite reaction mechanisms and physical conditions during retrograde reactions in the Marble Formation, Franklin, New Jersey. *Contributions to Mineralogy and Petrology*, **88**(3), 299–306, <http://doi.org/10.1007/bf00380175>.
- Yavorskyy, V.Y. & Hughes, R.W. 2010. *Terra Spinel: Terra Firma*. Ivy, New York, New York, USA, 203 pp.
- Zaw, K. 1990. Geological, petrological and geochemical characteristics of granitoid rocks in Burma: With special reference to the associated W-Sn mineralization and their tectonic setting. *Journal of Southeast Asian Earth Sciences*, **4**(4), 293–335, [http://doi.org/10.1016/0743-9547\(90\)90004-w](http://doi.org/10.1016/0743-9547(90)90004-w).
- Zaw, K. 2017. Overview of mineralization styles and tectonic–metallogenic setting in Myanmar. *Geological Society, London, Memoirs*, **48**(1), 531–556, <https://doi.org/10.1144/m48.24>.
- Zaw, K., Acharyya, S.K. & Maung, H. 1989. Comments and reply on “Transcurrent movements in the Burma–Andaman Sea region”. *Geology*, **17**(1), 93–98, [http://doi.org/10.1130/0091-7613\(1989\)017<0093:carotm>2.3.co;2](http://doi.org/10.1130/0091-7613(1989)017<0093:carotm>2.3.co;2).
- Zaw, K., Sutherland, L., Yui, T.-F., Meffre, S. & Thu, K. 2015. Vanadium-rich ruby and sapphire within Mogok gemfield, Myanmar: Implications for gem color and genesis. *Mineralium Deposita*, **50**(1), 25–39, <http://doi.org/10.1007/s00126-014-0545-0>.
- Zhu, J. & Yu, X. 2018. Inclusions of spinel from Burma. *Journal of Gems and Gemmology*, **20**(Supp.), 18–23 (in Chinese with English abstract).

The Authors

**Myint Myat Phyo and
Prof. Dr Leander Franz**

Department of Mineralogy and Petrology,
Basel University, CH-4056 Basel, Switzerland
Email: myintmyat.phyo@unibas.ch

Eva Bieler

Swiss Nano Imaging Lab,
Swiss Nanoscience Institute,
Basel University, CH-4056 Basel, Switzerland

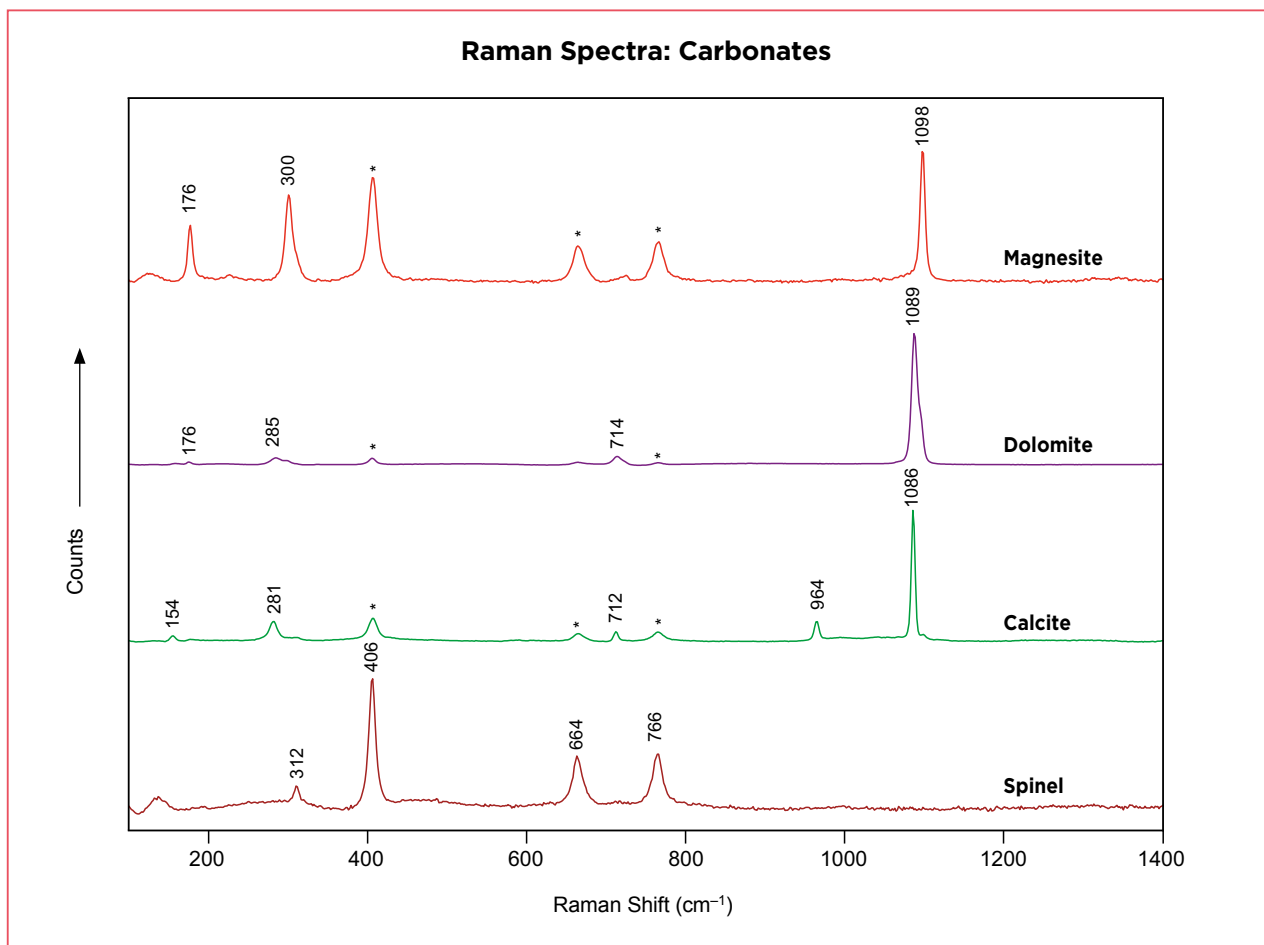
Walter Balmer and

Dr Michael S. Krzemnicki FGA
Swiss Gemmological Institute SSEF,
Aeschengraben 26, 4051 Basel, Switzerland

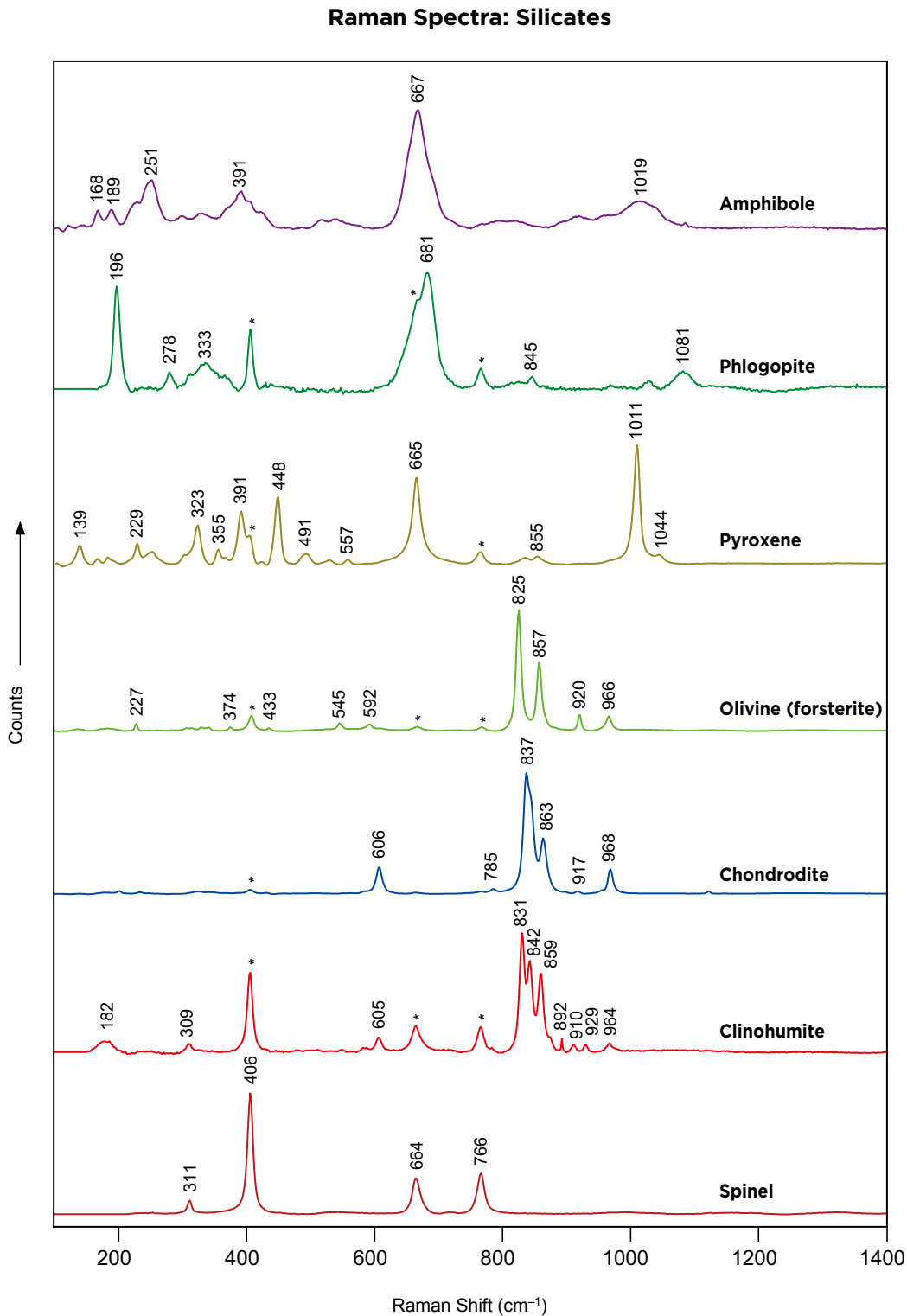
Acknowledgements

The authors thank Ma Mie, Ko Chu (Kyauksaung mine), Dr Takahito Mori, Ko Kyaw Swar and Ko Nay for all their support and for providing samples of gem-quality spinel and host rock. Further thanks to Sebastian Hänsel, U Aung Kyaw Htoon and Ko Ja Mu for their help with fieldwork. Special thanks to Ah Ba, Aunty Phyu and the local people and miners of the Mogok area for their kind encouragement during the fieldwork. Many thanks to Judith Braun, Dr Tashia Dzikowski and Dr Laurent E. Cartier FGA (all of the Swiss Gemmological Institute SSEF, Basel) for their help, advice and fruitful discussions on this paper. This study was financed by a grant from Kanton Basel (Stipendienkommission für Nachwuchskräfte aus Entwicklungsländern), by a research grant from FAG (Freiwillige Akademische Gesellschaft Basel) and by the Swiss Gemmological Institute SSEF. We also thank the three peer reviewers for their helpful suggestions and information.

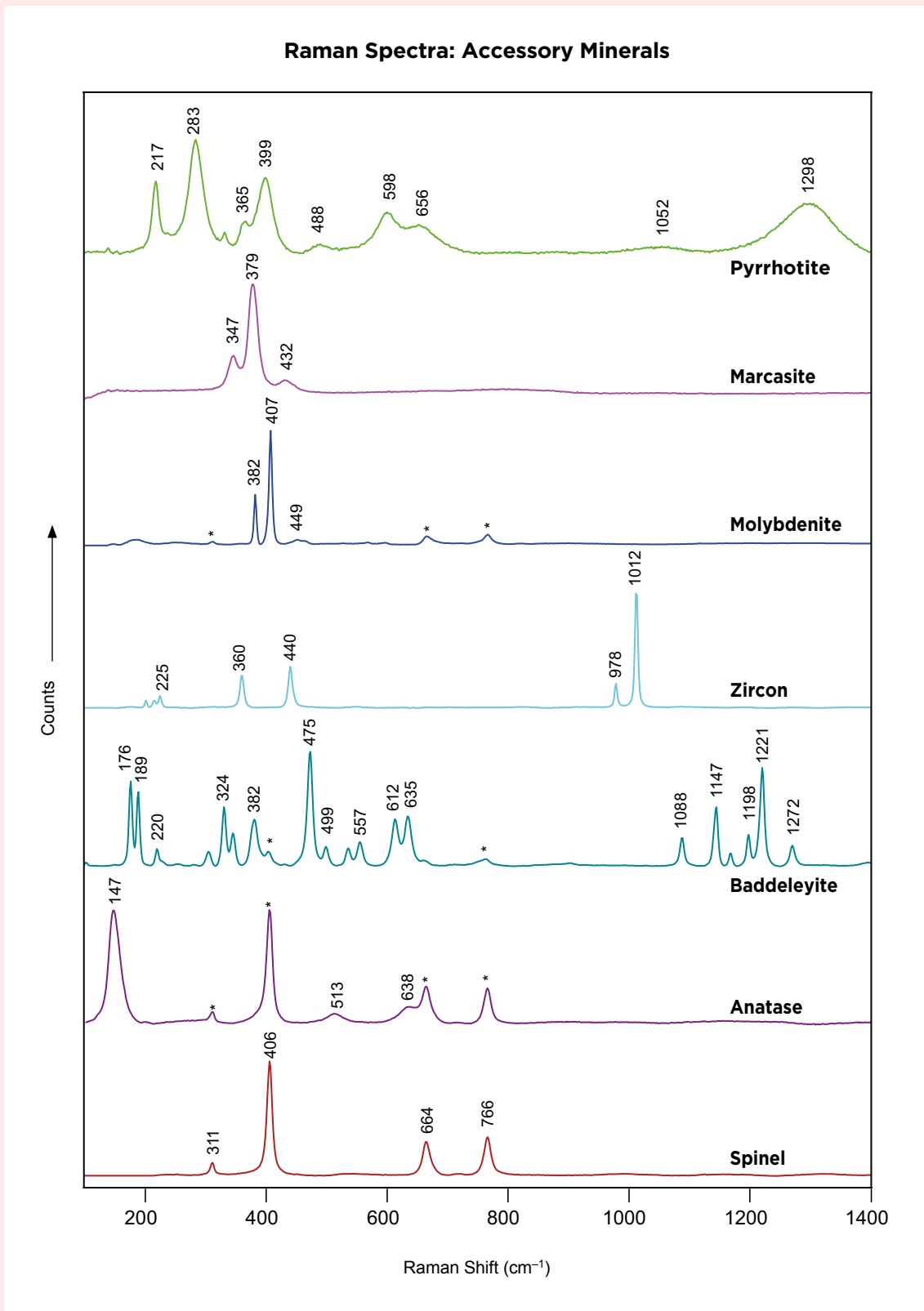
APPENDIX



Representative Raman spectra are shown for carbonate mineral inclusions analysed in our samples from Mogok, together with a spectrum of the host spinel. Peaks in the inclusion spectra that are marked with an asterisk are from the host spinel.



Representative Raman spectra are shown for various silicate mineral inclusions analysed in our samples from Mogok, together with a spectrum of the host spinel. Peaks in the inclusion spectra that are marked with an asterisk are from the host spinel.



Representative Raman spectra are shown for various accessory mineral inclusions analysed in our samples from Mogok, together with a spectrum of the host spinel. Peaks in the inclusion spectra that are marked with an asterisk are from the host spinel.



Figure 1: Peridots from Yiqisong, Jilin Province, China (left), and from North Korea (right) were investigated for this article. The Yiqisong sample weighs 2.15 ct and displays a yellowish green colour, while the North Korean peridot is 2.75 ct and is more brownish green. Photo by Z. Zhang.

Characterisation of Peridot from China's Jilin Province and from North Korea

Zhiqing Zhang, Min Ye and Andy H. Shen

ABSTRACT: Peridot from Neogene olivine-bearing basalt in the Yiqisong District of Jilin Province, China, and from North Korea are available in the global gem market. We characterised 100 stones from each of these two localities, and found similar RI, birefringence and SG values, but slightly different colour ranges, UV-Vis-NIR spectral characteristics and internal features. The most common inclusions in both the Yiqisong and North Korean samples were 'lily pad' discoid fractures; also present were diopside, chromite, enstatite and lizardite (the latter two were observed only in Yiqisong peridot). Chemical analyses indicated that most samples had forsterite contents ranging from 89.4 to 92.2 mol.%, with a trend toward slightly higher Fe in the North Korean samples. Statistical processing of the trace-element data with Fisher linear discriminant analysis (Fisher-LDA) showed that Al, Zn, Ti, Na and Ge are useful for separating peridot from these two localities.

The Journal of Gemmology, 36(5), 2019, pp. 436–446, <http://doi.org/10.15506/JoG.2019.36.5.436>
© 2019 Gem-A (The Gemmological Association of Great Britain)

Gem-quality peridot has been reported in the gemmological literature from several sources, including Zabargad Island, Egypt (Gübelin 1981); San Carlos, Arizona, USA (Koivula 1981); Kilbourne Hole, New Mexico, USA (Fuhrbach 1992); Tanzania (Stockton & Manson 1983); Kohistan, Pakistan (Jan & Khan 1996); Sardinia, Italy (Adamo *et al.* 2009); and the Central Highlands of

Vietnam (Huong *et al.* 2012; Nguyen *et al.* 2016). In addition, pallasitic peridot has been investigated to separate it from its terrestrial counterpart (Shen *et al.* 2011). Furuya & Davies (2015) used statistical analysis of trace-element data to establish the geographic origin of peridot from some locations.

Chinese peridot has been known since the 1980s, initially from the Zhangjiakou-Xuanhua area of Hebei

Province (Koivula & Fryer 1986) and later from the Jiaohe and Baishan areas in Jilin Province (Wang 1996; Liu 2001; Chen & Xing 2011; Gu *et al.* 2015). In 2016, a new deposit of gem-quality peridot (see, e.g., the left-hand stone in Figure 1) was discovered in the Yiqisong District (43°47' N, 127°56' E), located approximately 5 km north-east of the previously known Dashihe peridot mine near Jiaohe (Figure 2). The deposit covers an area of ~5.1 km² and is hosted by Neogene basalts in the Dunhua-Mishan fault zone (Wang 1996, 2017). Known as the Yiqisong South Mountain mine, this deposit has been worked since 2016 by Yanbian Fuli Peridot Mining Industry Co. Ltd (Dunhua, Jilin, China) using the room-and-pillar method of underground mining. According to an unpublished company report supplied by Yanbian Fuli Peridot Mining Industry Co. Ltd, the reserves are estimated at approximately 450 tonnes of gem-quality peridot. The rough material is fractured but contains transparent areas and can attain large sizes of 3–10 cm and exceptionally up to 25 cm (Wang 2017). The company report indicates that the amount of faceted peridot could reach 20 million carats per year. The stones are sold under the Fuli Jewelry brand.

Because of the high quality of Yiqisong peridot (i.e. attractive yellowish green colour and high clarity) and its significant mineral reserves, it is expected to play an

increasingly important role in the global gem market. However, some traders and consumers are confusing Yiqisong peridot with that from North Korea (again, see Figure 1). Although details of the North Korean peridot deposit are not well known, its regional setting places it within the Rangrim massif (cf. Yang *et al.* 2010), and mining takes place in the Changyon District of South Hwanghae Province (see Figure 2).

To provide a scientifically based separation of peridot from the two localities, we performed a detailed gemmological characterisation on numerous samples from Yiqisong and North Korea, focusing on their inclusions, as well as on spectroscopic and chemical data, and the latter were processed using statistical analysis.

MATERIALS AND METHODS

We studied 200 samples of peridot from Yiqisong and North Korea, consisting of 50 rough and 50 faceted stones from each locality (Figure 3). The rough was prepared by polishing windows to facilitate observation of the inclusions. Standard gemmological testing and spectroscopy were performed at the Gemmological Institute of China University of Geosciences (Wuhan).

Colour analysis was performed by taking digital photographs of all rough samples using a Nikon D810

Figure 2: The Yiqisong peridot deposit is located in Jilin Province, north-eastern China, approximately 5 km from the Dashihe peridot mine and ~200 km from another Chinese peridot locality near Baishan. An additional peridot deposit in North Korea is located near the Yellow Sea in South Hwanghae Province. The different colours of the inset map refer to administrative divisions of Jilin Province (yellowish green = Jilin City and pink = Yanbian Autonomous Prefecture).



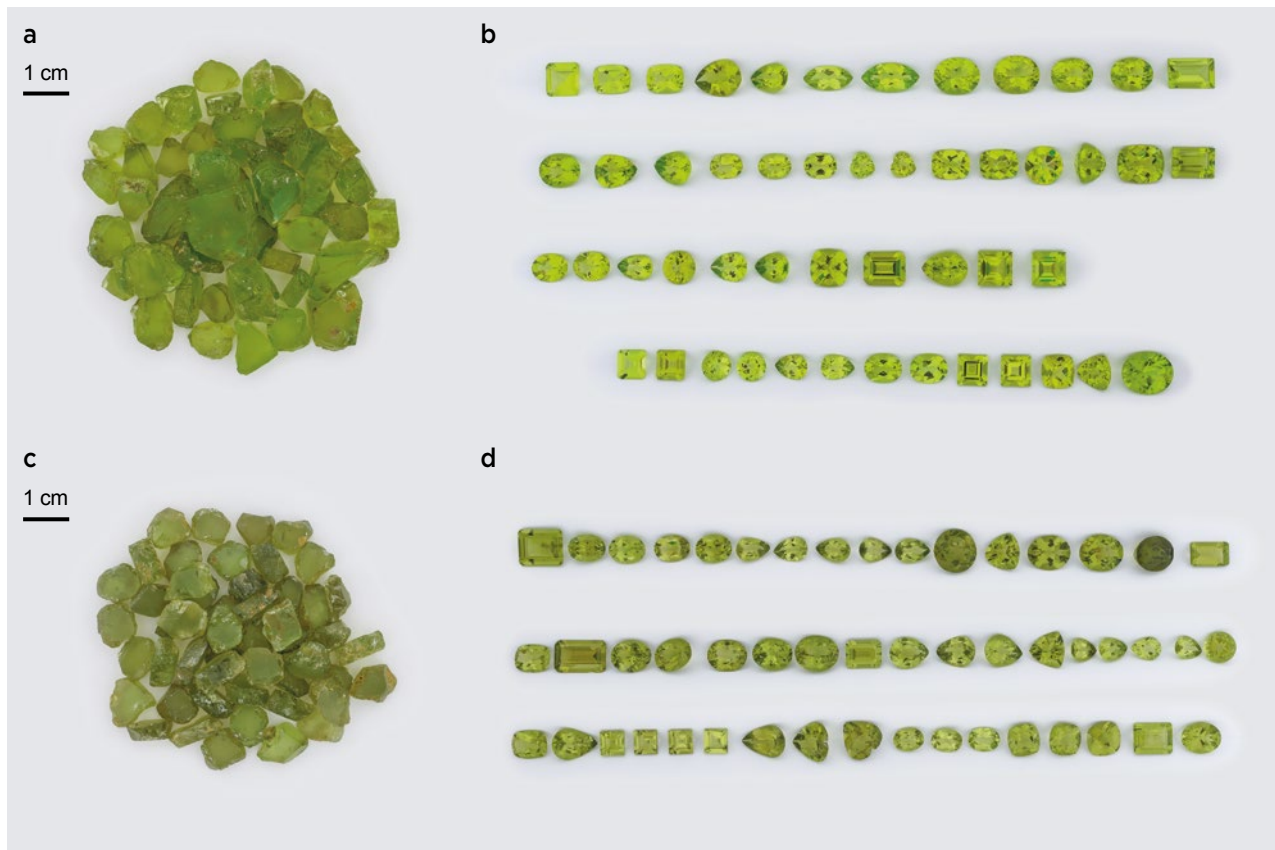


Figure 3: A total of 200 peridot samples from Yiqisong (a: rough and b: faceted) and North Korea (c: rough and d: faceted) were included in this study. Photos by M. Ye.

camera in a light box (6,500 K colour temperature), and camera settings were calibrated using a ColorChecker Gray Balance card. We then used Adobe Photoshop to determine colour parameters ($L^*a^*b^*$; see, e.g., Berns 2000) with the 5-by-5 Average colour picker.

Refractive indices were measured on 20 faceted samples (10 from each locality) with a GR-6 refractometer produced by Wuhan Xueyuan Jewelry Technology Co. Ltd, and SG values were determined hydrostatically using a Sartorius BT 224 S balance. Microscopic observations and photomicrography of internal features were done with a Leica M205 A microscope equipped with transmitted and fibre-optic illumination.

Raman spectra of inclusions were collected in the range of $1550\text{--}100\text{ cm}^{-1}$ using a Bruker Senterra R200-L Raman microspectrometer equipped with a 532 nm laser. The laser output power was 20 mW and the spot size was $50\text{ }\mu\text{m}$. The inclusions were identified using Opus and CrystalSleuth software, and compared to the RRUFF database of mineral Raman spectra (<http://rruff.info>).

Polarised ultraviolet-visible-near infrared (UV-Vis-NIR) spectra were obtained on two rough samples (one each from Yiqisong and North Korea) in the $360\text{--}1650$

nm range with a resolution of 0.5 nm using a JASCO MSV-5200 spectrometer. Spectra were collected along all three crystallographic directions.

Major-element chemical analysis was performed on 10 rough samples (five from each locality, selected as representative by their trace-element data) using a JEOL JXA-8230 electron probe microanalyser (EPMA) in the Center for Global Tectonics, School of Earth Sciences at China University of Geosciences (Wuhan). The following operating conditions were employed: 15 kV accelerating voltage, 20 nA current and a $3\text{ }\mu\text{m}$ beam diameter.

Trace-element analysis was done on all the samples by laser ablation inductively coupled plasma mass spectrometry (LA-ICP-MS) at Wuhan Sample Solution Analytical Technology Co. Ltd, using an Agilent 7700 Series ICP-MS coupled with a GeoLasPro 193 nm excimer laser. The laser employed a 5 Hz pulse rate and a $44\text{ }\mu\text{m}$ diameter spot size. Reference materials included USGS (BCR-2G, BHVO-2G and BIR-1G) and NIST (SRM 610) glasses, and ^{29}Si was used as the normalised element to calculate the concentrations of 55 trace elements with ICPMSDataCal software (Liu *et al.* 2008).

Statistical processing of the trace-element data

was done with the Fisher linear discriminant analysis (Fisher-LDA) model (Fisher 1936; Hastie *et al.* 2009; Blodgett & Shen 2011). We randomly selected 40 samples (20 from each origin) as ‘unknowns’ and left these samples out while building the LDA model from 160 ‘known location’ samples, using the SPSS statistical analysis software platform (Denis 2018). The results of discriminant analysis were expressed as two linear equations called discriminant functions (or classification functions) and plotted in diagrams.

RESULTS

As shown in Table I, the Yiqisong and North Korean samples had similar RI, birefringence and SG values, but there were some differences in their colour, pleochroism and internal features.

Colour

In general, the Yiqisong samples were yellowish green (Figure 3a, b), while many of the North Korean ones were brownish green (Figure 3c, d) and therefore they also showed brownish pleochroic colours. The colours were plotted in $L^*a^*b^*$ colour space (defined by the International Commission on Illumination [CIE] in 1976), which expresses colour as three numerical values: L^* for lightness, and a^* and b^* for saturation of green-red and blue-yellow colour components, respectively (Berns 2000). As shown in Figure 4a, most stones from

Yiqisong had a somewhat higher L^* value than those from North Korea, which means Yiqisong peridot tends to be brighter than material from North Korea. In Figure 4b, the samples from Yiqisong tended to have lower a^* values, which demonstrates that they are inclined to show less brownish green.

Table I: Gemmological properties of peridots from Yiqisong (China) and North Korea.

Property	Yiqisong, China	North Korea
Colour	Light yellowish green to darker yellowish green	Brownish green to darker brownish green
Pleochroism	Weak: light yellowish green to yellowish green	Weak: light brownish green to brownish green
Diaphaneity	Transparent	Transparent to translucent
RI	1.654-1.695	1.654-1.694
Birefringence	0.035-0.038	0.036-0.038
SG	3.33-3.36	3.33-3.38
Internal features	‘Lily pad’ inclusions; partially healed fractures; chromite, diopside, enstatite and lizardite (in one sample) inclusions; brown staining	‘Lily pad’ inclusions; partially healed fractures and smoke-like veils; chromite and diopside inclusions; brown staining

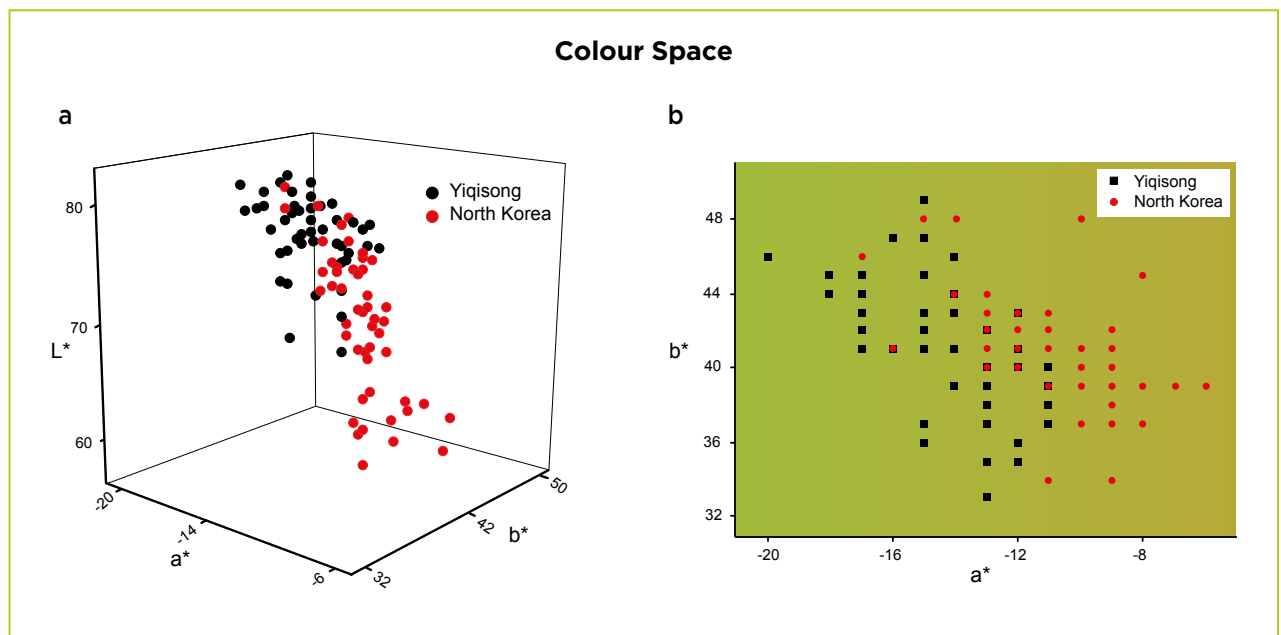


Figure 4: (a) A three-dimensional scatter diagram shows how representative peridot samples from Yiqisong and North Korea plot in L^*,a^*,b^* colour space. (b) A plot of a^* vs. b^* for $L^* = 75\%$ shows that peridot samples from Yiqisong generally have lower a^* values, indicative of less brown colouration than the North Korean samples.

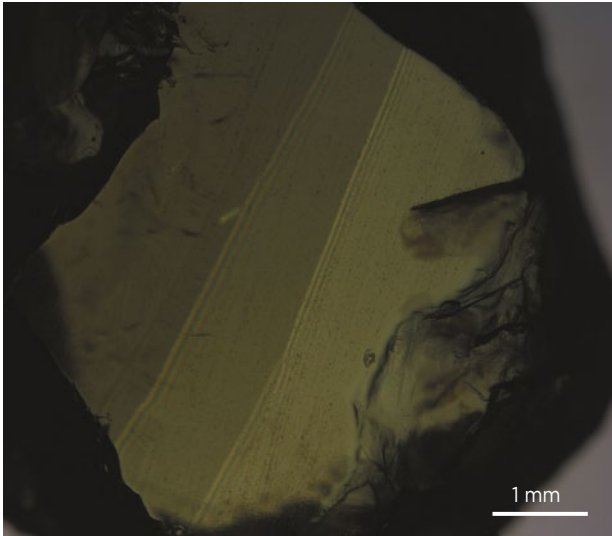


Figure 5: A rough peridot sample from Yiqisong shows wavy extinction between crossed polarisers. Photomicrograph by Z. Zhang.

Internal Features

Some stones from both localities showed wavy extinction between crossed polarisers (Figure 5), which is probably due to plastic deformation that occurred during formation and/or uplift.

In peridot from Yiqisong, inclusions most commonly consisted of ‘lily pads’ (Figure 6a). This feature is formed by a decrepitation halo, usually surrounding a rounded transparent negative crystal (Gübelin & Koivula 1986) or a dark chromite inclusion (Figure 6b). The surrounding decrepitation halo consisted of two- or three-dimensional

planes with radial or geometric shapes. Partially healed fractures were also common in Yiqisong peridot, showing forms such as feathers, veils, etc. (Figure 6c). We did not observe any smoke-like veils in Yiqisong peridot. Occasionally, isolated dark inclusions of chromite (identified by Raman analysis) occurred as needles and flakes, and some samples also contained green and brownish green crystals (Figure 6d, e) that were identified by Raman microspectroscopy as diopside and enstatite, respectively. One Yiqisong sample contained a dark inclusion that proved to be lizardite (Figure 7).

The North Korean peridot also contained ‘lily pads’ which, in most cases, consisted of a dark crystal (probably chromite) in the centre of one or more decrepitation halos (Figure 8a, b). Partially healed fractures showing feather- and veil-like patterns were common (Figure 8c), and smoke-like veils were often seen in faceted samples of North Korean peridot (Figure 8d). Isolated dark chromite inclusions were relatively more common than in Yiqisong peridot, and they formed octahedral, needle-like or columnar crystals. In addition, isolated transparent green diopside inclusions were also present (Figure 8e). Rough samples of North Korean peridot often showed brownish yellow staining.

Absorption Spectra

The UV-Vis-NIR absorption spectra (Figure 9) of peridots from Yiqisong and North Korea showed differences that were consistent with their colour appearance. In the visible-light region, Yiqisong stones had a transmission

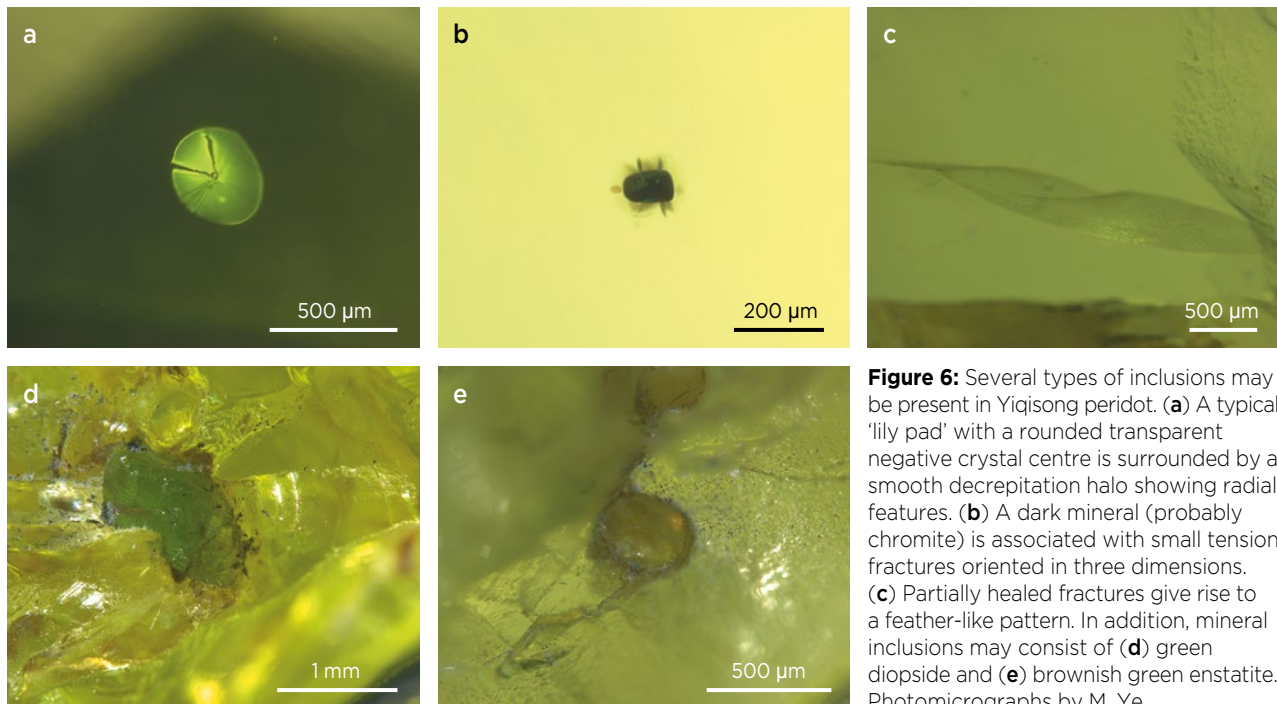


Figure 6: Several types of inclusions may be present in Yiqisong peridot. (a) A typical ‘lily pad’ with a rounded transparent negative crystal centre is surrounded by a smooth decrepitation halo showing radial features. (b) A dark mineral (probably chromite) is associated with small tension fractures oriented in three dimensions. (c) Partially healed fractures give rise to a feather-like pattern. In addition, mineral inclusions may consist of (d) green diopside and (e) brownish green enstatite. Photomicrographs by M. Ye.

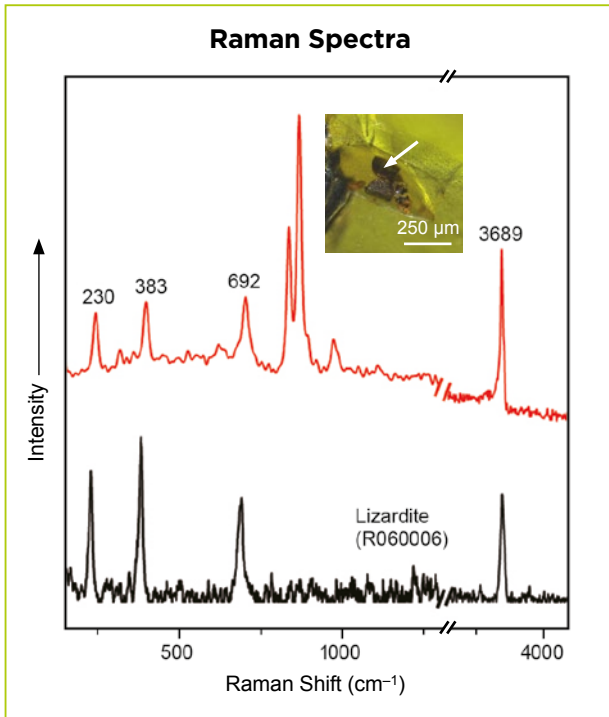


Figure 7: Raman peaks at 230, 383, 692 and 3689 cm^{-1} show clearly that a dark inclusion in a peridot from Yiqisong is lizardite (see spectrum of RRUFF sample R060006 for comparison). This common serpentine species forms as a secondary mineral during metamorphism at relatively low temperatures. Inset photomicrograph by M. Ye.

window centred at 557 nm resulting in a yellowish green colour, while in North Korean ones this window was centred at 565 nm corresponding to a brownish green colour. A broad band at 635 nm was present in all of

the spectra and an additional broad absorption at 528 nm was recorded mainly in the β direction. Peaks at 426, ~450, 470 and 490 nm were also noted, particularly in the North Korean samples, and they showed differences in relative absorbance along the α , β and γ directions. In the NIR region, samples from both localities presented similar absorption bands located near 862 nm (α direction) and at 1047 and 1226 nm (α and γ directions). In the β direction, the main band was centred at 1066 nm in Yiqisong peridot, while in North Korean samples it tended to occur at longer wavelengths near 1079 nm.

Chemical Composition

Major Elements. The composition of major elements is listed in Table II. Samples from Yiqisong showed a narrower range of Fe content compared to those from North Korea, with a forsterite component of 90.7–92.2 mol.% for Yiqisong versus 89.4–91.9 mol.% for North Korean peridot.

Trace Elements. The trace-element content of peridots from the two origins was quite similar overall (Table III), but in general the Yiqisong stones contained less Al and Zn than the North Korean samples. Nickel was the most abundant trace element, ranging from 2692 to 3240 ppm (2984 ppm on average) in Yiqisong samples and from 2291 to 3127 ppm (2887 ppm on average) in North Korean samples, followed by, in order of decreasing abundance, Mn, Ca, Co, Cr and Al.

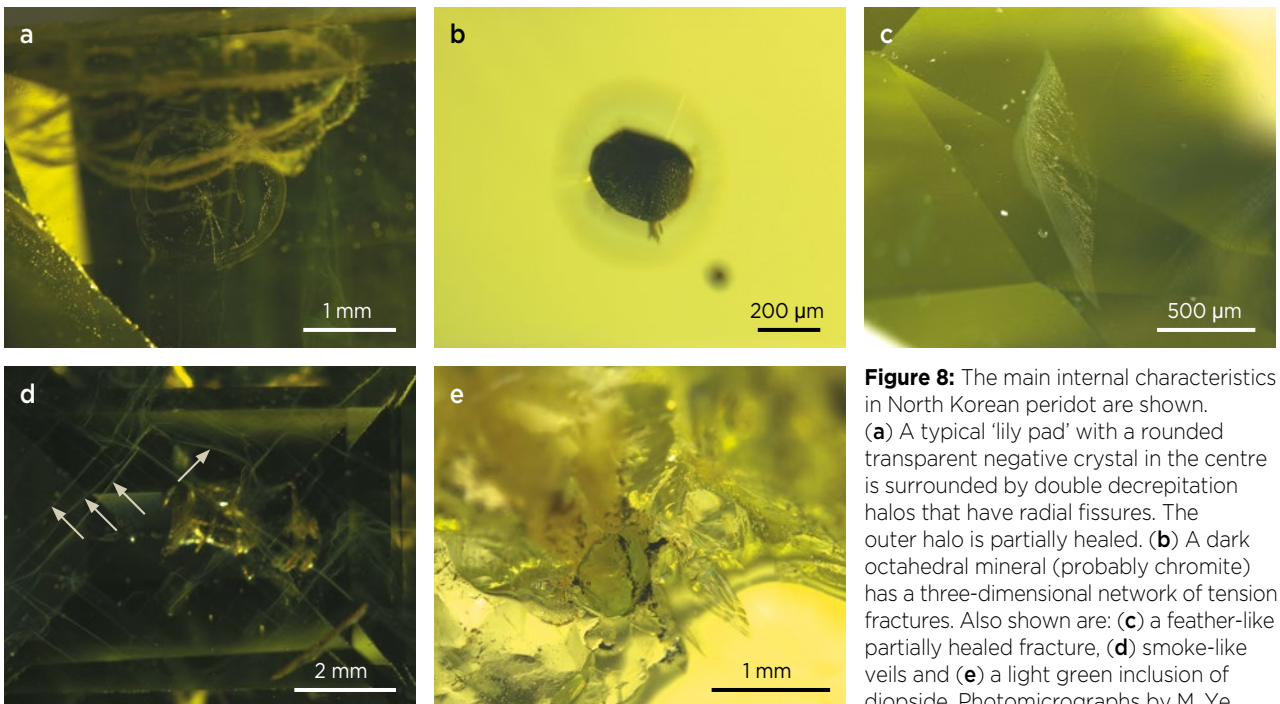


Figure 8: The main internal characteristics in North Korean peridot are shown. (a) A typical ‘lily pad’ with a rounded transparent negative crystal in the centre is surrounded by double decrepitation halos that have radial fissures. The outer halo is partially healed. (b) A dark octahedral mineral (probably chromite) has a three-dimensional network of tension fractures. Also shown are: (c) a feather-like partially healed fracture, (d) smoke-like veils and (e) a light green inclusion of diopside. Photomicrographs by M. Ye.

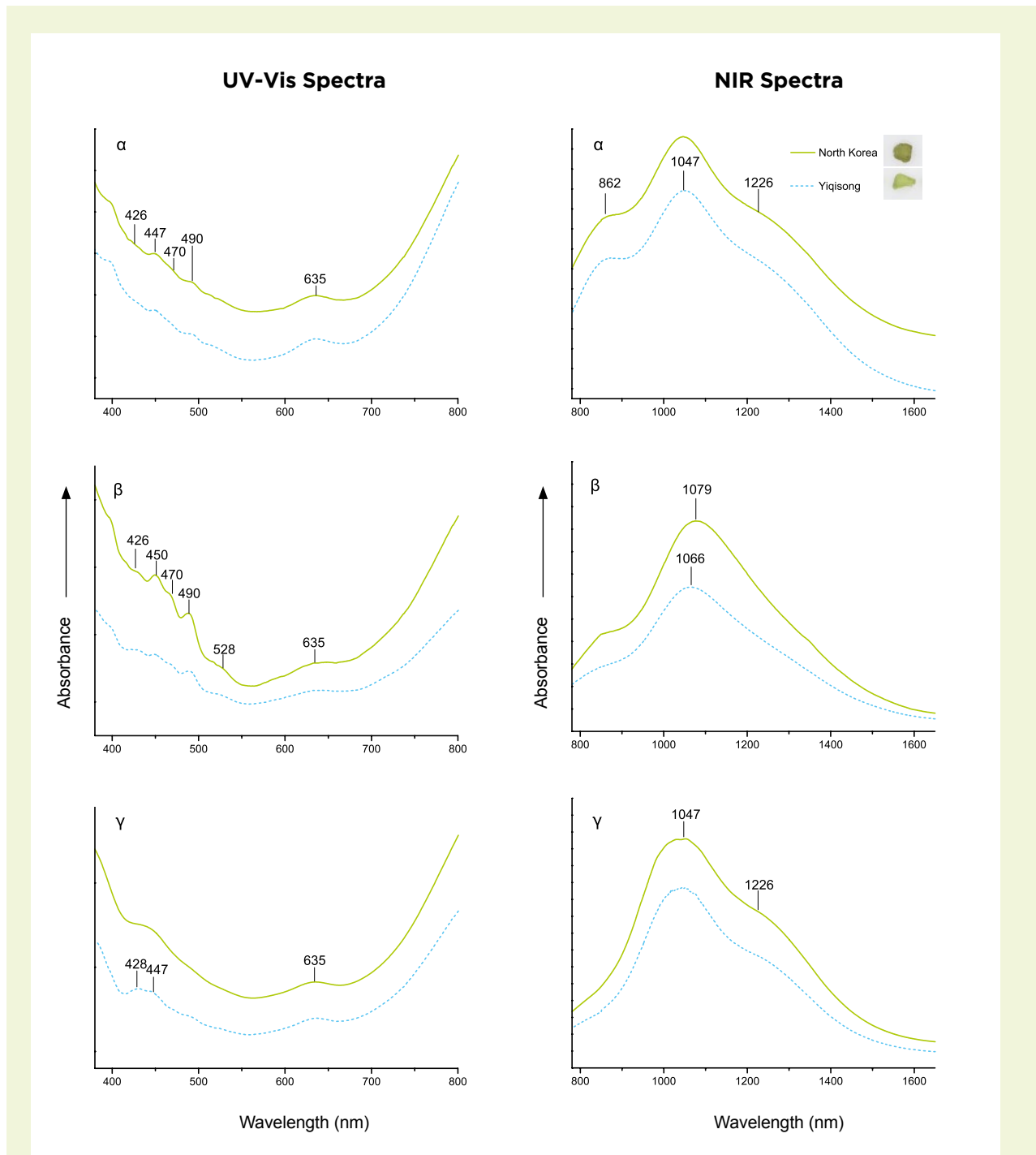


Figure 9: UV-Vis spectra (left) and NIR spectra (right) of peridot samples from Yiqisong and North Korea are shown in α , β and γ directions. All spectra have been shifted vertically for clarity. The approximate path lengths are 1.45 mm for the Yiqisong sample and 1.60 mm for the North Korean peridot.

Fisher-LDA Analysis of Trace-Element Data. For Fisher-LDA statistical analysis, five selected variables were used: Al, Zn, Ti, Na and Ge. Together they provide well-defined fields for peridots from the two origins, with an accuracy of up to 93.8% (cross-validation results). The results gave rise to two linear equations

(discriminant functions):

$$x = -15.146 + (0.060 \times C_{Al}) + (0.511 \times C_{Zn}) + (0.105 \times C_{Ti}) - (0.033 \times C_{Na}) + (3.850 \times C_{Ge})$$

$$y = -30.279 + (0.142 \times C_{Al}) + (0.584 \times C_{Zn}) + (0.228 \times C_{Ti}) + (0.049 \times C_{Na}) + (1.958 \times C_{Ge})$$

Table II: Chemical composition of peridots from Yiqisong (China) and North Korea by EPMA.*

Oxide (wt.%)	Yiqisong, China	North Korea
SiO ₂	41.10–41.99 (41.48)	41.26–42.10 (41.69)
FeO	7.42–8.76 (7.97)	7.81–10.19 (8.77)
MgO	48.03–49.87 (49.09)	48.14–49.51 (48.66)
Total	98.00–99.64 (98.53)	98.00–100.17 (99.12)
Average composition	Fo _{91.7} :Fa _{8.3}	Fo _{90.8} :Fa _{9.2}

* Average amounts are shown in parentheses. Abbreviations: Fo = forsterite, Fa = fayalite.

Table III: Trace-element concentration range of peridots from Yiqisong (China) and North Korea by LA-ICP-MS.*

Element (ppmw)	Yiqisong, China	North Korea
Li	0.92–2.21 (1.37)	0.90–3.94 (1.54)
Na	7.46–77.7 (29.8)	13.8–123 (71.1)
Al	35.4–129 (54.5)	55.2–231 (118)
Ca	96.4–822 (343)	216–1208 (495)
Sc	2.32–6.04 (4.00)	2.90–6.53 (4.34)
Ti	0.84–28.0 (7.17)	1.93–41.9 (15.9)
V	1.55–4.01 (2.49)	1.22–5.57 (3.10)
Cr	37.3–199 (93.0)	29.1–205 (126)
Mn	934–1093 (1002)	958–1489 (1104)
Co	128–144 (136)	127–148 (137)
Ni	2692–3240 (2984)	2291–3127 (2887)
Cu	<7.73 (1.33)	0.15–21.8 (1.91)
Zn	38.0–56.0 (44.9)	44.0–116 (56.3)
Ge	<1.69 (0.075)	0.062–1.48 (0.72)
Sn	<5.81 (1.88)	0.13–7.47 (2.06)

* Average amounts are shown in parentheses.

Figure 10 plots the resulting Fisher-LDA classification function values (x,y) for Yiqisong and North Korean peridots based on the LA-ICP-MS data. We also plotted the 40 ‘unknown’ samples (20 from each locality that we set aside for this purpose) on the two diagrams to check for accuracy. Every Yiqisong and North Korean ‘unknown’ sample fell into its respective oval field. Only four Yiqisong ‘unknown’ and seven North Korean ‘unknown’ samples fell into the overlapping area covered by fields from both localities. Although this is undesirable, the fact that these 11 spots still fell within their respective oval regions (and none of them fell outside of their corresponding field) indicates that our statistical model is valid. A table showing the results from both the initial and cross-validation stages of the Fisher-LDA analysis is available in the online data depository on *The Journal's* website.

DISCUSSION

The RI, birefringence and SG values for peridot samples from Yiqisong and North Korea (again, see Table I) are similar to those previously reported for peridot from some sources (i.e. Egypt, USA [Arizona], China, Vietnam and Italy; see references given in the Introduction). However, the SG range of our samples from both localities is lower than that of peridot from New Mexico and Pakistan (again, see references given in the Introduction). Chinese peridot (i.e. from the Zhangjiakou, Baishan and Jiaohe areas) is typically yellowish green, while North Korean peridot appears more like some of the material from Arizona, with a somewhat brownish green colour.

Internal features such as ‘lily pads’ (associated with negative crystals or chromite grains), crystals of chromite or green diopside, and veil-like partially healed fractures have also been observed in peridots from various origins. The lizardite that we documented in one peridot from Yiqisong may provide evidence of serpentinisation (Li 1993).

Since peridot is an idiochromatic gem material, the typical features of its UV-Vis spectra (Figure 9) are mainly due to the presence of Fe²⁺. Specifically, bands near 470, 490 and 526 nm are caused by Fe²⁺, while those at 426 and 635 nm are likely due to Ni²⁺, and the feature at ~450 nm might be associated with Fe²⁺ and Mn²⁺ (Burns 1970; Rossman *et al.* 1981). Since Fe²⁺ is mainly responsible for the colouration in peridot (Tang *et al.* 2012, 2016), we are inclined to infer that the 447 nm feature is related to Fe²⁺ rather than Mn²⁺. In the NIR region, along the β direction, the main band associated with Fe²⁺ content at

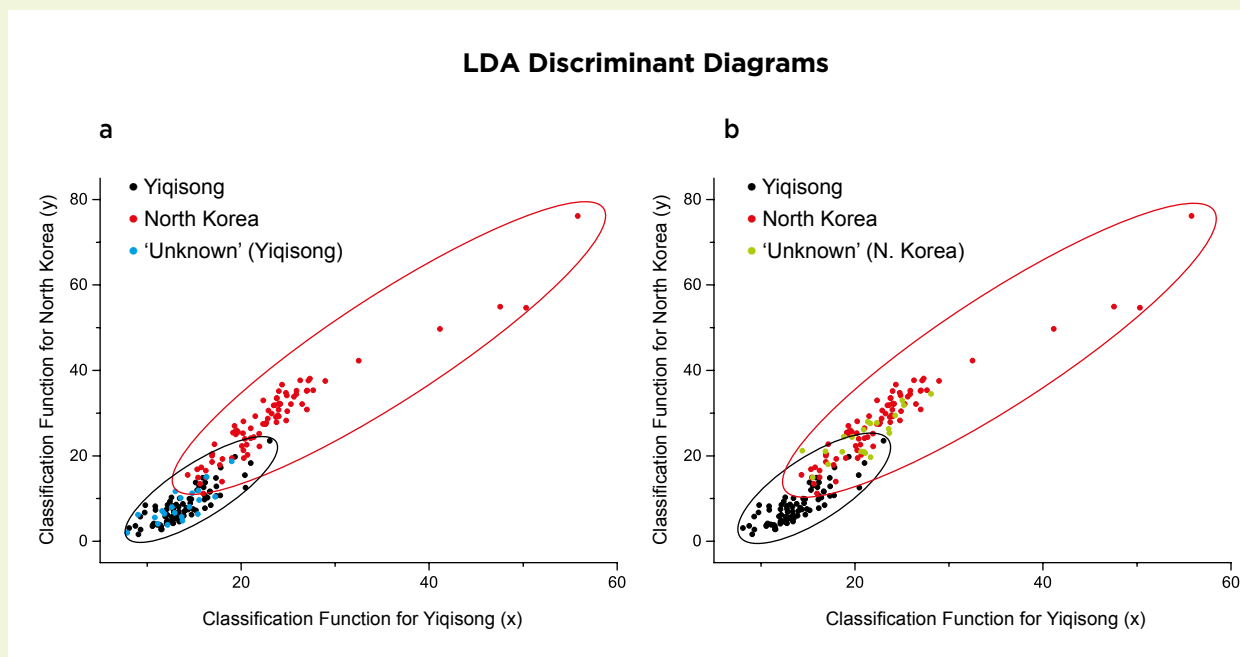


Figure 10: Scatter diagrams of Fisher-LDA classification function values (x , y) are shown for Yiqisong and North Korean peridot based on LA-ICP-MS data. Although the fields show some overlap between the two localities, data for randomly selected 'unknown' samples from Yiqisong (a) and North Korea (b) plot with their respective groups.

1066 nm in Yiqisong peridot shifts to longer wavelengths near 1079 nm in North Korean material, consistent with the greater Fe content measured in those stones by EPMA (see Table II; Burns 1970).

The chemical constituents of olivine fall along the forsterite (Mg_2SiO_4 ; abbreviated Fo) to fayalite (Fe_2SiO_4 ; expressed as Fa) solid-solution series, in which Mg^{2+} and Fe^{2+} can substitute for each other completely. Gem-quality peridot typically contains about 8–10% FeO (Gübelin 1981), otherwise reported as falling within the ranges of Fo_{88-93} (Jan & Khan 1996), $\text{Fo}_{88.3-92.0}$ (Embey-Isztin & Dobosi 2007) or $\text{Fo}_{88.6-96.0}$ (Shen *et al.* 2011). Our samples from both localities correspond to $\text{Fo}_{89.4-92.2}$, consistent with the ranges shown by gem-quality peridot from elsewhere.

Trace-element data and statistical analysis provided reliable means to help separate peridot from Yiqisong and North Korea. The cross-validation results indicated a 93.8% accuracy, while our 40 randomly selected 'unknown' samples all fell in their correct fields (as plotted in Figure 10). However, 11 of them plotted in the overlapping area for the two localities, supporting the fact that any final conclusion of a sample's origin should be drawn from a combination of characteristics, including colouration, distinctive inclusions and chemical evidence. The statistical analysis of

trace-element chemistry is just one piece of evidence to reach a sensible conclusion.

CONCLUSIONS

Peridot from Yiqisong (e.g. Figure 11) and North Korea have gemmological characteristics and inclusion features similar to those of peridot from other deposits worldwide. In addition, stones from both localities have forsterite contents that are typical for gem-quality peridot. While both Yiqisong and North Korean peridot have the well-known 'lily pad' inclusions, smoke-like veils were seen only in North Korean samples, whereas enstatite and lizardite were documented only in peridot from Yiqisong. Comprehensive statistical analysis (i.e. Fisher-LDA) of LA-ICP-MS data has shown that most peridot from these two localities can be separated by their trace-element contents.

In conclusion, the key factors for separating Yiqisong from North Korean peridot are: (1) colour, (2) the distinctive inclusions and (3) trace-element composition combined with Fisher-LDA statistical analysis. To successfully determine the origin of a sample, it is important to consider a combination of information covering all of these aspects so that a consistent set of data supports the conclusion.



Figure 11: The centre stone in this pendant is a peridot from Yiqisong that weighs 4.35 ct. Photo courtesy of Yanbian Fuli Olivine Mining Co. Ltd.

REFERENCES

- Adamo, I., Bocchio, R., Pavese, A. & Prosperi, L. 2009. Characterization of peridot from Sardinia, Italy. *Gems & Gemology*, **45**(2), 130–133, <http://doi.org/10.5741/gems.45.2.130>.
- Berns, R.S. 2000. *Billmeyer and Saltzman's Principles of Color Technology*. 3rd edn. John Wiley & Sons, New York, New York, USA, 272 pp.
- Blodgett, T. & Shen, A.H. 2011. Application of discriminant analysis in gemology: Country-of-origin separation in colored stones and distinguishing HPHT-treated diamonds. *Gems & Gemology*, **47**(2), 145.
- Burns, R.G. 1970. Crystal field spectra and evidence of cation ordering in olivine minerals. *American Mineralogist*, **55**(9–10), 1608–1632.
- Chen, J. & Xing, C. 2011. Metallogeny of the gem deposits in basalt in Baishan area, Jilin Province. *Geology and Resources*, **20**(4), 255–257, <https://doi.org/10.13686/j.cnki.dzyzy.2011.04.003>.
- Denis, D.J. 2018. *SPSS Data Analysis for Univariate, Bivariate, and Multivariate Statistics*. Wiley, Hoboken, New Jersey, USA, 224 pp.
- Embey-Isztin, A. & Dobosi, G. 2007. Composition of olivines in the young alkali basalts and their peridotite xenoliths from the Pannonian Basin. *Annales Historico-Naturales Musei Nationalis Hungarici*, **99**, 5–22.
- Fisher, R.A. 1936. The use of multiple measurements in taxonomic problems. *Annals of Human Genetics*, **7**(2), 179–188, <https://doi.org/10.1111/j.1469-1809.1936.tb02137.x>.

- Fuhrbach, J.R. 1992. Kilbourne Hole peridot. *Gems & Gemology*, **28**(1), 16–27, <http://doi.org/10.5741/gems.28.1.16>.
- Furuya, M. & Davies, S. 2015. Gemological features of pallasitic peridot of six different meteorites. *34th International Gemmological Conference*, Vilnius, Lithuania, 27–30 August, 85–88.
- Gu, J., Zhao, Q., Lai, J., Wang, C. & Yin, Z. 2015. Gemmological characteristic of peridot from Jiaohe, Jilin Province. *Journal of Gems & Gemmology*, **17**(5), 24–31.
- Gübelin, E. 1981. Zabargad: The ancient peridot island in the Red Sea. *Gems & Gemology*, **17**(1), 2–8, <http://doi.org/10.5741/gems.17.1.2>.
- Gübelin, E.J. & Koivula, J.I. 1986. *Photoatlas of Inclusions in Gemstones*. ABC Edition, Zurich, Switzerland, 532 pp.
- Hastie, T., Tibshirani, R. & Friedman, J. 2009. *The Elements of Statistical Learning*. 2nd edn. Springer Nature, New York, New York, USA, 763 pp.
- Huong, L.T.-T., Häger, T., Hofmeister, W., Hauzenberger, C., Schwarz, D., Van Long, P., Wehrmeister, U., Khoi, N.N. & Nhung, N.T. 2012. Gemstones from Vietnam: An update. *Gems & Gemology*, **48**(3), 158–176, <http://doi.org/10.5741/gems.48.3.158>.
- Jan, M.Q. & Khan, M.A. 1996. Petrology of gem peridot from Sapat mafic-ultramafic complex, Kohistan, NW Himalaya. *Geological Bulletin of the University of Peshawar*, **29**, 17–26.
- Koivula, J.I. 1981. San Carlos peridot. *Gems & Gemology*, **17**(4), 205–214, <http://doi.org/10.5741/gems.17.4.205>.
- Koivula, J.I. & Fryer, C.W. 1986. The gemmological characteristics of Chinese peridot. *Gems & Gemology*, **22**(1), 38–40, <http://doi.org/10.5741/gems.22.1.38>.
- Li, M. 1993. Thermodynamic investigation of the serpentinization, talcization and brucitization for the forsterite and clinoenstatite. *Journal of Mineralogy and Petrology*, **13**(3), 81–85.
- Liu, R. 2001. Geologic feature and ore-forming conditions of Jiaohe peridot gem deposit in Jilin. *Geology and Prospecting*, **37**(6), 17–19.
- Liu, Y., Hu, Z., Gao, S., Günther, D., Xu, J., Gao, C. & Chen, H. 2008. *In situ* analysis of major and trace elements of anhydrous minerals by LA-ICP-MS without applying an internal standard. *Chemical Geology*, **257**(1–2), 34–43, <http://doi.org/10.1016/j.chemgeo.2008.08.004>.
- Nguyen, T.M.T., Hauzenberger, C., Nguyen, N.K., Cong, T.D., Chu, V.L., Nguyen, T.M., Nguyen, H. & Häger, T. 2016. Peridot from the Central Highlands of Vietnam: Properties, origin, and formation. *Gems & Gemology*, **52**(3), 276–287, <http://doi.org/10.5741/gems.52.3.276>.
- Rossmann, G.R., Shannon, R.D. & Waring, R.K. 1981. Origin of the yellow colour of complex nickel oxides. *Journal of Solid State Chemistry*, **39**(3), 277–287, [http://doi.org/10.1016/0022-4596\(81\)90261-9](http://doi.org/10.1016/0022-4596(81)90261-9).
- Shen, A.H., Koivula, J.I. & Shigley, J.E. 2011. Identification of extraterrestrial peridot by trace elements. *Gems & Gemology*, **47**(3), 208–213, <http://doi.org/10.5741/gems.47.3.208>.
- Stockton, C.M. & Manson, D.V. 1983. Peridot from Tanzania. *Gems & Gemology*, **19**(2), 103–107, <http://doi.org/10.5741/gems.19.2.103>.
- Tang, W., Guo, Y. & Ma, L. 2012. Influence of Fe²⁺ on the color appearance of yellow-green peridot. *Key Engineering Materials*, **492**, 370–373, <https://doi.org/10.4028/www.scientific.net/KEM.492.370>.
- Tang, J., Guo, Y., Lai, X., Liu, Y. & Wu, Q. 2016. Study on the correlation between Fe²⁺ and peridot's yellow green color and quality evaluation of color based on CIE1976 L*a*b* uniform color space. *5th International Conference on Environment, Materials, Chemistry and Power Electronics*, Zhengzhou, China, 11–12 April, 599–604, <https://doi.org/10.2991/emcpe-16.2016.123>.
- Wang, L. 1996. The occurrence of Dashihe olivine deposit in Jilin Province, China. *Journal of Changchun University of Earth Sciences*, **26**(1), 43–46, <https://doi.org/10.13278/j.cnki.jjuese.1996.01.007>.
- Wang, J. 2017. Geological characteristics and metallogenic rules of peridotite gem mine in Yiqisong district, Dunhua city, Jilin Province (China). *Resource Information and Engineering*, **32**(4), 50–52, <https://doi.org/10.19534/j.cnki.zyxygc.2017.04.024>.
- Yang, J., O'Reilly, S., Walker, R.J., Griffin, W., Wu, F., Zhang, M. & Pearson, N. 2010. Diachronous decratonization of the Sino-Korean craton: Geochemistry of mantle xenoliths from North Korea. *Geology*, **38**(9), 799–802, <https://doi.org/10.1130/G30944.1>.

The Authors

Zhiqing Zhang, Min Ye and Prof. Andy H. Shen

Gemmological Institute and Center for Innovative Gem Testing Technology
China University of Geosciences,
No. 388 Lumo Rd., 430074 Wuhan, China
Email: ahshen1@live.com

Acknowledgements

The authors are grateful to Yanbian Fuli Olivine Mining Co. Ltd for supplying samples and financial support. Special thanks to William Rohtert, geologist and gemologist with SRK Consulting China office in Beijing, for his helpful assistance. Comments from three anonymous reviewers helped improve this article.



PAUL WILD

EXCELLENCE IN
GEMSTONE INNOVATION



SPINEL

*Found in the most famous crown jewels of the world, the treasured spinel
rivals ruby's vibrant colour, is singly refractive and highly transparent.*

MINING • CUTTING • CREATION

PAUL WILD OHG • AUF DER LAY 2 • 55743 KIRSCHWEILER • GERMANY
T: +49.(0)67 81.93 43-0 • F: +49.(0)67 81.93 43-43 • E-MAIL: INFO@PAUL-WILD.DE • WWW.PAUL-WILD.DE

VISIT US AT

The Modern History of Gemstone Faceting in Sri Lanka

Justin K Prim

ABSTRACT: Drawing on information provided by cutters, factory owners and machine manufacturers, this article traces the evolution of gem-cutting technology in Sri Lanka, from the use of traditional machines such as the *hanaporuwa* and the *bannku opa pattalaya*, to the birth of the modern cutting industry that started in the 1970s with the introduction of the Imahashi faceting machine from Japan. Modifications to its design by visionary Sri Lankan companies such as Bandu Wickrama Engineering Works and Sterling Gems & Lapidary provided further innovations that facilitated the introduction of affordable and precision-quality machines into commercial cutting facilities, leading to great improvements in the quality of gemstone faceting in Sri Lanka.

The Journal of Gemmology, 36(5), 2019, pp. 448–455, <http://doi.org/10.15506/JoG.2019.36.5.448>
© 2019 Gem-A (The Gemmological Association of Great Britain)

The art of fashioning stones in Sri Lanka (formerly Ceylon) goes back more than 2,000 years, and gems have been mined on the island for even longer (ICA Congress 2017). Gemstones are deeply tied to Sri Lanka's history, and the island is referenced in many historical texts, from Pliny in 77 AD (Corso *et al.* 1988) to Marco Polo in ~1300 (Moule & Pelliot 1938). Polo tells us, 'You must know that rubies are found in this Island and in no other country in the world but this. They find there also sapphires and topazes and amethysts, and many other stones of price' (Moule & Pelliot 1938). In 1344, the Islamic traveller and scholar Ibn Battuta wrote (Gray 1996, p. 45):

Gems are met with in all localities of the island of Ceylon. In this country the whole of the soil is private property. An individual buys a portion of it and digs to find gems. He comes across stones white blanchéd: in the interior of these the gem is hidden. The owner sends it to the lapidaries who scrape it until it is separated from the stones which conceal it. There are the red (rubies), the yellow (topazes), and the blue (sapphires) which they call neilem (nilem)¹.

The modern history of Sri Lankan gem cutting began in the early 1980s, and its evolution since then has resulted

in dramatic improvements in the faceting of stones there (e.g. Figure 1). Prior to the modern era, a more ancient narrative was in progress that is much harder to pin down. The Sri Lankan cutting industry initially developed around the south-western coastal towns of Galle, Gintota and Beruwala, at a time when the Sri Lankan gem trade was mainly in the hands of Middle Eastern traders who settled in the country between 400 and 800 AD (Ahmed Shareek, pers. comm. April 2017). They had caravans that travelled inland to buy rough from miners in gem-bearing localities such as Ratnapura and Eheliyagoda, and then brought the stones back to the seaports of Colombo and Galle for export on Arab ships (Mahroof 1989).

Efforts to modernise the gem industry in Sri Lanka (e.g. Kularatnam 1975) were mostly unsuccessful until the 1980s. Among the many subsequent developments were important advances in the Sri Lankan gem-cutting industry, which are described here and based on information provided by cutters, factory owners and machine manufacturers. As the industry has developed, it has also grown, and it is now estimated that there are around 15,000 coloured stone cutters in Sri Lanka (National Gem and Jewellery Authority 2014) that facet free-size, calibrated and melee gems for the jewellery and watch industries.

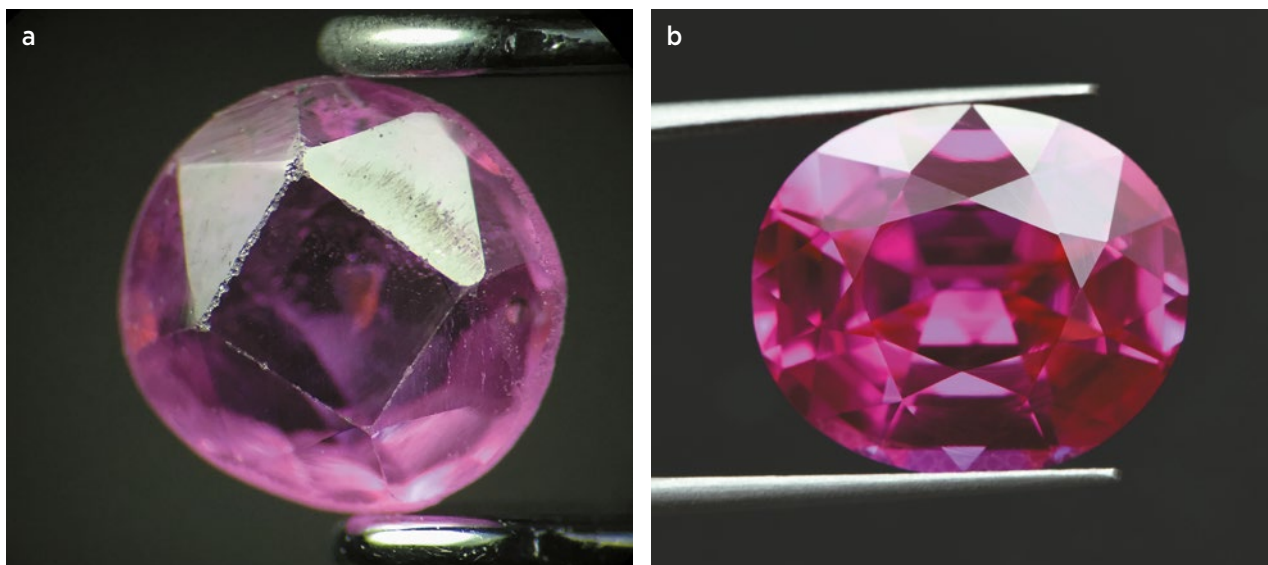


Figure 1: These pink sapphires demonstrate the dramatic improvement in Sri Lankan gem-cutting. (a) This 1.5 ct stone was cut on a *hanaporuwa* cutting machine in the 1970s and shows a so-called native cut appearance. (b) By comparison, this 19 ct gem was faceted on a modern Sri Lankan machine in a well-executed 'Ceylon' mixed-cut style. Photos by J. Prim.

TRADITIONAL CUTTING TECHNIQUES

The traditional machine used for cutting gems in Sri Lanka is called the *hanaporuwa*, and this bow-driven device was typically used to both preform and facet stones (Zwaan 1982). The cutter sits in front of the machine and draws the bow back and forth with his right hand (Figure 2) in order to spin a vertical lap disc that is made of lead embedded with carborundum powder. The stone is pressed against the lap with the left hand. The cutter rotates the stone with his fingers to cut a cabochon, and this is still the preferred method of cutting star sapphires in Sri Lanka. Flat facets are created by holding the stone steady against the lap (ICA Congress 2017; Naji Sammoon, pers. comm. September 2018). Cutting in this freehand style often results in so-called native-cut proportions (e.g. Figure 1a). The stone is then taken to another machine, the *bannku opa pattalaya*, for polishing.

Bannku opa pattalaya literally means 'bench machine'. It consists of a large (20 in., or 51 cm) copper wheel built into a table and connected to a crank with a rope (Figure 3a). One person would crank the machine (e.g. Figure 4), which would cause the copper wheel to spin, and the lapidary would use a handpiece called a *thanaasuwa* (or *sanaasuwa*) to press the stone against the wheel. In Beruwala, until the late 1980s such machines were typically cranked by men from nearby rice fields who made INR10 (GBP1.15) per day (Naji Sammoon, pers. comm. April 2017). The legs of this heavy machine had

to be very strong, and consisted of large wooden timbers (6 × 6 in. or ~15 × 15 cm) that suspended the 5 cm-thick wooden table.

The *thanaasuwa* handpiece represents an interesting example of early faceting technology because we see a similar design—called a *cadran* (or quadrant)—in Prague in 1609 (de Boodt 1609) and in France in the 1670s (e.g. Figure 3b; Félibien 1676). The origin of the handpiece has passed out of living memory in Sri Lanka, but it seems to have been in use for about a



Figure 2: A Sri Lankan lapidary operates a traditional *hanaporuwa* in Ratnapura. The stone is held against a vertical lap, which is spun by drawing the bow back and forth. Photo by J. Prim.

¹ The modern Sinhalese word for sapphire is *nila*.

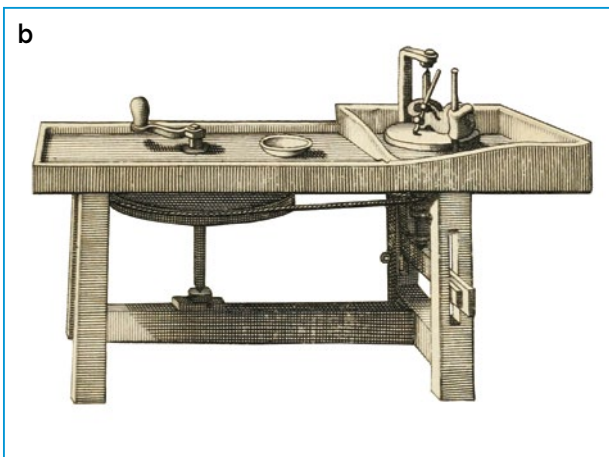


Figure 3: A 20th-century *bannku opa pattalaya* machine (a) shows similarities to a French cutting machine from 1676 (b). Photo courtesy of Dmitry Petrochenkov; engraving from Félibien (1676).

century, indicating that it would have made its way to Sri Lanka in the 1860s, possibly from Burma, which by then had already had 100 years of political interactions with France.

A homemade polishing compound was used on the *bannku opa pattalaya* machines until diamond powder was first adopted in the 1970s. According to Keerthi Jayasinghe (pers. comm. October 2017), the traditional polishing compound (*wadi*) was made from the ashes of midribs from *kitul* palm fronds, plus the ashes of burned rice husks. The ashes were cooked together in equal parts along with a trace of lime (CaCO_3) to make fist-sized balls. The balls were burned for a few hours using rice shells, and the ashy remains were then partially dissolved in water. Several rounds were required to get the mixture down to the finest particles, which would then be used for polishing. Jayasinghe maintained that this ash-based compound produced a better polish than the finest diamond grit.



Figure 4: A lapidary polishes a stone with a *bannku opa pattalaya* machine, while an assistant turns the large wooden crank wheel. Photo courtesy of Ika Dayananda.

INTRODUCTION OF THE IMHASHI MACHINE

The traditional Sri Lankan cutting machines started going out of fashion in the mid-1960s as new technology from Thailand, and then Japan, entered the country. Although a government-sponsored gem-cutting programme was proposed in 1939 (Anonymous 1939), it seems that official cutting classes were not offered until the early 1970s, when Badra Marapana started one at the Gem Bureau in Ratnapura. The class combined traditional Sri Lankan cutting methods that had developed over centuries (Mahroof 1989) with Japanese and European techniques (Zwaan 1982; Naji Sammoon, pers. comm. April 2017) in order to teach modern cutting methodology to a new generation of lapidaries.

The Japanese-made Imahashi machine was first introduced to the island by M. S. M. Hamza of Universal Gems, a leading gem dealer from Galle. He visited the Imahashi factory in Japan and saw the potential of using these machines in Sri Lanka. In 1976, with the help of the State Gem Corporation, the machines were placed in the Technical College of Ratnapura (Keerthi Jayasinghe, pers. comm. October 2017). Initially they were used only for training purposes, but subsequently a few individuals imported the machines for personal use. This style of machine had not been seen before in Sri Lanka. Its handpiece ‘faceter’ design descended from an older German company called EDUS (Figures 5a and 5b; Sandun Aponsu, pers. comm. September 2017). According to Keerthi Jayasinghe (pers. comm. October 2017), when it was introduced the Imahashi machine cost INR15,000 (GBP160), while the Graves machine from the USA cost around INR75,000 (GBP800).



Figure 5: Shown here are faceting handpieces from EDUS (a), Imahashi (b) and Sterling Gems & Lapidary (c). Photos by J. Prim.

By the time two groups of students had graduated from the Technical College, the demand for Imahashi machines began to grow. A government-funded institute called the National Youth Services Council established faceting schools in many districts around Sri Lanka. In the late 1970s and early 1980s, a few cutters were already using imported machines such as those made by Graves, Ultratec and 3M, but for the most part it was a huge challenge for these new types of motor-driven machines to become accepted in Sri Lanka (Keerthi Jayasinghe, pers. comm. October 2017). The dealers strongly believed that the motorised machines unnecessarily wasted weight during cutting, and that the polish was not as good as that produced with the *bannku opa pattalaya*. The adherence to traditional beliefs was noted 40 years earlier when the Sub-Committee of the Executive Committee of Labour, Industry and Commerce reported that ‘there is an inherent prejudice towards new innovations however efficient they may be’ (Anonymous 1939, p. 26). During this transitional period, a lot of education was needed within the gem community to

convince people about the precision and efficiency of the modern machines (Naji Sammoon, pers. comm. April 2017). As the demand for (what became known as) ‘machine cut’ stones increased, and older members of the gem trade retired, a new generation of gem cutters adopted the motorised machines. These younger cutters knew little about the old ways of cutting and polishing, including the aversion to motor-driven machines.

In the late 1970s, Thai-style machines (Figure 6a) were brought to Sri Lanka by Thai gem dealers who were buying cheap Sri Lankan pale ‘geuda’ rough for heating into valuable blue sapphires (Naji Sammoon, pers. comm. April 2017). Some cutters, such as those around Beruwala, Ratnapura and Eheliyagoda, liked the Thai machines because they seemed good for retaining weight, meaning they could produce heavier and therefore more valuable gems. In general, though, the Thai machines did not gain widespread traction in Sri Lanka. In some cases, the Thai machines were modified to use Imahashi-style handpieces, or they were replaced completely by Imahashi-style machines (Figure 6b).

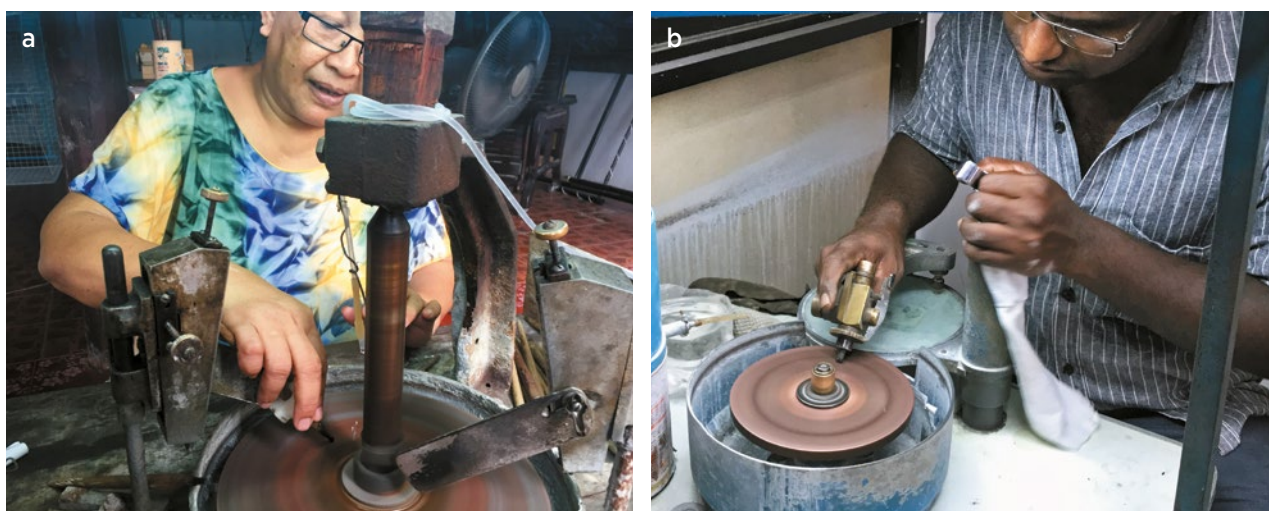


Figure 6: Thai jamb-peg-type cutting machine (a) is shown in comparison with a Sri Lankan Imahashi-style handpiece machine (b). Photos by J. Prim.

MODERN CUTTING ERA

Innovations by Bandu Wickrama Engineering Works

The early 1980s marked the beginning of a mass technological change in Sri Lanka's gem-cutting industry. An example of this was provided by Naji Sammoon, who ran a cutting factory in Hong Kong until it became too expensive for him to stay profitable there. He returned to Sri Lanka and started a new factory in Colombo. Sammoon first bought an Imahashi 'Faceter C' machine in 1982 from M. S. M. Hamza, who by then had become the director of Unique Gemstones, an Imahashi agent. Sammoon wanted to equip his factory with these machines, but they were too expensive to buy in large quantities. Furthermore, he felt the Imahashi handpiece was too complicated for the Sri Lankan cutting industry, so Sammoon gave one to Bandu Wickrama Engineering Works in Galle and asked the two brothers who ran the company, Aloysius and Bandu, to modify it for use in his factory (Naji Sammoon, pers. comm. April 2017). Bandu did the drawings and manufacturing for several variations of the handpiece, and the final design (Figure 7a) was modified to eliminate the oval cam movement and reduce its weight (Bandu Wickramasingha, pers. comm. September 2018). In addition, the machine employed a rubber V-belt to connect the motor to the lap wheel, rather than the flat leather belt of the Thai-style devices. Both the motor and wheel were fixed on a small steel table (Figure 7b), and the machine was designed to use three laps: a diamond lap for cutting and two cast-iron laps for polishing, instead of the single large cast-iron lap used in the Thai machines (Bandu Wickramasingha, pers. comm. September 2018).

Bandu Wickrama Engineering Works made about six of the cutting machines for Sammoon over six

months, all the while tweaking the design. Since their first one was completed in 1980, Bandu Wickrama Engineering Works has continued to make various types of faceting machines for the gem industry in Sri Lanka (www.gemlapidary.com/about-us). By 1992, Aloysius left the faceting machine business and his brother Bandu took over as the sole leader of Bandu Wickrama Engineering Works, which now sells their machine under the company name Gem Lapidary (Bandu Wickramasingha, pers. comm. September 2018).

Innovations by Sterling Gems & Lapidary

In the suburb of Moratuwa, located 20 km south of Colombo, the family-run Sterling Gems & Lapidary company was started by Palitha Aponsu in 1982. The author visited the Aponsu family home and workshop in September 2017, and Palitha and his son Sandun related their role in introducing modern gem-cutting methods to Sri Lanka. Palitha's father was the chief draftsman of the mechanical department in the local university. Palitha was an engineer by training who had studied gem cutting at the Gem Bureau in Ratnapura under Badra Marapana. He saw a photo of the Imahashi handpiece in the early 1980s and constructed a modified version of it (Sandun Aponsu, pers. comm. September 2017). In 1984, Palitha began manufacturing several types of gem-cutting machines (e.g. Figure 8), which are now used throughout the world.

During the initial development of their machines, Sterling made various modifications and enhancements and then started mass production. The Sterling handpiece (Figure 5c) is lightweight and user-friendly, which makes it easier to retain a stone's weight while cutting accurately. When the machine first appeared on the market, it cost about half the price of the one imported from Imahashi, which made it an affordable option for

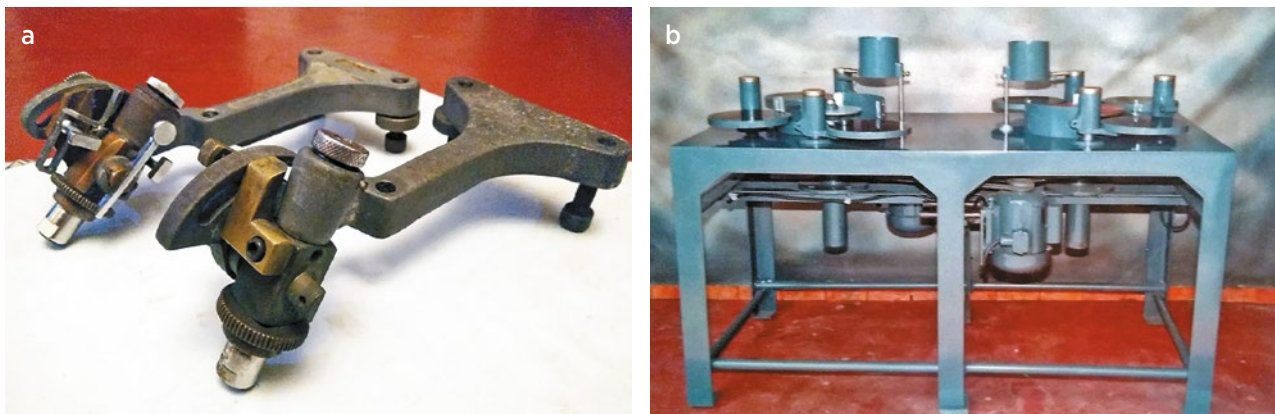


Figure 7: (a) A handpiece modified by Bandu Wickrama Engineering Works (front) is shown next to an original Imahashi handpiece (back). (b) These early dual faceting machines from Bandu Wickrama Engineering Works were designed with three laps: a diamond lap for cutting and two cast-iron laps for polishing. Photos courtesy of Bandu Wickrama Engineering Works.

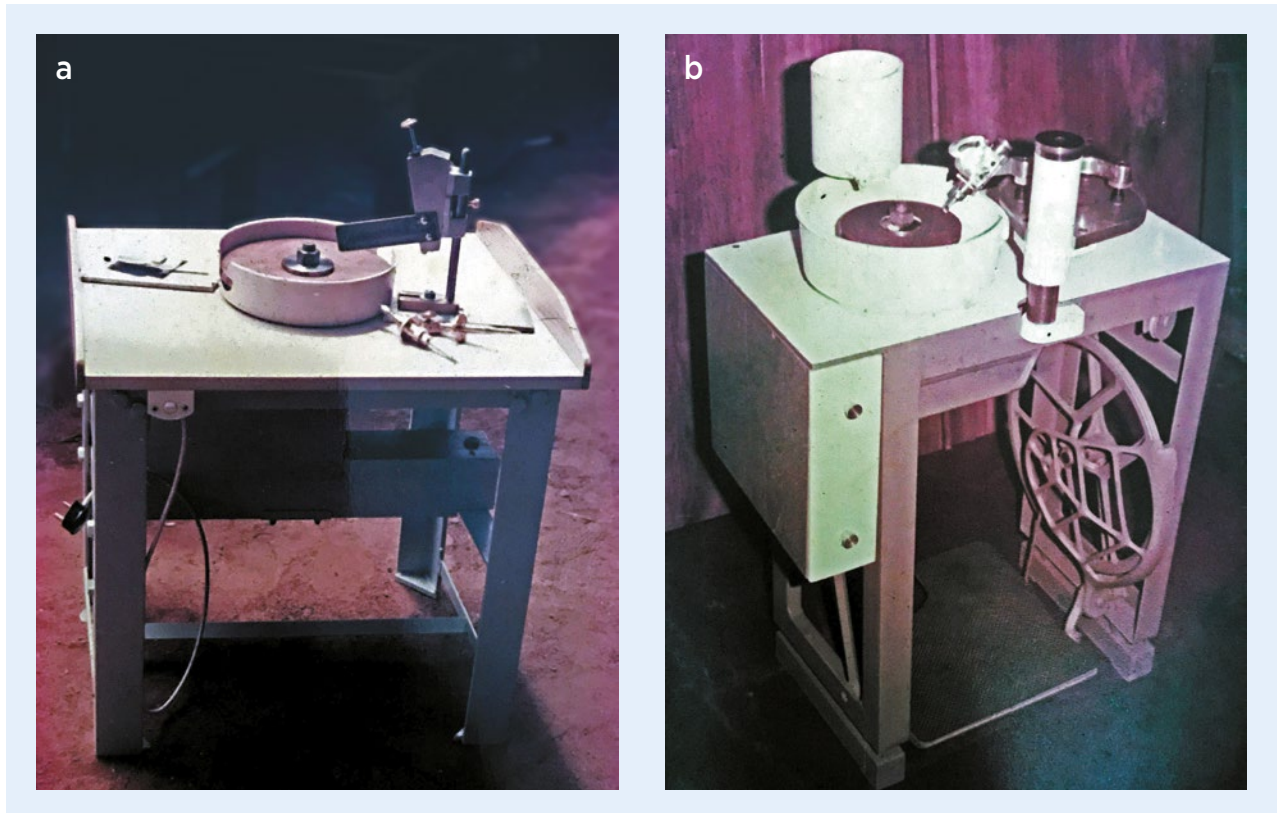


Figure 8: Early Sterling-made faceting machines include: (a) Thai-style and (b) a foot-powered Sri Lankan variation. Photos courtesy of Sterling Gems & Lapidary.

local cutting factories (Sandun Aponsu, pers. comm. September 2017). Some of these first-generation Sterling machines were delivered to Sammoon in Colombo for his cutting factory (Naji Sammoon, pers. comm. April 2017).

The company continues to hand-make their machines with a crew of six part-time workers. They recycle as much aluminium as possible from local machine shops, car parts and any other source they can find. When they need more than the recycling market can provide, they buy new aluminium from a local source. In their casting factory, the aluminium is melted and poured into moulds to make their handpieces, faceter heads and machine bodies. The cast pieces are then moved to another building for cleaning, polishing, powder coating and final assembly. Sterling can make a complete faceting machine in a single day within their small workshop.

RAISING THE BAR ON CUTTING STANDARDS

Since 1980, redesigned cutting machines have become the main faceting implements in Sri Lanka. The author has visited a dozen different cutting workshops in Ratnapura and Beruwala, and every cutter was using these handpiece-based machines alongside a few

hanaporuwas. In one shop, the *hanaporuwa* and handpiece cutters were sitting side-by-side, working together (Figure 9). The person on the handpiece machine would cut a stone and then hand it to the lapidary who would polish it on the *hanaporuwa*. This integration of old and new technology was a delightful surprise. Despite the fact that Sri Lankans can do every step of the cutting process on a single machine, they still choose to combine the best qualities of each type of machine to produce a high-quality product, while keeping relevant the older cutters with their different specialities (Lucas *et al.* 2014).

Because of this kind of innovation and ingenuity, Sri Lanka has risen to the top of the world's commercial stone-cutting industry. The Sri Lankan cutters are able to quickly cut a well-proportioned stone (e.g. Figure 10), while maintaining a reasonable wage. The author's research indicates that cutters in Thailand make about GBP1 for every carat they cut, whereas in Sri Lanka cutters make about GBP2 per carat (Naji Sammoon, pers. comm. April 2017). This means that a Sri Lankan cutter can theoretically spend a little more time per stone to ensure the cut quality is high.

In Sri Lanka, as well as in other commercial cutting countries, an important distinction is made between



Figure 9: In this Ratnapura cutting shop, a traditional lapidary using a *hanaporuwa* works side-by-side with a modern cutter using a handpiece machine. Photo by J. Prim.

cutters and polishers. Insight on this was provided during a visit by the author to the family home of Hiflan Sala, reputedly one of the best cutting families in Beruwala. According to Hiflan, the job of the cutter is considered the more advanced skill. The cutter must be able to evaluate the shape of the rough and any mineral inclusions that it contains, and navigate around the inclusions to create a pleasing final form for the gemstone (Hiflan Sala, pers. comm. April 2017).

Hiflan demonstrated his technique to the author by preforming a stone freehand on a Sri Lankan-made machine. He took an irregular rough ruby and turned it into a pleasing oval shape with a table, crown, pavilion, girdle and keel. As Hiflan worked, he spoke with pride about the skill of the preformers and cutters. His family preforms the rough and then cuts the facets into the stones. The stones are then sent to a polisher who makes the facets shine. In the author's experience, the polishing process has its own challenges, but it takes a master to properly preform a stone, as Hiflan pointed out. Preforming is the hardest part of cutting a gemstone from rough starting material and has the greatest influence on a stone's finished value.



Figure 10: Modern Sri Lankan cutting reveals the beauty of this 25 ct tanzanite. Photo by J. Prim.

CONCLUSION

It is incredible to consider how recently the gem-cutting industry in Sri Lanka has changed. Nearly all of the technology in use today has been around for only the past 35 years or so. This shift in technology and the mentality accompanying it has enabled Sri Lanka to develop some of the best cutters in the world. Sri Lanka's history with sapphires and rubies, and the steady rise in cutting quality, has caused a lot of the faceting work to move from India and Thailand to Sri Lanka. Since the 1990s, many Sri Lankan cutting factories have transitioned into producing stones that

meet the highest international cutting standards (e.g. Figures 1b and 10; Lucas *et al.* 2014), as opposed to the 'native cuts' they were known for in previous decades (Anonymous 1939). They have even secured some precision-cutting work from Switzerland for its gem-encrusted watch industry (Ahmed Shareek, pers. comm. November 2017; Yavorsky 2018). This is not surprising, considering how adaptable the people of Sri Lanka have proved to be and how active they are in the gem industry. Sri Lanka has one of the oldest relationships with gemstones, as well as a unique story within the world of gem cutting. As an industry, we can look forward to the next 2,000 years.

REFERENCES

- Anonymous 1939. *Report of the Sub-Committee of the Executive Committee of Labour, Industry and Commerce on the Marketing and Cutting of Ceylon Gems*. Colombo, Sri Lanka, 34 pp.
- Corso, A., Mugellesi, R. & Rosati, G. (eds and transl) 1988. *Gaio Plinio Secondo: Storia Naturale. V: Mineralogia e Storia dell'Arte, Libri 33–37*. Giulio Einaudi, Turin, Italy, 966 pp.
- de Boodt, A.B. 1609. *Gemmarum et Lapidum Historia*. C. Marnium et heredes J. Aubrii, Hanover, Germany, 294 pp, <https://books.google.com/books?id=upxkAAAAcAAJ>.
- Félibien, A. 1676. *Des Principes de l'Architecture, de la Sculpture, de la Peinture, et des Autres Arts qui en Dépendent*. Jean-Baptiste Coignard, Paris, France, 267 pp, <https://digi.ub.uni-heidelberg.de/diglit/felibien1676>.
- Gray, A. 1996. *Ibn Battuta in the Maldives and Ceylon*. Asian Educational Services, New Delhi, India, 64 pp.
- ICA Congress 2017. Jack Ogden – Sri Lankan Legacy: A History of Sapphires. YouTube, www.youtube.com/watch?v=DOKxNif8d5U, accessed May 2017.
- Kularatnam, K. 1975. Lapidary—Scope and potential (The Ceylon Daily News). *Rocks & Minerals*, **50**(2), 80–82, <http://doi.org/10.1080/00357529.1975.11762201>.
- Lucas, A., Sammoon, A., Jayarajah, A.P., Hsu, T. & Padua, P. 2014. Sri Lanka: Expedition to the island of the jewels. *Gems & Gemology*, **50**(3), 174–201, <http://doi.org/10.5741/gems.50.3.174>.
- Mahroof, M.M.M. 1989. The Muslim lapidary: Some aspects of the gem folkways in Sri Lanka. *Journal of Gemmology*, **21**(7), 405–410, <http://doi.org/10.15506/JoG.1989.21.7.405>.
- Moule, A.C. & Pelliot, P. 1938. *Marco Polo: The Description of the World*. George Routledge & Sons Ltd, London, 595 pp, <https://archive.org/details/descriptionofwor01polo>.
- National Gem and Jewellery Authority 2014. Gemstone Faceting Industry. www.ngja.gov.lk/en/gem-cutting-industry, accessed January 2019.
- Yavorsky, V.Y. 2018. *Sri Lanka Gems*. Yavorsky Co. Ltd, Hong Kong, 172 pp.
- Zwaan, P.C. 1982. Sri Lanka: The gem island. *Gems & Gemology*, **18**(2), 62–71, <http://doi.org/10.5741/gems.18.2.62>.

The Authors

Justin K Prim

Institute of Gem Trading, Chartered Square Building
15-04, 15th Floor, 152 North Sathorn Road, Bangrak,
Bangkok, Thailand 10500
Email: justinkprim@gmail.com

Acknowledgements

Special thanks to the following people for answering my many questions, without whom I would not have been able to write this history: Sandun Aponsu and family (Sterling Gems & Lapidary, Moratuwa, Sri Lanka);

Arnil and Naji Sammoon and family (Sri Lanka Gem & Jewellery Association, Colombo, Sri Lanka); Bandu Wickramasingha (Bandu Wickrama Engineering Works, Galle, Sri Lanka); Muhammed Raihan, Hiflan Sala and families (Beruwala, Sri Lanka); Ahmed Shareek (Crescent Gems, Colombo, Sri Lanka); Keerthi Jayasinghe (Prima Gems Ltd, Arusha, Tanzania); Ika Dayananda (Squire Mech Engineering, Maharagama, Sri Lanka); Herathlaga Sarath Chandrasiri (Yavorsky Co. Ltd, Bangkok, Thailand); and Dmitry Petrochenkov (Russian State Geological Prospecting University, Moscow, Russia).

Figure 1: These examples of Connemara marble jewellery were produced by Harry Grant & Co., Torquay, in the early 1900s: a harp-shaped brooch and a harp-and-harp necklace, as well as four amulets (e.g. heart- and boot-shaped charms) worn by Irish soldiers in World War I (Dougherty 2015). The harp in the centre is 4.5 cm long and the amulets are up to 2 cm long. Photo by Pat O'Connor.



Mineral Liberation Analysis and Scanning Electron Microscopy of Connemara Marble: New Mineral Distribution Maps of an Iconic Irish Gem Material

Martin Feely, Derek H. Wilton, Alessandra Costanzo, Albert D. Kollar, Dylan J. Goudie and Ambrose Joyce

ABSTRACT: This article reports results from mineral liberation analysis–scanning electron microscopy (MLA-SEM) of six samples of the iconic Irish gem material, Connemara marble. New false-colour mineral distribution maps along with quantitative mineral abundance data for each sample facilitate correlations between marble mineralogy and millimetre- to centimetre-scale colour variations in banding observed in each sample. The modal mineral data were used to classify each of the samples, and indicate that they define a petrological continuum from calc-silicate to metacarbonate rocks. The results demonstrate the efficacy of MLA-SEM methodology for generating mineral distribution maps along with quantitative modal analysis that inform and enhance the study of inhomogeneous gem materials such as the Connemara marble. Finally, this study demonstrates the potential for MLA-SEM analyses to aid in the fingerprinting and authentication of other polymineralic gems akin to Connemara marble.

The Journal of Gemmology, 36(5), 2019, pp. 456–466, <http://doi.org/10.15506/JoG.2019.36.5.456>
© 2019 Gem-A (The Gemmological Association of Great Britain)

Connemara marble is the standout Irish geological and gem material, and is therefore recognised as the iconic stone of Ireland (Horgan 2002; Walsh 2014). Its use in jewellery (e.g. Figure 1) can be regarded as one of Ireland’s indigenous industries, and the quarrying of Connemara marble is a centuries-old endeavour (Feely 2002). The stone exhibits intricate millimetre- to metre-scale corrugated layers that range from white through sepias to various shades of green. The polished stone’s appeal was described by American art critic Charles Caffin (1897, p. 955) as ‘the exquisite mystery of graded greens and greys and black, their tempestuous streakings and tender veining, and the perfect texture of their polished surface’.

The colour variations displayed by Connemara marble derive from the relative abundance of the coloured silicate minerals present (e.g. deep green hues appear when serpentine predominates). By contrast, white-to-grey marble such as that quarried at Carrera, Italy, consists of relatively pure metamorphosed calcite- and/or dolomite-bearing limestone. Max (1985) noted that only a small portion of the Connemara marble horizons contain sufficient proportions of carbonate minerals to be properly termed ‘marble’, and furthermore it is the other minerals (i.e. mainly calc-silicates and serpentine) that impart the colour varieties so typical of the stone traded as Connemara marble.

Despite a number of reports on the mineralogy of Connemara marble (Cronshaw 1923; Leake *et al.* 1975; Max 1985), descriptions of the relationship between the mineralogy and colour variations are absent from the literature. We present new mineral distribution maps and mineral abundance statistical data (expressed as area percent) from six polished thin sections of Connemara marble, using a novel analytical technique called mineral liberation analysis–scanning electron microscopy (MLA-SEM). The mineral distribution maps highlight the correlations between mineralogical composition and the layered, polychromatic characteristics of the marble. In addition, a triangular discriminant plot of the quantitative mineral abundance data indicates that the marble samples display a petrological continuum from calc-silicate to metacarbonate rock. The mixture of these components in the rock results in mineralogical and textural variations that impart the interesting ornamental characteristics to this gem material.

GEOLOGICAL SETTING

The Connemara region of western Ireland (Figure 2) is composed of a number of major rock units (Leake & Tanner 1994; Pracht *et al.* 2004). The central zone comprises the Connemara Metamorphic Complex (CMC) containing Dalradian metasediments (ca. 650 million

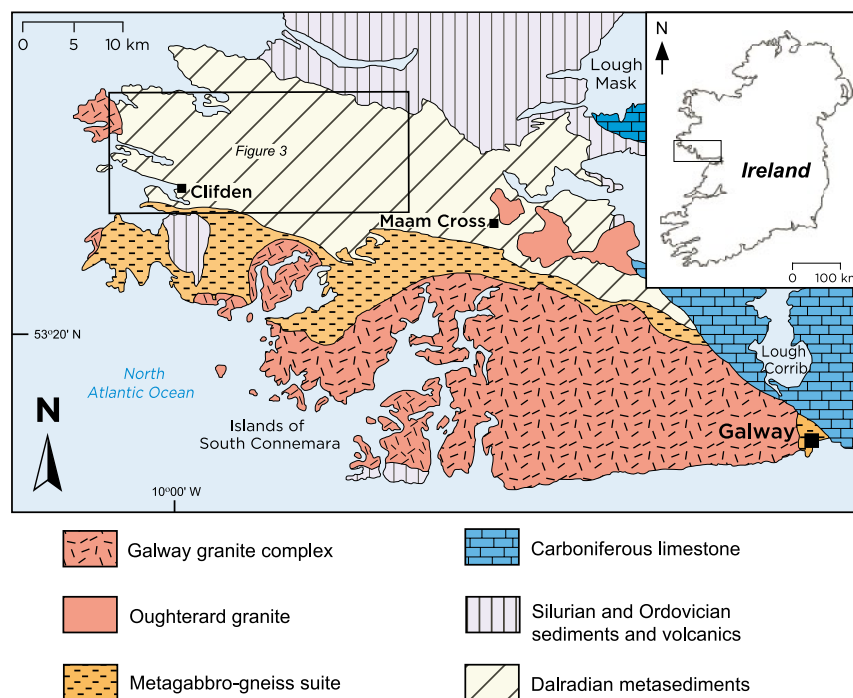


Figure 2: This map of the Connemara area shows the distribution of the main geological units. The Connemara Metamorphic Complex comprises the ca. 470 Ma metagabbro-gneiss suite and the Dalradian metasedimentary rocks that contain the Connemara Marble Formation. Adapted from Leake & Tanner (1994), Pracht *et al.* (2004), Feely *et al.* (2006) and Lees & Feely (2016, 2017).

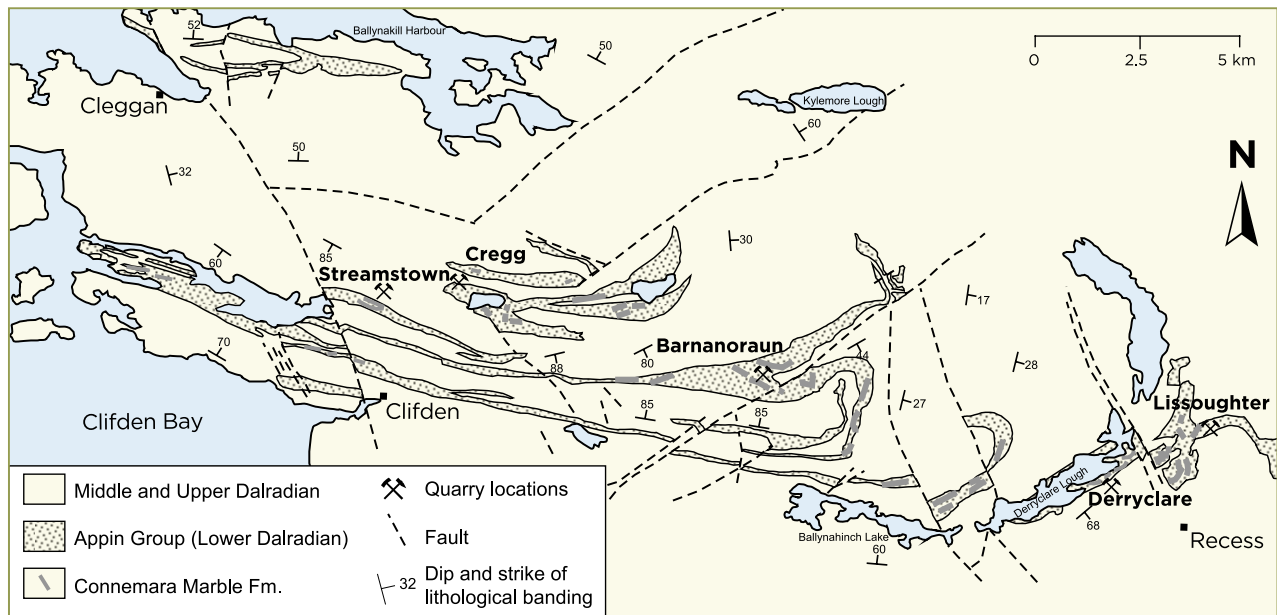


Figure 3: This simplified geological map shows the distribution of the Connemara Marble Formation, which forms part of the Lower Dalradian Appin Group. The five main Connemara marble quarry locations are: Streamstown, Cregg, Barnanoraun, Derryclare and Lissoughter. The folded nature of the Appin Group and the east-west distribution of the marble reflect the regional structural trend of the Connemara Metamorphic Complex. Adapted from Max (1985).

years old [Ma]) and a 475–463 Ma metagabbro-gneiss suite (Leake 1989; Dewey & Ryan 2016; Friedrich & Hodges 2016). The intrusion of the Oughterard granite, east of Maam Cross (Friedrich & Hodges 2016), occurred during the end stage of the Grampian orogeny (ca. 475–462 Ma). The CMC is bounded to the north by Silurian and Ordovician sedimentary and volcanic rocks (Leake & Tanner 1994), and to the east it is in faulted contact with Carboniferous limestones (Lees & Feely, 2016; 2017). To the south lie the younger Caledonian Galway granites (~425–380 Ma; see Feely *et al.* 2010; 2018). Some exposures of Ordovician sedimentary and volcanic rocks occur just south of Clifden and further south on the islands of South Connemara (Figure 2).

Horizons of Connemara marble typically range up to 80 m thick (Leake and Tanner 1994) and are hosted by the Connemara Marble Formation, which belongs to Lower Dalradian (=Appin Group) metasediments (Figure 3). The marble is a metamorphosed impure siliceous dolomitic limestone (Leake *et al.* 1975; Tanner & Shackleton 1979; Treloar 1982; Max 1985). Amphibolite-greenschist facies metamorphism during the Grampian orogeny induced the formation of silicate minerals that include olivine, diopside, tremolite, talc and chlorite. In addition, calcite and dolomite occur throughout, locally representing significant portions of the mineralogical assemblages. Indeed, the relative proportions of all of these minerals vary widely due to the different compositional layers present in the marble protoliths. Later hydrothermal

metamorphism led to wholesale serpentinisation of the earlier-formed high-grade olivine, diopside and tremolite (Cronshaw 1923; Leake *et al.* 1975; Max 1985). The serpentinisation, in part, may be linked to the generation of hydrothermal fluids syn- or post-emplacment of the Galway granites (Jenkin *et al.* 1997; O’Reilly *et al.* 1997).

CULTURAL HERITAGE

Connemara marble has played a key role in the development of the renowned cachet that characterises the Irish jewellery design and manufacturing sector. The marble’s popularity in jewellery and souvenir gift items during the Victorian era (Horgan 2002) initiated the prestige that it still enjoys to this day. The deep green variety known as *Irish Jade* was in particularly high demand. When Queen Victoria visited Ireland in 1900 she was presented with an ornamental harp (~30 cm tall) fashioned from Connemara marble.

Birmingham, England, was one of the major centres for the manufacture of Connemara marble jewellery, and many of the antique brooches (e.g. harps and shamrocks), pendants and bracelets have the anchor hallmark of the Birmingham Assay Office. Harry Grant & Co., located in Torquay (1847 to early 1980s), produced a large range of silver and gold jewellery inlaid with Connemara marble. During World War I, Irish soldiers carried heart-, boot-, bean- and shamrock-shaped amulets of Connemara marble manufactured by Harry Grant & Co. (see Figure 1;

Dougherty 2015). Stamping dyes and samples from Harry Grant & Co. are on display in the Connemara Marble Visitor Centre, Moycullen, County Galway, Ireland. Records of marble quarrying go back to at least the 18th century (Feely 2002; Feely & Costanzo 2014). Indeed, lyrical descriptions of the marble are to be found in the stone trade's literature. For example, Hoyt (1903, p. 122) described its colour as ranging from 'the light greens, almost verging on yellow, to the deep, dark lustrous greens that suggest in turn the emerald, the depths of the sea and the moss of the forest covert'.

Connemara marble is currently in the process of being proposed as a candidate for Global Heritage Stone status in recognition of its widespread utilisation in architectural and ornamental masterpieces, particularly in the UK and USA. During the Gilded Age (late 19th to early 20th century) of architecture in the USA, many of the great public buildings in Boston, New York, Chicago, Washington DC, Harrisburg and Pittsburgh incorporated classical ornamental stones from Europe, including Connemara marble (Wyse Jackson *et al.* in press).

Five main quarries for Connemara marble occur along a west-to-east-trending corridor from Clifden to Recess in County Galway: Streamstown, Cregg, Barnanoraun, Derryclare and Lissoughter (Figure 3). Their spatial distribution reflects the exposures of folded Appin Group rocks and the dominant east-west structural trend of the CMC. The history of marble quarrying at these localities is outlined in Naughton *et al.* (1992) and Feely (2002). An image of the Streamstown quarry was used by Stanley (1999, figure 2.26, p. 53) to highlight the ornamental use of metamorphic rocks such as Connemara marble.

MATERIALS AND METHODS

The six Connemara marble samples used for this study came from the Streamstown quarry, located approximately 3 km north of the town of Clifden. The quarry contains typical examples of folded and banded green marble (Figures 4a and b). Four of the samples (nos. 3–6) were supplied by author ADK and are representative of Connemara marble used as ornamental inlays (Figure 4c)



Figure 4: (a) In this photo of the Streamstown quarry, near Clifden, the folded and banded Connemara marble is clearly visible. This image is a frame taken from a LiDAR (light detection and ranging) survey of the quarry by McCaffrey *et al.* (2008). (b) A polished slab of Connemara marble (image width 30 cm) from the Streamstown quarry displays typical centimetre-scale banding and colour variations. (c) Streamstown Connemara marble inlays decorate the Carnegie Museum in Pittsburgh, Pennsylvania, USA (see pen for scale). Photos by M. Feely.

during the early 20th century construction of the Carnegie Museum in Pittsburgh, Pennsylvania, USA (Kollar *et al.* 2017). Samples 1 and 2 are from a recently obtained quarry floor drill core supplied by author AJ.

A polished thin section (0.03 mm thick) was prepared for each sample. The thin sections were imaged using a digital scanner at Memorial University, St Johns, Newfoundland, Canada, and the corresponding marble samples from which they were cut were photographed (Figure 5). The thin sections then underwent MLA-SEM analysis (Box A).

RESULTS AND DISCUSSION

The MLA-SEM analyses (a) identified the major, minor and accessory mineral phases in each marble sample; (b) provided quantitative data on the contents of all the mineral phases present as a percentage of the total sample area (see Table I and Figure 5); and (c) created false-colour mineral distribution maps for each of the thin sections that are easily compared with the actual thin sections and the rock slabs from which they were

BOX A: MLA-SEM INSTRUMENTATION AND METHODOLOGY

Mineral liberation analysis–scanning electron microscopy (MLA-SEM) can identify the mineral phases present and quantitatively define their modal abundances in polished rock thin sections. The basis for MLA studies is the derivation of an energy-dispersive X-ray (EDX) spectrum for each mineral in a sample. The MLA software compares the analysed EDX spectra with a library of mineral spectra to identify the particular phases that are present in a sample.

The MLA-SEM facility in the CREAT laboratories at Memorial University (Figure A-1; Sylvester 2012; Grant *et al.* 2016; Wilton *et al.* 2017) consists of a 2011-model FEI Quanta FEG 650 scanning electron microscope (SEM) equipped with mineral liberation analysis (MLA) software written by the University of Queensland's Julius Kruttschnitt Mineral Research

Centre in Australia. The Memorial University group has developed a sophisticated, proprietary library of species identification protocols (SIPs) that can be used to indicate almost all minerals present within a sample, down to <0.3% detected unknowns (e.g. Wilton & Winter 2012; Wilton *et al.* 2015, 2017), using a matching threshold of 70% in the MLA software. The confidence level for the spectral match is set during the initial analysis. The software scales the probability between 0% and 100%, where 100% is a perfect match (probability of 1) and 50% is an 'average match' (Mateo 2010). New mineral spectra are added to the SIP library as they are identified.

The SEM at Memorial University is equipped with a dual Bruker EDS detector, and utilises a field emission gun at an operating voltage of 25 kV and a beam current of 10 nA. The working distance between the sample and detector is 13.5 mm, and for the present study the spot size was ~2.5 µm. The imaging scan speed was 16 microseconds, with a resolution of 500 pixels per frame (each frame 1.5 × 1.5 mm) and X-ray collection at 12 milliseconds.

The MLA software provides a false-colour digital map of the mineral phases present within a rock thin section and it also yields mineral abundance data (as a function of the area percent of the analysed thin section). In this study, the samples each took 4–6 hours to analyse and obtain thin-section maps.

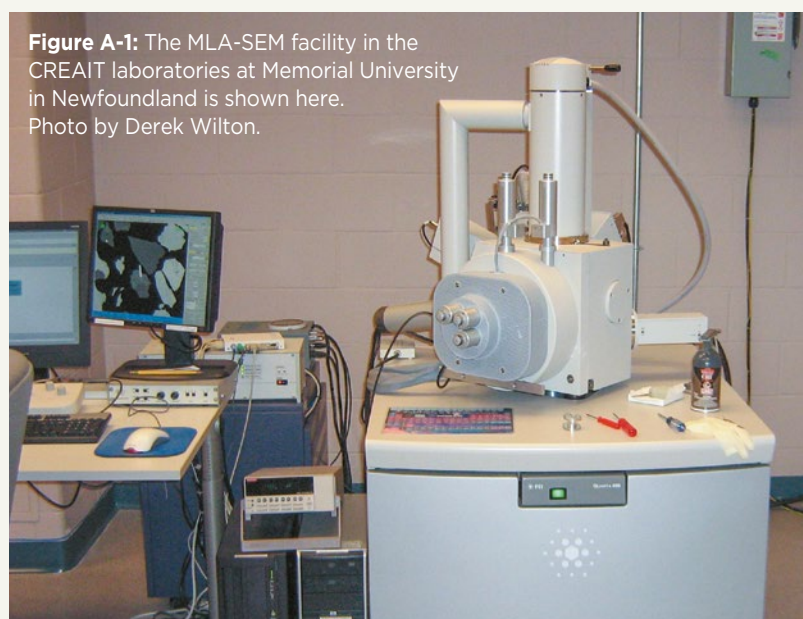


Figure A-1: The MLA-SEM facility in the CREAT laboratories at Memorial University in Newfoundland is shown here. Photo by Derek Wilton.

Table I: Mineral abundance data (area %) generated by the MLA-SEM analyses of six Connemara marble samples.

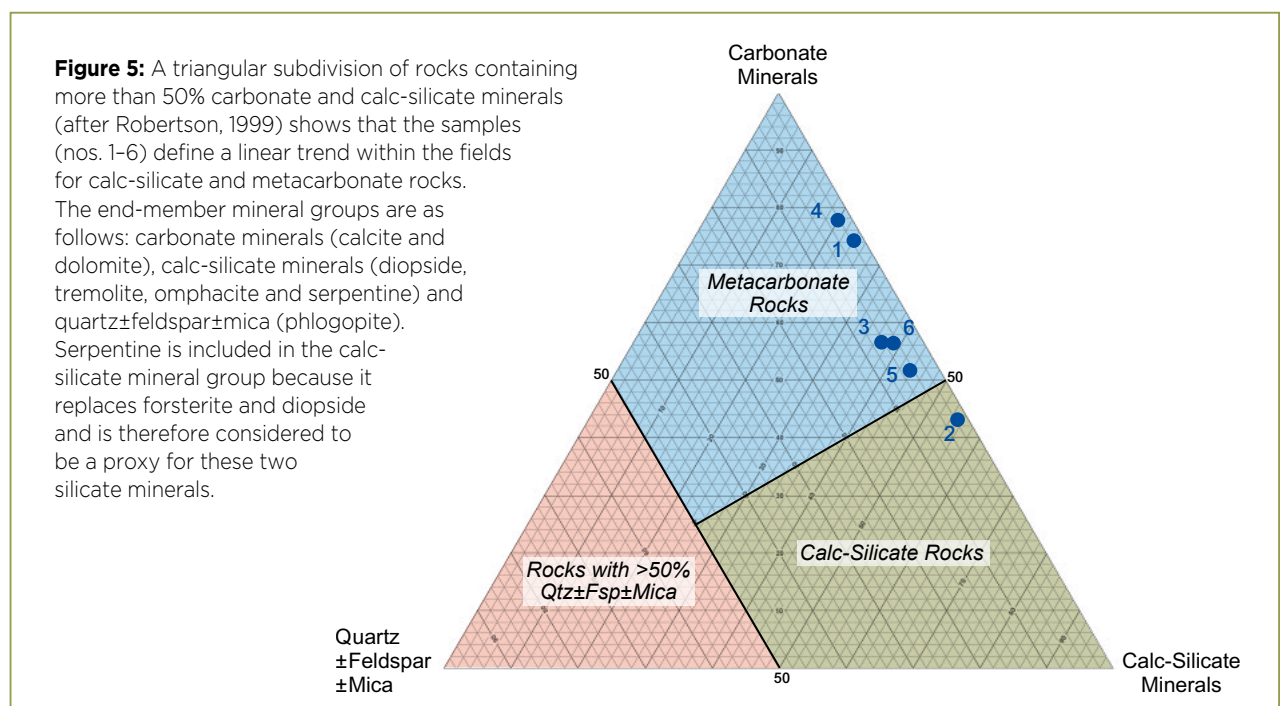
Mineral	Sample 1	Sample 2	Sample 3	Sample 4	Sample 5	Sample 6
Dolomite	58.67	21.64	24.70	44.85	13.52	14.99
Calcite	16.18	15.40	32.17	32.55	37.62	41.49
Serpentine	15.40	25.50	27.17	17.93	27.26	34.37
Clinochlore	1.46	15.34	0.46	0.92	0.18	0.40
Diopside	3.27	11.67	4.17	0.26	12.17	0.82
Tremolite	3.51	7.74	3.26	1.17	3.22	1.72
Phlogopite	1.02	0.41	6.97	1.63	5.57	5.84
Omphacite	0.40	1.87	0.68	0.29	0.36	0.33
Talc	0.04	0.19	0.28	0.04	0.09	0.03
Accessory phases	0.05	0.24	0.14	0.36	0.01	0.01
Total	100.00	100.00	100.00	100.00	100.00	100.00
Carbonates	74.9	37.0	56.9	77.4	51.1	56.5
Other minerals	25.1	63.0	43.1	22.6	48.9	43.5

cut (Figures 6 and 7). In addition, Figure 7 shows the relative abundance of each mineral phase present.

The mineral-phase abundance data indicate that dolomite (14–59%), calcite (15–41%) and serpentine (15–34%) were the dominant minerals in all six samples. Less abundant mineral phases were clinochlore (0.20–15%), diopside (0.30–12%), tremolite (1–8%), phlogopite (0.40–7%) and omphacite (0.30–2%). Accessory phases, including zircon, were < 0.50%.

The modal mineral abundances were plotted on a triangular discriminant diagram (Figure 5) adapted from

Robertson (1999). The samples define a linear trend extending from the calc-silicate to the metacarbonate rock fields. However, as noted earlier, the stone has been referred to as Connemara ‘marble’ for centuries even though Figure 5 indicates that it is composed of significant amounts of silicate minerals along with calcite and dolomite. Small-scale patches of true marble were evident in all six of our samples. Suffice it to say that the variable mineralogical nature of Connemara marble from millimetre to metre scale makes it a challenging rock to classify, and it should be viewed as occurring



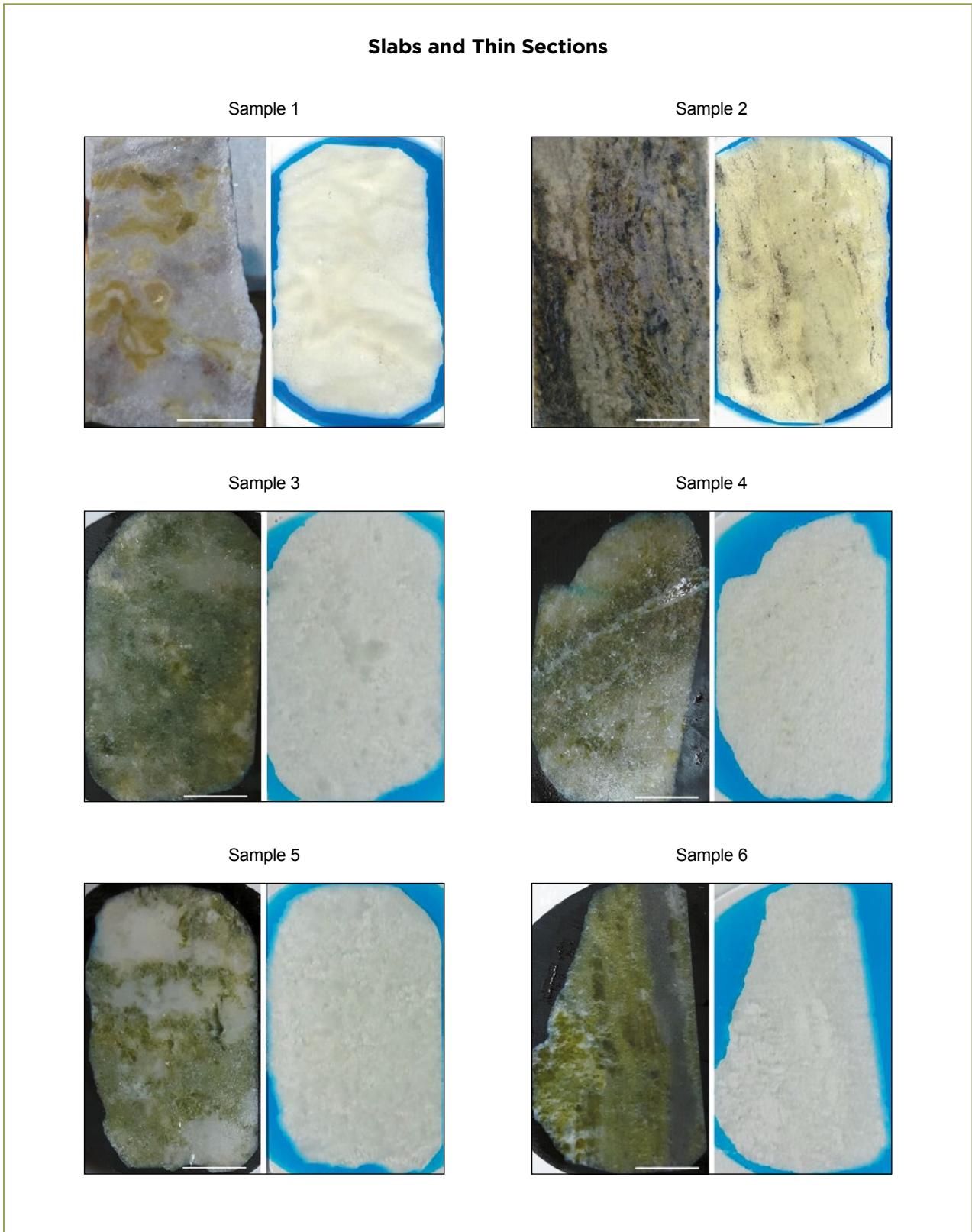


Figure 6: Six samples of Connemara marble from the Streamstown quarry were analysed using MLA-SEM. Samples 1 and 2 were recently collected, while nos. 3–6 represent marble quarried during the late 19th to early 20th centuries and used as decorative stone tiling in the Carnegie Museum (see Figure 4c). For each sample, a photo of a sawn slab (left) is shown together with its matching polished thin section (right, surrounded by blue epoxy). Samples 2, 4 and 6 display characteristic millimetre- to centimetre-scale banding that reflects the mineral composition of each layer. Samples 1, 3 and 5 have a more inhomogeneous appearance with white areas intimately admixed with coloured patches. Photos by M. Feely and A. Costanzo; the scale bar in the slab photos is ~1 cm long.

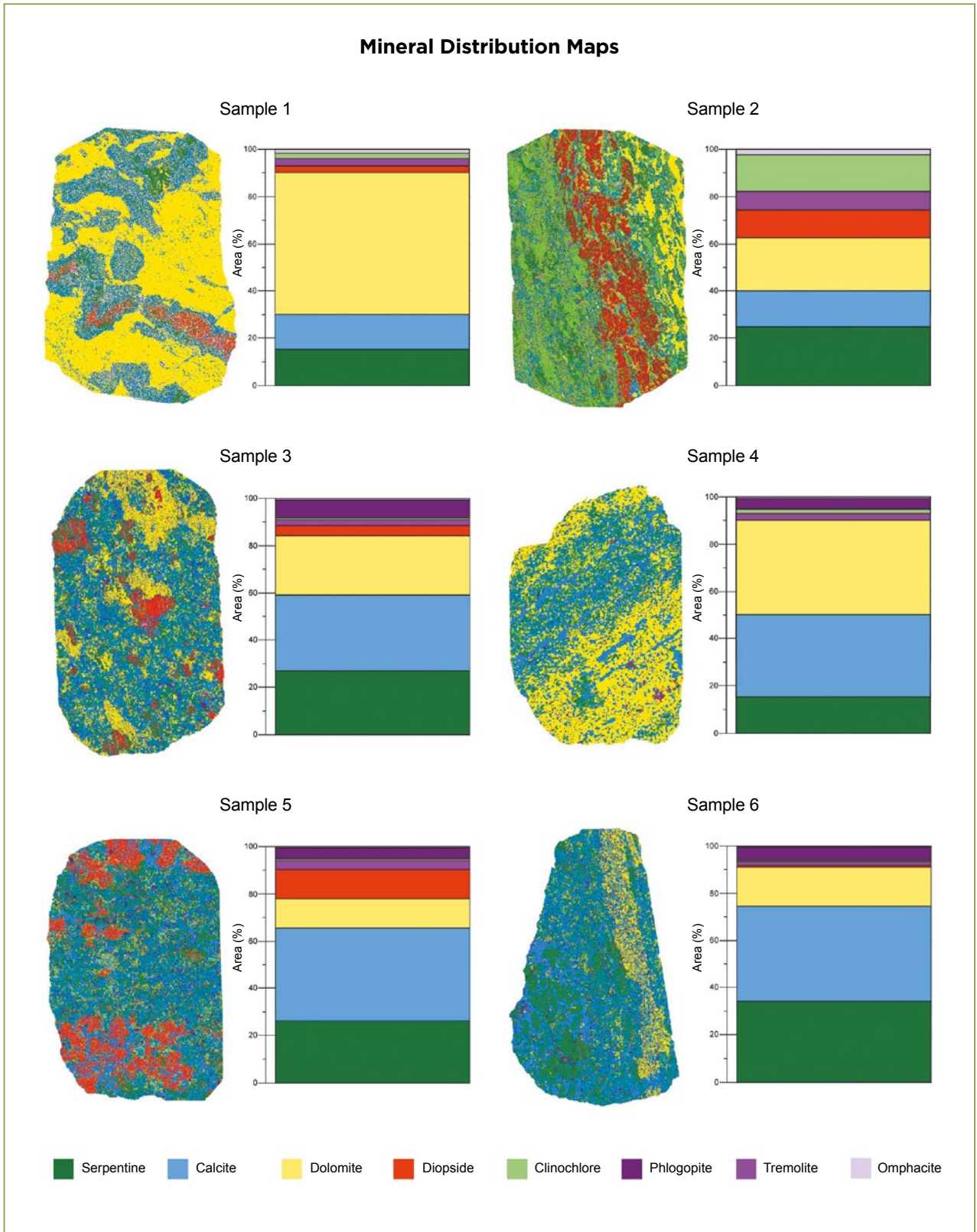


Figure 7: False-colour mineral distribution maps are shown for each marble sample along with graphic representations of the mineral phase area-percent data that were generated by MLA analysis. The maps display the correlation between mineral phases, their spatial distribution and the ensuing colours observed in the marble (as seen in Figure 6). Calcite and dolomite, for example, correlate with the white to grey areas and bands seen in the marble. Diopside commonly occurs in association with these carbonates, and correlates with pale green areas of the marble. A more intense green colour in the marble is primarily produced by serpentine, which is pervasive and present in each sample. Furthermore, clinocllore in association with serpentine defines the layering on the left side of sample 2.

Figure 8: Connemara marble products displaying the characteristic range of colours and textures typical of this gem material are shown here. The Claddagh ring (upper left) and bracelet (top, 18 cm long) were produced by Harry Grant & Co. in the early 1900s. The shamrock-themed silver brooch in the centre is a relatively recent creation (late 20th century) by Ambrose Joyce and is on display in the Connemara Marble Visitor Centre. Also in this photo are various cabochons, and the oval ones are up to 2.5 cm long. Photo by Pat O'Connor.



across the lithological spectrum from true marble to calc-silicate in nature.

The false-colour mineral-distribution maps (Figure 7) reflect the composite and banded nature of the marble and the mineralogical causes of the colour variations (from deep green to white) evident in the samples. Dolomite and calcite dominated the grey to white layers and patches, whereas the green layers and patches reflected the presence of serpentine and diopside. The mineral maps also showed that the layers were not monomineralic but consisted of aggregates of calcite and dolomite with variable calc-silicate mineral contents (mainly diopside) and serpentine. The anhedral character of the diopside (see in particular samples 1, 2 and 5 in Figure 7) and its spatial relationship to the serpentine reflects serpentinisation of the diopside, along with the formation of forsterite and tremolite, during late-stage hydrothermal metamorphism (Wyse Jackson *et al.* in press).

CONCLUDING REMARKS

Connemara marble (Figure 8) is an iconic Irish gem material, and until now the relationship between its mineralogy and colour variations had not been reported. MLA-SEM analysis was used to generate a series of mineral distribution maps and mineral abundance data that:

- allow for the study and correlation of the mineralogically driven colour variations and banding in the marble samples;

- facilitate the classification of the marble using quantitative modal abundance data;
- illustrate mineralogical textures that result from the pervasive serpentinisation of early-formed minerals, particularly diopside (indeed, the serpentine is a proxy mineral for other minerals such as forsterite and tremolite); and
- demonstrate the potential for MLA-SEM analyses to aid the fingerprinting and authentication of polymineralic gem materials akin to Connemara marble.

REFERENCES

- Caffin, C.H. 1897. Architecture and mural painting: Columbia College library. *Harper's Weekly*, **41**, 953, 955.
- Cronshaw, H.B. 1923. The Connemara serpentine rocks. *Geological Magazine*, **60**(10), 467–471, <http://doi.org/10.1017/s001675680008835x>.
- Dewey, J.F. & Ryan, P.D. 2016. Connemara: Its position and role in the Grampian orogeny. *Canadian Journal of Earth Sciences*, **53**(11), 1246–1257, <http://doi.org/10.1139/cjes-2015-0125>.
- Dougherty, T. 2015. The things they carried. *Irish America*, **30**(2), 25, https://issuu.com/irishamerica/docs/ia.february_march_2015.
- Feely, M. 2002. *Galway in Stone – A Geological Walk in the Heart of Galway*. Geoscapes, Dublin, Ireland, 48 pp.
- Feely, M. & Costanzo, A. 2014. *Galway City Walks: Buildings in Stone*. National University of Ireland Galway, Ireland, 64 pp.

- Feely, M., Leake, B.E., Baxter, S., Hunt, J. & Mohr, P. 2006. *A Geological Guide to the Granites of the Galway Batholith, Connemara, Western Ireland*. Geological Survey of Ireland, Dublin, 62 pp.
- Feely, M., Selby, D., Hunt, J.O.N. & Conliffe, J. 2010. Long-lived granite-related molybdenite mineralization at Connemara, western Irish Caledonides. *Geological Magazine*, **147**(6), 886–894, <http://doi.org/10.1017/S0016756810000324>.
- Feely, M., Gaynor, S., Venugopal, N., Hunt, J. & Coleman, D.S. 2018. New U-Pb zircon ages for the Irish granite pluton, Galway Granite complex, Connemara, western Ireland. *Irish Journal of Earth Sciences*, **36**, 1–7, <http://doi.org/10.3318/ijes.2018.36.2>.
- Friedrich, A.M. & Hodges, K.V. 2016. Geological significance of $^{40}\text{Ar}/^{39}\text{Ar}$ mica dates across a mid-crustal continental plate margin, Connemara (Grampian orogeny, Irish Caledonides), and implications for the evolution of lithospheric collisions. *Canadian Journal of Earth Sciences*, **53**(11), 1258–1278, <http://doi.org/10.1139/cjes-2016-0001>.
- Grant, D.C., Goudie, D.J., Shaffer, M. & Sylvester, P. 2016. A single-step trans-vertical epoxy preparation method for maximising throughput of iron-ore samples via SEM-MLA analysis. *Applied Earth Science*, **125**(1), 57–62, <http://doi.org/10.1080/03717453.2015.1104056>.
- Horgan, D. 2002. *The Victorian Visitor in Ireland: Irish Tourism 1840–1910*. Imagimedia, Cork, Ireland, 108 pp.
- Hoyt, F.W. 1903. American and British marbles. *Stone*, **27**(2), 112–123, https://quarriesandbeyond.org/articles_and_books/pdf/american_and_british_marbles-stone-dec_1903.pdf.
- Jenkin, G.R.T., O'Reilly, C., Feely, M. & Fallick, A.E. 1997. The geometry of mixing of surface and basinal fluids in the Galway granite, Connemara, western Ireland. *Geofluids II '97: Second International Conference on Fluid Evolution, Migration and Interaction in Sedimentary Basins and Orogenic Belts*, Belfast, Northern Ireland, 10–14 March, 374–377.
- Kollar, A.D., Feely, M., Joyce, A., Fedosick, R. & Hughes, K. 2017. The industrial archaeology of the Connemara marble: Cross-Atlantic connections between western Ireland and the Carnegie Museum of Natural History, Pittsburgh, Pennsylvania. *Geological Society of America Abstracts with Programs*, **49**(2), Paper No. 44-1, <http://doi.org/10.1130/abs/2017NE-289712>.
- Leake, B.E. 1989. The metagabbros, orthogneisses and paragneisses of the Connemara complex, western Ireland. *Journal of the Geological Society*, **146**(4), 575–596, <http://doi.org/10.1144/gsjgs.146.4.0575>.
- Leake, B.E. & Tanner, P.W.G. 1994. *The Geology of the Dalradian and Associated Rocks of Connemara, Western Ireland*. Royal Irish Academy, Dublin, Ireland, 96 pp.
- Leake, B.E., Tanner, P.W.G. & Senior, A. 1975. The composition and origin of the Connemara dolomitic marbles and opicalcites, Ireland. *Journal of Petrology*, **16**(1), 237–257, <http://doi.org/10.1093/petrology/16.1.237>.
- Lees, A. & Feely, M. 2016. The Connemara eastern boundary fault: A review and assessment using new evidence. *Irish Journal of Earth Sciences*, **34**, 1–25, <http://doi.org/10.3318/ijes.2016.34.1>.
- Lees, A. & Feely, M. 2017. The Connemara eastern boundary fault: A correction. *Irish Journal of Earth Sciences*, **35**, 55–56, <http://doi.org/10.3318/ijes.2017.35.55>.
- Mateo, S. 2010. *MLA v 3.0 Regional Training Manual 2010*, unpublished.
- Max, M.D. 1985. *Connemara Marble and the Industry Based upon it*. Geological Survey of Ireland, Dublin, 32 pp.
- McCaffrey, K.J.W., Feely, M., Hennessy, R. & Thompson, J. 2008. Visualization of folding in marble outcrops, Connemara, western Ireland: An application of virtual outcrop technology. *Geosphere*, **4**(3), 588–599, <http://doi.org/10.1130/ges00147.1>.
- Naughton, E., Feely, M. & Bell, A. 1992. *The Assessment of the Connemara Marble Resources*. Connemara Marble Producers Group, Department of Earth and Ocean Sciences, National University of Ireland Galway, Ireland, unpublished.
- O'Reilly, C., Jenkin, G.R.T., Feely, M., Alderton, D.H.M. & Fallick, A.E. 1997. A fluid inclusion and stable isotope study of 200 Ma of fluid evolution in the Galway granite, Connemara, Ireland. *Contributions to Mineralogy and Petrology*, **129**(2–3), 120–142, <http://doi.org/10.1007/s004100050327>.
- Pracht, M., Lees, A., Leake, B.E., Feely, M., Long, B.C., Morris, J. & McConnell, B. 2004. *Geology of Galway Bay: A Geological Description to Accompany the Bedrock Geology 1:100,000 Map Series, Sheet 14, Galway Bay*. Geological Survey of Ireland, Dublin.
- Robertson, S.J. 1999. *BGS Rock Classification Scheme, Volume 2, Classification of Metamorphic Rocks*. British Geological Survey, Keyworth, Nottingham, 24 pp, <http://nora.nerc.ac.uk/id/eprint/3226/1/RR99002.pdf>.
- Stanley, S.M. 1999. *Earth System History*. 3rd edn. W.H. Freeman, New York, New York, USA, 615 pp.
- Sylvester, P.J. 2012. Use of the mineral liberation analyzer (MLA) for mineralogical studies of sediments and sedimentary rocks. In: Sylvester, P. (ed) *Quantitative Mineralogy and Microanalysis of Sediments and Sedimentary Rocks*. Mineralogical Association of Canada Short Course Vol. 42, Quebec, Canada, 1–16.
- Tanner, P.W.G. & Shackleton, R.M. 1979. Structure and stratigraphy of the Dalradian rocks of the Bennabeola area, Connemara, Eire. *Geological Society, London, Special Publications*, **8**, 243–256, <http://doi.org/10.1144/GSL.SP.1979.008.01.25>.
- Treloar, P.J. 1982. The stratigraphy and structure of the rocks of the Lissoughter area, Connemara. *Proceedings of the Royal Irish Academy*, **82**(5), 83–107.
- Walsh, S. 2014. *Connemara Marble: Ireland's National Gem*. O'Brien Press, Dublin, Ireland, 128 pp.

Wilton, D.H.C. & Winter, L.S. 2012. SEM-MLA (scanning electron microprobe – mineral liberation analyser) research on indicator minerals in glacial till and stream sediments – An example from the exploration for awaruite in Newfoundland and Labrador. *In: Sylvester, P. (ed) Quantitative Mineralogy and Microanalysis of Sediments and Sedimentary Rocks*. Mineralogical Association of Canada Short Course Vol. 42, Quebec, Canada, 265–283.

Wilton, D.H.C., Thompson, G.M. & Evans-Lamwood, D.M. 2015. MLA-SEM examination of sulphide mineral breakdown and preservation in till, Voisey’s Bay Ni-Cu-Co deposit, Labrador: The distribution and quantitative mineralogy of weathered sulphide phases in a transect from massive sulphide through gossanous regolith to till cover. *In: Williamson, M.-C. (ed) Environmental and Economic Significance of Gossans*. Geological Survey of Canada Open File 7718, Ottawa, Ontario, Canada, 29–39, <http://doi.org/10.4095/296577>.

Wilton, D.H.C., Thompson, G.M. & Grant, D.C. 2017. The use of automated indicator mineral analysis in the search for mineralization – A next generation drift prospecting tool. *Explore*, 174, 1, 5–6, 8, 11–18, www.appliedgeochemists.org/images/Explore/Explore_Number_174_March_2017.pdf.

Wyse Jackson, P.N.W., Caulfield, L., Feely, M., Joyce, A. & Parkes, M.A. (in press). Connemara marble, Co. Galway, Ireland: A Global Heritage Stone resource proposal. *Geological Society, London, Special Publications*, 17.

The Authors

Prof. Martin Feely and Dr Alessandra Costanzo FGA DGA
 Earth and Ocean Sciences,
 National University of Ireland Galway, Ireland
 Email: martin.feely@nuigalway.ie

Prof. Derek H. Wilton
 Department of Earth Sciences, Memorial University,
 St Johns, Newfoundland, Canada

Albert D. Kollar
 Carnegie Museum of Natural History, Pittsburgh,
 Pennsylvania, USA

Dylan J. Goudie
 CREAT Network, Memorial University, St Johns,
 Newfoundland, Canada

Ambrose Joyce
 Connemara Marble Industries Ltd., Moycullen,
 County Galway, Ireland

Acknowledgements

We thank the three anonymous peer reviewers for their helpful comments and suggestions.

Gem-A INSTRUMENTS

Did you know we sell **gift vouchers?**

If you're looking for a special gift for a gemmologist but are unsure of what to buy, our gift vouchers are the ideal solution!

Gem-A Instruments have a range of products to suit budding or professional gemmologists and our gift vouchers are available in any denomination.

Contact:
instruments@gem-a.com
 today and have your gift card created.

How to use this gift voucher
 Simply hand to a member of staff when purchasing an item. Gem-A Instruments stocks a wide range of books and equipment, including laptops, microscopes and more. To consult a catalogue visit www.gem-a.com/gem-a-shop

How to use this gift voucher
 Simply hand to a member of staff when purchasing an item. Gem-A Instruments stocks a wide range of books and equipment, including laptops, microscopes and more. To consult a catalogue visit www.gem-a.com/gem-a-shop

How to use this gift voucher
 Simply hand to a member of staff when purchasing an item. Gem-A Instruments stocks a wide range of books and equipment, including laptops, microscopes and more. To consult a catalogue visit www.gem-a.com/gem-a-shop

Name: _____
 Voucher number: G10004
 (front)

How to use this gift voucher
 Simply hand to a member of staff when purchasing an item. Gem-A Instruments stocks a wide range of books and equipment, including laptops, microscopes and more. To consult a catalogue visit www.gem-a.com/gem-a-shop

How to use this gift voucher
 Simply hand to a member of staff when purchasing an item. Gem-A Instruments stocks a wide range of books and equipment, including laptops, microscopes and more. To consult a catalogue visit www.gem-a.com/gem-a-shop

How to use this gift voucher
 Simply hand to a member of staff when purchasing an item. Gem-A Instruments stocks a wide range of books and equipment, including laptops, microscopes and more. To consult a catalogue visit www.gem-a.com/gem-a-shop

An innovator in gemstone reporting

- Identification of colored gemstones • Country of origin determination • Full quality and color grading analysis



AMERICAN GEMOLOGICAL LABORATORIES



580 5th Ave • Suite 706 • New York, NY 10036, USA
www.agilgemlab.com • +1 (212) 704 - 0727

A Brief Study of Three Reported ‘Coconut Pearls’ from Southeast Asia

Henry A. Hänni and Chiara Parenzan

ABSTRACT: We investigated three so-called coconut pearls loaned to us by a private collector. The white, roundish ‘pearls’ possessed peculiar longitudinal surface grooves, and on one side they had either one or three small bulges. The samples were found to consist of polycrystalline aragonite, as shown by Raman spectroscopy, supported by SG measurements and their reaction to hydrochloric acid. They revealed a parallel-layered structure that is consistent with shell material. The surface grooves showed evidence of filing, and it was obvious that the samples had been manually shaped. Based on the thickness of the shell that must have been used to make these imitations, and the similar structures seen in *Tridacna* shell material, we infer that they were manufactured from giant clam shell. There are no indications to suggest the samples actually derived from a coconut-related origin.

The Journal of Gemmology, 36(5), 2019, pp. 468–471, <http://doi.org/10.15506/JoG.2019.36.5.468>
© 2019 Gem-A (The Gemmological Association of Great Britain)

So-called coconut pearls have been reported as curiosities since the 13th century (Kunz & Stevenson 1908, p. 78), and they have been postulated as originating from the giant clam, *Tridacna gigas*, in Singapore (Kunz & Stevenson 1908, p. 351) or in the Celebes Sea between Indonesia and the Philippines (Anonymous 1947). These ‘pearls’ have also been described as ‘*Mestica calappa*’ (or ‘*Mystica klapa*’), being related to a coconut palm from Ambon (Indonesia) in which they reportedly were occasionally found (Cleyern *et al.* 1704).

On the Internet, ‘coconut pearls’ are described as extreme rarities and often very high prices are asked. But so far, the present authors have found no documented examples of these exotic formations that prove such material formed in coconuts, and there is no clear source of the reported ‘coconut pearls’ given in the literature (see further discussion at www2.palomar.edu/users/warmstrong/ww0601b.htm). Furthermore, ‘coconut pearls’ from various countries in Southeast Asia have been described regularly as objects of questionable authenticity, and for decades they have been widely believed to be hoaxes (e.g. Anonymous 1947). Some references regarding ‘coconut pearls’ include Reyne (1951),

Child (1974), Armstrong (2000), Veldkamp (2002) and Campbell Pedersen (2010).

In November 2018 a private collector, Peter Bauer, supplied three ‘coconut pearl’ samples (Figure 1) for our examination that measured 11.85–19.45 mm in maximum dimension. The specimens reportedly were collected in Indonesia by his father, Swiss aviation pioneer Joseph Bauer, while crop spraying in Southeast Asia in 1969. This article describes our identification of the material constituting these objects and our interpretation of its probable origin.

RESULTS AND DISCUSSION

Material Identification

Using a hydrostatic balance, we found the three samples had SG values of 2.80, 2.84 and 2.85, which is in agreement with that of aragonite (i.e. shell; cf. Bolman, 1941). In addition, testing of an inconspicuous area with a droplet of 10% hydrochloric acid showed the effervescent reaction expected for carbonate-based substances. The Raman spectrum produced with a Gem-Ram desk-model spectrometer (Hänni & Hunziker 2011) also indicated aragonite.



Figure 1: The three 'coconut pearl' samples investigated for this study are shown here from their top and side views. Sample 1 weighs 42.30 ct and measures 19.45 × 16.55 mm, sample 2 weighs 36.54 ct and measures 18.10 × 17.45 mm, and sample 3 weighs 9.11 ct and measures 11.85 × 9.40 mm. Composite photo © H. A. Hänni.

Microscopic Features

The surface of the spherules was roughly polished, with longitudinal grooves that locally intersected one another and appeared to have been made by a file (Figure 2). In addition, the basal portion of one sample showed a small bulge and the other two had three such bulges (see Figure 1, bottom row). Strong fibre-optic illumination of the objects revealed a parallel-layered structure (Figure 3). In addition, all of them were crossed by multiple fractures in various directions independent of the layered structure.

This internal structure is similar to the texture reported in some shell material used to manufacture bead nuclei for cultured pearls (e.g. Figure 4; Strack 2006). This material, also consisting of aragonite, is polished into beads that are larger than those that are commonly cut from common freshwater shells such as mussels from Mississippi and Tennessee, USA. Such thick-walled shell may be produced by *Tridacna* spp. giant clams, which have been protected since 1985 and are listed in CITES Appendix II (<http://checklist.cites.org>). Recent unpublished research on some large cultured pearl bead nuclei by one of the authors (HAH) showed that besides recent *Tridacna* shell, older giant clam shell material

is also possibly used. Carbon-14 dating at the ETH Zurich Laboratory of Ion Beam Physics was performed on two large beads from Tahitian and South Sea cultured pearls that had cracked during the drilling process. The dating gave ages more than 300 years old, which may explain the presence of fractures in the bead nuclei. This



Figure 2: Indications of filing on the surface of 'coconut pearl' sample 2 are clearly visible as longitudinal grooves. Photomicrograph © H. A. Hänni; magnified 20×.



Figure 3: Layered growth structures and fine fissures (seen here as vertical dark lines) were visible in all three ‘coconut pearl’ samples, shown here for sample 3 in transmitted light. Photomicrograph © H. A. Hänni; magnified 20×.

indicates that material used for beads is available from giant clam shell derived from other than recently living individuals. The source of the aged white aragonite shell material is not currently known, but it may be from Papua New Guinea (cf. Kinch 2008).

A thin section of the dated bead material (Figure 5a) displays structures similar to those seen in Figure 3. By contrast, recent *Tridacna* shell material shows layered structures with a different appearance and without any noticeable cracks (Figure 5b).

In addition to being polished for use as bead nuclei, giant clam shell has also been worked and shaped into pearl imitations (Krzemnicki & Cartier 2017), and an object that was very similar to those described here was documented by Hainschwang (2011).

Origin

Accounts of ‘coconut pearls’ are always rather vague when it comes to the exact origin of the objects. The reports underline spiritual forces with enthusiastic descriptions, but documented evidence of a link to coconuts remains missing. When we take into account the SG of plant-derived materials, which may only approach 1.5, this is quite unlike the SG range of 2.80–2.85 measured for the (aragonite) samples in this study. Furthermore, botanists have not reported any plants producing pure CaCO_3 , either regularly or by exception. Therefore, there is no plant tissue known that can precipitate aragonite. The densest material found in plants is probably vegetable ivory produced from the large nuts of several species of palm tree, which has an SG of 1.40–1.43 (i.e. tagua palm nut: O’Donoghue, 2006). This is roughly half the SG of aragonitic calcium carbonate. It is thus another point that sends ‘coconut pearls’ into the realm of fantasy.

No flame structure such as is found in *Tridacna* shell material or conch shell (cf. Hänni 2010) was visible on the present samples because their surfaces were not polished, and preparation of thin sections for more detailed examination was not possible. As described above, their layered growth structure is similar to that seen in older shell bead material that is sometimes used for large bead nuclei in cultured pearls. Note that if such spherical samples were formed naturally, any layered appearance would be expected to form concentric rather than flat-parallel patterns.

CONCLUSION

Our examination of three ‘coconut pearls’ indicates that they consist of aragonite shell material that was shaped into rough spheres with a grooved surface appearance. Such objects can be identified by their worked appearance and by their SG value of ~ 2.8 , layered internal growth structure and Raman spectral identification as aragonite, all of which are consistent with shell material such as that derived from *Tridacna* spp. giant clams (either recent or older animals). Although the intersecting surface grooves and overall worked appearance are helpful for distinguishing the artisanal-made character of such objects, even highly polished samples would be straightforward to identify by their non-concentric internal layering, as well as the other identifying characteristics of aragonite—a mineral with no known botanical origin.

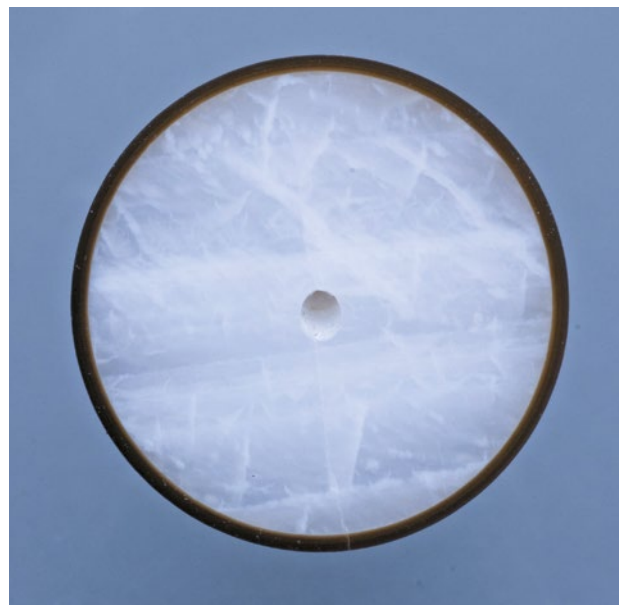


Figure 4: This 10-mm-diameter Tahitian cultured pearl contains a bead nucleus of atypical aragonite material that is characterised by a layered growth structure (typical of giant clam shell), superimposed by crossing fissures. Photo © H. A. Hänni.

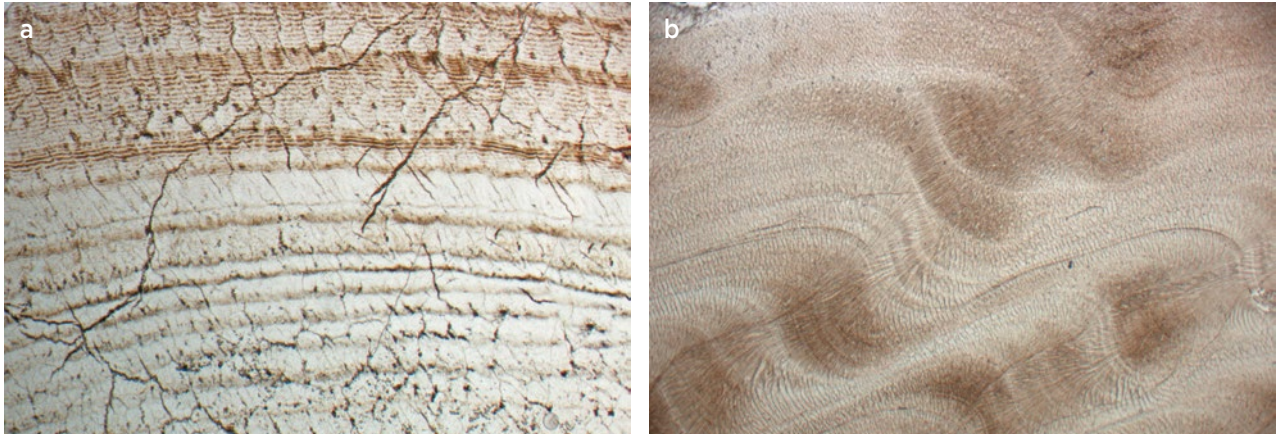


Figure 5: Thin sections of inferred *Tridacna* bead material are shown for (a) a specimen more than 300 years old (as determined by radiocarbon dating) with layered structures that strongly resemble those seen in the three 'coconut pearls' examined in this study, and (b) a recent specimen that shows wavy structures. Note also the presence of cracks in the old shell material and the uncracked nature of the recent shell. Photomicrographs © H. A. Hänni; magnified 16×.

REFERENCES

- Anonymous 1947. No pearls in coco-nuts. *Nature*, **160**(4071), 653, <http://doi.org/10.1038/160653a0>.
- Armstrong, W.P. 2000. Botanical jewelry: Necklaces & bracelets made from plants. www2.palomar.edu/users/warmstrong/ww0901.htm, accessed 16 November 2008.
- Bolman, J. 1941. *The Mystery of the Pearl*. Vol. 39 of Internationales Archiv für Ethnographie, E. J. Brill, Leiden, The Netherlands, 170 pp.
- Campbell Pedersen, M. 2010. *Gem and Ornamental Materials of Organic Origin*. Robert Hale Ltd, London, 282 pp.
- Child, R. 1974. *Coconuts*. 2nd edn. Longmans Group Ltd, London, 335 pp.
- Cleyern, D.A., Rumphen, G.E., de Jager, H. & ten Rhyne, W. 1704. *Oost-Indianische Send-Schreiben*. Verlegung Johann David Zunners, Frankfurt, Germany, 119 pp.
- Hainschwang T. 2011. Gem News International: A skillfully crafted non-nacreous pearl imitation. *Gems & Gemology*, **47**(1), 70–71.
- Hänni, H.A. 2010. Explaining the flame structure of non-nacreous pearls. *Australian Gemmologist*, **24**(4), 85–88, <https://static1.squarespace.com/static/5948e09029687f8edc3e3f99/t>.
- Hänni, H.A. & Hunziker, J.C. 2011. A portable Raman system for gemstone identification: The GemExpert Raman probe. *International Gemmological Conference*, Interlaken, Switzerland, 13–17 July, 167–168.
- Kinch, J. 2008. From prehistoric to present: Giant clam (*Tridacnidae*) use in Papua New Guinea. In: Antczak, A. & Cipriani, R. (eds) *Early Human Impact on Megamolluscs*. BAR International Series 1865, Archaeopress, Oxford, 179–188.
- Krzemnicki, M.S. & Cartier, L.E. 2017. Fake pearls made from *Tridacna gigas* shells. *Journal of Gemmology*, **35**(5), 424–429, <http://doi.org/10.15506/JoG.2017.35.5.424>.
- Kunz, G.F. & Stevenson, C.H. 1908. *The Book of the Pearl*. The Century Co., New York, New York, USA, 548 pp, <https://archive.org/details/bookofpearlhisto00kunz/page/n12>.
- O'Donoghue, M. (ed) 2006. *Gems*. 6th edn. Butterworth-Heinemann, Oxford, 873 pp [see p. 666].
- Reyne, A. 1951. On the structure of shells and pearls of *Tridacna squamosa* Lam. and *Hippopus hippopus* (Linn.). *Archives Néerlandaises de Zoologie*, **8**(1), 206–241, <http://doi.org/10.1163/187530151x00027>.
- Strack, E. 2006. *Pearls*. Rühle-Diebener-Verlag, Stuttgart, Germany, 707 pp.
- Veldkamp, J.F. 2002. Mestica calappa, the coconut pearl, trick or true? *Flora Malesiana Bulletin*, **13**, 143–153, <http://repository.naturalis.nl/document/570927>.

The Author

Prof. Dr Henry A. Hänni FGA
GemExpert GmbH
Postfach 921, CH-4001 Basel, Switzerland
email: h.a.haenni@gmail.com

Chiara Parenzan

Swiss Gemmological Institute SSEF
Aeschengraben 26, 4051 Basel, Switzerland

Acknowledgements

We thank Peter Bauer (Illnau-Effretikon, Switzerland) for loaning the samples and providing valuable information. Dr Irka Haidas is acknowledged for the carbon-14 age determination of cultured pearl bead nucleus material. Dr Laurent Cartier FGA provided valuable information and a review of an initial draft of this article.

Conferences

AGA TUCSON CONFERENCE

The 2019 Accredited Gemologists Association Conference in Tucson, Arizona, USA, took place 6 February and was attended by 138 people from nine countries. The event was moderated by AGA president **Stuart Robertson** (Gemworld International Inc., Glenview, Illinois, USA) and featured five presentations. The day closed with the AGA Gala and award presentations (Figure 1; see the end of this report for a full list of awardees).

Jeffery Bergman (Primagem, Bangkok, Thailand) described the history, gemmological properties, clarity enhancement (with cedarwood oil) and marketing of emeralds from the Halo mine in the Shakiso area of Ethiopia. Their main internal features are colour zoning, biotite inclusions, growth tubes and blocky two- and three-phase fluid inclusions, and their similarity to Zambian emeralds means that trace-element analysis is necessary for distinguishing them from one another.

Gina Latendresse (American Pearl Company, Nashville, Tennessee, USA) covered the history, production and varieties of freshwater natural pearls from USA. Approximately one in 10,000 freshwater mussels contains a pearl, and of those only 5% have a symmetrical shape and 1% are round; the remainder have various baroque shapes that are termed 'feathers', 'rose buds', 'turtle-backs', etc. Latendresse then touched on natural pearls

of marine origin such as those from quahog, abalone and conch molluscs, and also described various pearl imitations made from polished shell material.

Dr Claudio Milisenda (DSEF German Gem Lab, Idar-Oberstein, Germany) reviewed the composition and structure of the tourmaline group, and then described the properties and sources of various colour varieties of gem tourmaline, which most commonly consist of the elbaite, liddicoatite and dravite-uvite species. He indicated that clarity enhancement of tourmaline with oils and polymers is becoming more common, particularly for rubellite.

Dr Daniel Nyfeler (Gübelin Gem Lab, Lucerne, Switzerland) discussed the traceability of gemstones. Barriers to attaining full transparency along the supply chain from source to end consumer include the remoteness of the deposits, the numerous transactions during which stones change hands frequently and the informal/artisanal nature of mining of many coloured stones. Nyfeler described the Emerald Paternity Test for implanting an invisible barcode (using DNA tagging technology) into newly mined emeralds, and explained how the new Provenance Proof initiative uses blockchain technology to provide a digital tracer of a stone's journey through the supply chain. Anyone can sign up to use the blockchain for free at www.provenanceproof.io.

Jon Phillips (Corona Jewellery Co., Toronto, Ontario,



Figure 1: Dr Karl Schmetzer holds his 2019 Antonio C. Bonanno Award for Excellence in Gemology, while a long list of his publications is displayed by Antoinette Matlins (left), Stuart Robertson (centre-left) and Dr Lore Kiefert (right), as Kathryn Bonanno (blue dress) and Karen Bonanno DeHaas (pink dress) look on. Photo courtesy of AGA.

Canada) reviewed diamond mining activities in Canada including Ekati (where underground operations are under development at the Misery pit), Diavik (where the third open pit [A21 pipe] was started in August 2018), Victor (which will close in 2019) and Gahcho Kué (where a 60.59 ct yellow octahedral diamond was found in October 2018). Phillips also covered the cutting and marketing of Canadian diamonds.

The conference featured workshops by **Dr Çiğdem Lüle** (Kybele LLC, Buffalo Grove, Illinois, USA) on gem treatments and their influence on the market, **Gary Smith** (Smith's Jewelers, Montoursville, Pennsylvania, USA) on precious metal testing and **Samantha Lloyd** (Gem-A, London) on hand-held gemmological testing instruments.

The AGA Gala took place that evening, where awardees were honoured with the 2019 Antonio C. Bonanno Award for Excellence in Gemology in three categories: (1) for gemmological education, **Donna Hawrelko** (Vancouver Community College, British Columbia, Canada) was recognised for her contributions to the field and her commitment to numerous gemmology students; (2) for gemmological instruments, **Alberto Scarani** and **Mikko Åström** (Magilabs, Rome, Italy, and Helsinki, Finland) were honoured for making advanced spectroscopy technology more accessible and affordable to gemmologists; and (3) for gemmological research, **Dr Karl Schmetzer** (Petershausen, Germany) was lauded for over 50 years of publications and presentations on mineralogical and gemmological topics (again, see Figure 1).

Brendan M. Laurs FGA

21ST FEEG SYMPOSIUM AND CIBJO SEMINAR ON RESPONSIBLE SOURCING

The 21st symposium of the Federation for European Education in Gemmology (FEEG) was organised by the Istituto Gemmologico Italiano (IGI) as a joint event with a seminar presented by CIBJO, the World Jewellery Confederation, on responsible sourcing and sustainability. The event took place on 19 January 2019 during the Vicenzaoro jewellery trade show in Vicenza, Italy.

Dr Gaetano Cavalieri (CIBJO president, Milan, Italy) introduced and moderated the CIBJO seminar. He explained that consumer confidence, on which the entire premise of the gem business is built, requires more than just maintaining the integrity of the product. The ways in which the members of the jewellery industry behave

and impact society and the environment are fundamental components of consumer confidence.

This author (FEEG president, Brussels, Belgium) welcomed the delegates and introduced FEEG. He pointed out that we are confronted with an explosion of knowledge and an increasing need to serve a growing network of gem enthusiasts and jewellery professionals throughout Europe. Excellence in gemmological training is vital. It is the aim of FEEG to be the world's finest and fastest-growing gemmological education organisation to passionately teach industry members and consumers about gems.

Philip Olden (CIBJO, Bern, Switzerland) provided an overview of CIBJO's new 'blue book' on responsible sourcing, which is meant to provide guidance and a framework within which all members of the industry can perform responsible-sourcing due diligence, irrespective of their size and type of business.

Francesca Marino (CIBJO, Bern) looked at how the implementation of social responsibility practices could change through the application of blockchain technology. Blockchain makes the process of ethically evaluating the behaviour of a company more objective, eliminating the arbitrariness that sometimes accompanies other methods.

Rui Galopim de Carvalho (CIBJO and Portugal-Gemas Academy, Lisbon, Portugal) presented a gemmological and historical overview of gem-quality coral, and explained that it is critical to differentiate the eight precious coral species from the thousands of other common (i.e. reef-building) corals. In light of the current emphasis on sustainability and corporate social responsibility, it is important to educate members of the trade and consumers to the fact that coral used in jewellery does not pose a threat to coral reefs, although it does need to be sustainably harvested.

Vincenzo Liverino (CIBJO, Bern) described research being conducted at scientific institutes around the world with the support of the CIBJO Coral Commission. These efforts are yielding promising results that could help with the regrowth and repopulation of common corals affected by global warming. The CIBJO Coral Commission will soon launch an online course about coral and will assist gemmological education organisations with providing information on coral in their programmes.

Prof. Roberto Vona (Business Management Department, University of Naples Federico II, Italy) considered how blockchain technology could be applied to manage the precious coral supply chain, and so provide opportunities to improve the quality and sustainability of the product. Blockchain could deliver objective and unalterable records



Figure 2: Speakers at the 21st FEEG symposium included (left to right) Clement Sabbagh, Valentina Gagliardi, Giacomo Diego Gatta, Andrea Zullino and Fabrizio Nestola. Photo courtesy of Italian Exhibition Group.

of what is known about a product as it moves along the chain of distribution, providing evidence that sustainable practices have been complied with throughout the harvesting, processing and sales activities.

For the afternoon session, the FEEG Symposium was opened by **Paolo Valentini** (IGI vice president, Milan, Italy), who welcomed the delegates and introduced the five speakers (Figure 2).

Clement Sabbagh (International Coloured Stone Association [ICA], Governador Valadares, Brazil) discussed the role ICA plays in the gem industry, as well as the networking power and services that ICA provides to its members.

Valentina Gagliardi (IGI, Milan, Italy) delved into the unambiguous identification protocols of jade, which consists of two different gem materials: jadeite and nephrite. Both are silicates and form aggregates. Jadeite is an Al-rich pyroxene and nephrite is an Mg-rich amphibole, and they can be separated by standard gemmological tests. The deposits as well as classifications (i.e. A, B and C jade) were discussed. Jadeite and omphacite are both pyroxenes that form a solid-solution series, and Raman spectroscopy can be used to differentiate them.

Prof. Giacomo Diego Gatta (University of Milan, Italy) discussed the potential of single-crystal X-ray diffraction as a non-destructive technique in gemmology. After a brief introduction to the basic aspects of X-ray diffraction theory, he described an actual case study: a 4 mm crystal was identified as chambersite [ideally $(\text{Mn}^{2+}, \text{Fe}^{2+})_3(\text{B}_7\text{O}_{13})\text{Cl}$] using a four-circle X-ray diffractometer combined with openly available databases containing basic crystallographic parameters of minerals.

Andrea Zullino (IGI, Milan, Italy) spoke about the role of defects in diamond classification. Optical defects occur in very low concentrations in diamond, and they may cause absorption features in the visible-range

spectrum to produce colour. Their presence can be detected using spectroscopic techniques. A novel indicator of the exposure of type Ia diamonds to artificial ionising radiation and subsequent annealing consists of narrow photoluminescence lines in the red region, between 681 and 725 nm, which result from vacancies trapped by interstitial carbon aggregates and platelets. The interstitial structures become sites of vacancy trapping—by thermal migration of radiation-induced vacancies—when a diamond undergoes treatment.

Prof. Fabrizio Nestola (University of Padua, Italy) described his research on determining the depth and growth mechanisms of diamond formation by characterising mineral and fluid inclusions. The presence of syngenetic inclusions of ringwoodite proves the super-deep formation of diamond. Ringwoodite constitutes 60% or more of the lower part of the earth’s transition zone, between 525 and 660 km depth, and this hydrous mineral indicates the presence of a significant amount of water in this region. ‘CLIPPIT’ (Cullinan-like, large, inclusion-poor, pure [type II], irregular-shaped, resorbed) diamonds are of such ‘super-deep’ origin. Their inclusion composition indicates that the deep mantle environment contains small pockets of oxygen-deficient metallic liquid from which the diamonds crystallised.

The day ended with the FEEG diploma ceremony (Figure 3), which celebrated 56 new graduates. They represent the future of gemmology. FEEG gemmologists master knowledge of the properties of gems and achieve academic excellence in gemmology. The next FEEG symposium will be held in Schoonhoven, The Netherlands, in January 2020.

*Guy Lalous (guy.lalous@outlook.com)
Brussels, Belgium*



Figure 3: Presenters at the FEEG diploma ceremony in 2019 were (left to right) IGI president Raffaele Maino, FEEG president Guy Lalous, CIBJO president Dr Gaetano Cavalieri and Charles Evans of Gem-A. Photo courtesy of Italian Exhibition Group.

Gem-A Notices

Gifts to the Association

Gem-A is most grateful to the following for their generous donations that will support continued research and teaching:

Andrew Hinds, F. Hinds, UK, for a signed and framed photograph of Eric Bruton sitting at Ayers Rock that was taken on NAG's 'Jewellers' Study Tour to Australia' in 1980.

Dennis Ho, Hong Kong, for three carvings, one bangle and a fragment of jadeite; six absorption spectra boxes; two interference figure boxes; and five bags of rough material: sapphire (Tanzania), kyanite (Myanmar), topaz (Brazil), chrome tourmaline (Myanmar) and spinel (Myanmar).

Mauro Panto, The Beauty in the Rocks, Italy, for a 'rhodosite' (magnesio-riebeckite) doublet from Jezkagan (Zhezkazgan), Kazakhstan.

Dr Marco Campos Venuti, Spain, for a selection of polished stones from Brazil: albite, scapolite, quartz with biotite(?) inclusions, quartz with triphylite inclusions, apatite in jasper and opal with dendrites.

New COO for Gem-A

A new year and a new start for Daniel Heath, Gem-A's new Chief Operating Officer. Joining us from his previous role at The Sports Grounds Safety Authority, where he was Head of Corporate Services, Daniel is a Chartered Management Accountant and has been heading up finance and operations at Gem-A since January 2019.



Gem-A

THE GEMMOLOGICAL ASSOCIATION
OF GREAT BRITAIN

Gem-A presents...

FREE
GEMMOLOGY
WEBINARS

Are you based outside of the UK? Do you find it difficult to get to Gem-A HQ in London for our workshops?

For the first time, Gem-A is pleased to offer a series of one-hour webinars, designed to boost your gemmological knowledge no matter where you are in the world. Our convenient webinars are targeted at beginners who want to get a grasp of the basics, fast. Each of our webinars is entirely free – just book your place by searching 'Gem-A' on Eventbrite and join us from the comfort of your own home or office.

Understanding Gemstones

18 Jul 2019

Start your gemmology journey with this accessible beginner's guide to gemstones. This tutor-guided webinar will explain the physical characteristics of popular gems such as sapphire, emerald and ruby, while explaining their origins, history and vital care techniques. At the end of this webinar, you will have a better grasp of basic gemmology and the terminology that makes it an exciting and varied field of study.

Understanding Diamonds

10 Oct 2019

Are you passionate about diamonds but want to know more? This tutor-guided webinar will explain how diamonds are formed, what makes them special and how to assess their value and qualities using the 4Cs: cut, colour, clarity and carat weight. You will learn the basics of diamond certification and begin to discover the broader issues of diamond synthetics and simulants. At the end of the webinar, participants will be one step closer to understanding the uniqueness of diamond.

Obituary

Edward Allan Jobbins

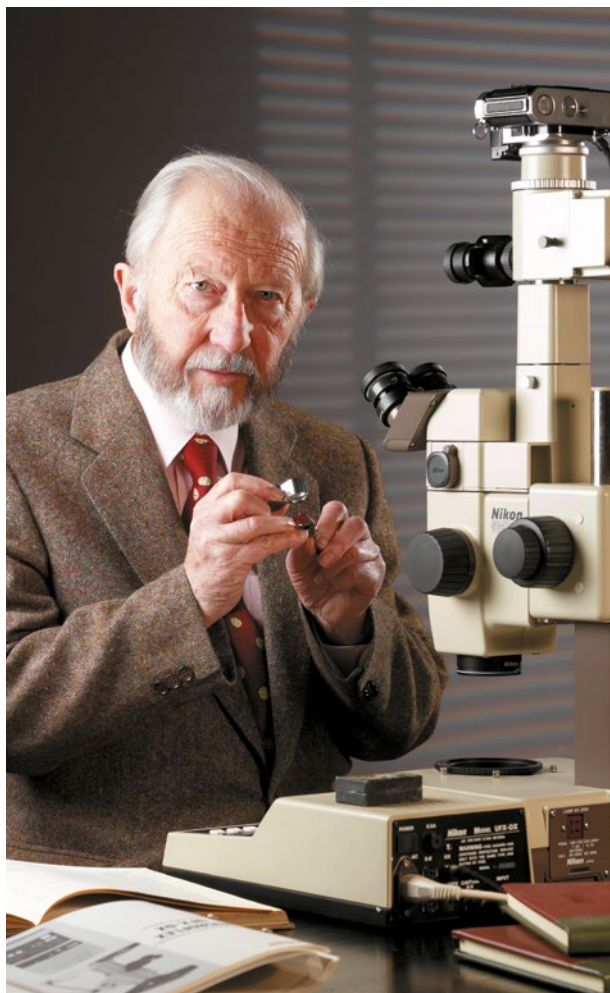
1923–2019

Alan, as he was known to his friends and colleagues (he rarely, if ever, used either 'Edward' or the second 'I'), was born on 14 December 1923 in Rotherhithe, London. He was educated at the John Roan School, Greenwich, where he first developed an interest in geology during field trips to the Lake District organised by his geography teacher. From 1939 to 1942, during World War II, Alan was evacuated to Ammonford, Wales, where he boarded with a solicitor and his family who helped Alan through his formative years.

Alan gained entry to King's College, London, but then joined the Queen's Regiment. He was declared 'Grade 3' due to his poor eyesight and was therefore sent to teach mathematics and English at the Army College in Scotland. He later returned to King's College to complete his degree in geology, where he not only gained First Class Honours, but also won the Myers prize in mineralogy and the Tennant prize in geology. In addition to his geology degree, Alan also became a qualified Civil Engineer, which possibly accounted for his interest in building stone.

In 1950 Alan joined The Geological Survey/The Geological Museum in London as a geologist, progressing to become curator of minerals and gemstones where he was responsible for the care and display of the gem and mineral collections, including acquisitions and organising exhibitions. He was responsible for the creation of a superb permanent display of gems at the museum, which not only showed the specimens at their best but also provided comprehensible and interesting information for visitors. Sadly, this display was subsequently dismantled when the collections were incorporated into The Natural History Museum. Alan also undertook research into many important gemmological and mineralogical subjects such as East African garnets, the structure and identification of synthetic opals, and the identification and characterisation of a new mineral, magnesio-axinite. He was also called to investigate the meteorite which fell on the town of Barwell, near Leicester, on 24 December 1965.

During his time at the museum, Alan was seconded to UN/UNESCO and the British Overseas Development Administration, where his assignments took him to numerous gem-producing areas in Brazil (the diamond mines and Piauí opal deposits), Myanmar (previously Burma), Cambodia (the Pailin ruby and sapphire



deposits), Guyana, India and Sri Lanka (surveying the gem mining and cutting industries). His work included carrying out geological and gemmological surveys of the deposits to determine how the resources could be developed and utilised. Much of this work became the subject of papers in a number of learned publications, including *The Journal of Gemmology*. Alan was particularly proud of his time in Burma (1967–1968), where he set up a research laboratory and taught gemmology to a class of Burmese students. Ten of them passed their Gemmology Diploma under his tutorship, with two progressing to doctorates at Cambridge and Durham Universities. It was during his time in Burma that Alan developed a love of and expertise in jade, and with jadeite in particular.

Although Alan retired from The Natural History Museum in 1983, he remained a consultant for a further

two years and continued his work with gems and gemmology. Both during his time at the museum and after his retirement, Alan was closely connected to the wider gemmological world and, in particular, with The Gemmological Association of Great Britain (now Gem-A). He assisted *Journal* editor J. R. H. Chisholm from 1973 until 1985 when, beginning with the April issue, he briefly acted as joint editor before becoming editor himself in 1986, a post he held until the end of 1993. Alan also helped to review papers, not just for *The Journal* but also for other publications. He was always happy to offer advice and guidance to authors, and he was often asked to review new books. Alan revised the 6th and 7th editions of Robert Webster's *Gemmologists' Compendium* and the 10th edition of Basil Anderson's *Gem Testing*.

Perhaps one of Alan's 'crowning' achievements was that, under commission of The Royal Collection, he assembled a team of expert gemmologists to carry out a comprehensive examination and description of the British Crown Jewels and royal regalia. The work was carried out between 1986 and 1989, and the results were detailed in *The Crown Jewels: The History of the Coronation Regalia in the Jewel House of the Tower of London*, a two-volume, leather-bound, numbered, limited-edition book published in 1995 by Her Majesty's Stationery Office. In fact, Alan's connection with The Royal Collection went further, as he was occasionally asked to examine other objects for confirmation of identity or updating of details prior to lending to external exhibitions.

Alan took his Gemmology Diploma examinations in 1972 and passed with a mark of 98% after the chief examiner, Basil Anderson, deducted two points for poor handwriting! His performance won him the Tully Medal. Alan was an examiner for the Gemmological Association's examinations from 1975 to 1995 and served on the Executive Committee/Council of Management from 1987 to 1993. He was elected president of the Association, a position he held from 2004 to 2008, after which he remained as vice president until his death on 9 February 2019.

Alan was a long-standing member of IGC (the International Gemmological Conference) and served on their Executive Committee. He was also a founding member of ICA (the International Colored Gemstone Association) and contributed to CIBJO's industry rules. In addition, he advised the laboratory at the London Chamber of Commerce, which later became the Gem Testing Laboratory of Great Britain. Closer to home, Alan taught a post-diploma class at Sir John Cass College for well over 20 years and was a key

member of the learned group JPH (Jewellery, Plate and Horology). He also served as president of the Society of Jewellery Historians.

Continuing his work for the Gemmological Association, Alan travelled to Wuhan and Beijing, China, on a number of occasions with Dr Jamie Nelson to introduce the Association's courses to China. This resulted in a significant increase in the number of students from China who gained their Gemmology Diploma, just at a time when the potential of the country's huge resources was being realised, coupled with a growth in the demand for gems in their domestic market.

In recognition of a lifetime dedicated to gemmology, Alan was presented with the 2005 Antonio C. Bonanno Award for Excellence in Gemology by the Accredited Gemologists Association.

Despite all his accomplishments and his high standing within the gem world, Alan always remained a modest man who was delighted to share his knowledge and experience without any material gain. Passing on his knowledge to others with the possibility to inspire was reward enough. He was renowned for the many and varied lectures that he gave without the 'safety net' of notes. 'My slides are my notes' was often his response when asked. It was not uncommon for members of the audience to comment afterwards that they had just heard the best talk they had ever attended. He would treat each audience with warmth and respect regardless of whether he was speaking to experts at a prestigious event, a small mineral society or a local interest group.

Aside from gems and geology, Alan also had a passion for birdwatching, and it was in 1970, on an organised birding holiday to the Algarve in Portugal, when Alan met his future wife and soulmate, Mary. It was apparently 'love at first sight'. Together, they enjoyed many happy holidays birdwatching, and they shared a love of fine food and wine, with Mary's culinary prowess complementing Alan's excellent knowledge of fine wine. They didn't keep such pleasures to themselves but, with their customary generosity and hospitality, would often entertain friends, colleagues and groups, both large and small.

Such was Alan's kindness and generosity of spirit that so many of his former colleagues and students regarded him as a true friend and will miss him deeply. I am honoured to consider myself one of those very fortunate people.

Alan is survived by Mary and by his son, Simon.

Peter Wates FGA DGA
Purley, Surrey

Learning Opportunities

CONFERENCES AND SEMINARS

46th Rochester Mineralogical Symposium

11–14 April 2019
Rochester, New York, USA
www.rasny.org/minsymp

16th Annual Sinkankas Symposium—Pearl

27 April 2019
Carlsbad, California, USA
www.sinkankassymposium.net

Swiss Gemmological Society Conference

28–30 April 2019
Meisterschwanden, Switzerland
<https://gemmologie.ch/en/current>

Scottish Gemmological Association Conference

3–6 May 2019
Cumbernauld, Scotland
www.scottishgemmology.org/conference

GAC-MAC-IAH (Geological Association of Canada–Mineralogical Association of Canada–International Association of Hydrogeologists) Conference

12–15 May 2019
Québec City, Québec, Canada
<https://gacmac-quebec2019.ca>
Session of interest: Recent Advances in the Study of Gems and Gem Deposits

NDNC 2019: 13th New Diamond and Nano Carbons Conference

12–17 May 2019
Hualien, Taiwan
www.ndnc2019.org

5th Mediterranean Gemmological & Jewellery Conference

17–19 May 2019
Limassol, Cyprus
<https://gemconference.com>

33rd Annual Santa Fe Symposium

19–22 May 2019
Albuquerque, New Mexico, USA
www.santafesymposium.org

48th Annual Society of North American Goldsmiths (SNAG) Conference

22–25 May 2019
Chicago, Illinois, USA
www.snagmetalsmith.org/conferences/the-loop

European Gemmological Symposium 2019

24–26 May 2019
Idar-Oberstein, Germany
www.dgemg.com/egs-2019-en.php

Sustainable Development in the Mining Industry (SDIMI 2019)

27–29 May 2019
Sydney, Australia
<http://sdimi.ausimm.com>

JCK Las Vegas

31 May–3 June 2019
Las Vegas, Nevada, USA
<http://lasvegas.jckonline.com>
Note: Includes a seminar programme

International Exposition of Agate

6–9 June 2019
Austin, Texas, USA
<https://ntrocks.com/international-exposition-of-agate>
Note: Includes a seminar programme

Jewelry of the 20th Century, 1900–1960s

9 June 2019
Boston, Massachusetts, USA
www.jewelryconference.com

PEG 2019: 9th International Symposium on Granitic Pegmatites

11–18 June 2019
Pala, California, USA
<http://peg2019.com>
Note: Includes field trips to gem-bearing pegmatites

18èmes Rendez-Vous Gemmologiques de Paris

~~17 June 2019~~ 9 September 2019
Paris, France
www.afgems-paris.com/rdv-gemmologique

**Mineralogical Society of America
Centennial Symposium**

20–21 June 2019

Washington DC, USA

www.minsocam.org/MSA/Centennial/MSA_Centennial_Symposium.html

Sessions of interest: Scientific Characterization of High-Value Gemstones; Mineral Inclusions in Diamonds from the Deep Earth; Museum Mineral Collections in the Next 100 Years

**ECROFI 2019: European Current Research
on Fluid and Melt Inclusions**

23–27 June 2019

Budapest, Hungary

<https://ecrofi2019.elte.hu>

**Sainte-Marie-Aux-Mines 56th Mineral
& Gem International Show**

27–30 June 2019

Sainte-Marie-aux-Mines, France

www.sainte-marie-mineral.com/english

Note: Includes a seminar programme

**19th International Meeting on Crystal Chemistry,
X-ray Diffraction and Spectroscopy of Minerals**

2–5 July 2019

Apatity, Russia

www.ksc.ru/en/xrd2019

**Goldsmiths' Company Jewellery
Materials Congress 2019**

8–9 July 2019

London

www.assayofficelondon.co.uk/events/the-goldsmiths-company-jewellery-materials-congress

2019 Antique Jewelry & Art Conference

27–28 July 2019

Newark, New Jersey, USA

www.jewelrystcamp.org

Northwest Jewelry Conference

9–11 August 2019

Seattle, Washington, USA

<http://northwestjewelryconference.com>

Goldschmidt Conference

18–23 August 2019

Barcelona, Spain

<https://goldschmidt.info/2019>

Session of interest: Origin and Evolution of Continental Mantle Lithosphere and its Resource Endowment

Dallas Mineral Collecting Symposium

23–25 August 2019

Dallas, Texas, USA

www.dallassymposium.org

**15th Biennial Meeting of the Society for Geology
Applied to Mineral Deposits**

27–30 August 2019

Glasgow, Scotland

www.sga2019glasgow.com

Session of interest: Supergenes, Gems and Non-Metallic Ores

36th International Gemmological Conference

27–30 August 2019

Nantes, France

www.igc-gemmology.org

Japan Jewellery Fair 2019

28–30 August 2019

Tokyo, Japan

www.japanjewelleryfair.com/en

Note: Includes a seminar programme

**42nd Joint Mineralogical Societies of
Australasia Seminar**

31 August–1 September 2019

Perth, Western Australia

www.minsocwa.org.au/gallery.html

International Jewellery London (IJL)

1–3 September 2019

London

www.jewellerylondon.com

Note: Includes a seminar programme

**Geological Society of Namibia
50th Anniversary Conference**

1–4 September 2019

Windhoek, Namibia

www.gssa.org.za/wp-content/uploads/GeolSocNam.pdf

Note: A field trip to diamond areas is planned.

**10th International Congress on the
Application of Raman Spectroscopy in
Art and Archaeology (RAA2019)**

3–7 September 2019

Potsdam, Germany

www.raa2019.de

30th International Conference on Diamond and Carbon Materials (DCM 2019)

8–12 September 2019

Seville, Spain

www.diamond-conference.elsevier.com**9th European Conference on Mineralogy and Spectroscopy (ECMS 2019)**

11–13 September 2019

Prague, Czech Republic

<http://ecms2019.eu>*Workshop of interest:* Gemstone Deposits**Denver Gem & Mineral Show**

13–15 September 2019

Denver, Colorado, USA

www.denvermineralshow.com*Note:* Includes a seminar programme**2019 National Association of Jewellers' Loughborough Conference**

14–16 September 2019

Loughborough

www.naj.co.uk/whats-on/2019-conference/8201?OccId=11716**Hong Kong Jewellery & Gem Fair**

16–22 September 2019

Hong Kong

<http://tinyurl.com/yyogn944>*Note:* Includes a seminar programme**14th International Congress for Applied Mineralogy (ICAM 2019)**

23–27 September 2019

Belgorod, Russia

www.geo.komisc.ru/icam2019/en*Themes of interest:* Precious Stones; Cultural Heritage**International Colored Gemstone Association (ICA) Congress**

12–15 October 2019

Bangkok, Thailand

www.gemstone.org/events/2019-congress**Chicago Responsible Jewelry Conference**

25–26 October 2019

Chicago, Illinois, USA

www.chiresponsiblejewelryconference.com**Munich Show/Mineralientage München**

25–27 October 2019

Munich, Germany

<https://munichshow.de/?lang=en>*Note:* Includes a seminar programme**Gem-A Conference 2019**

2–3 November 2019

London

<https://gem-a.com/event/conference-2019>**MAESA 2019: Earth Sciences and Sustainable Development**

30 November–1 December 2019

Yangon, Myanmar

www.maesa.org*Sessions of interest:* Mineralogy and Origin of Gem Deposits; Geographic Typing of Gemstones and Advances in Instrumentation**OTHER EDUCATIONAL OPPORTUNITIES****Gem-A Workshops and Courses**

Gem-A, London

<https://gem-a.com/education>**Lectures with Gem-A's Midlands Branch**

Fellows Auctioneers, Augusta House, Birmingham

Email louiseludlam@hotmail.com

- Charles Bexfield—Silverware, Assay Offices & Hallmarks
26 April 2019
- Shirley Mitchell—Valuations
25 October 2019

Lectures with the Society of Jewellery Historians

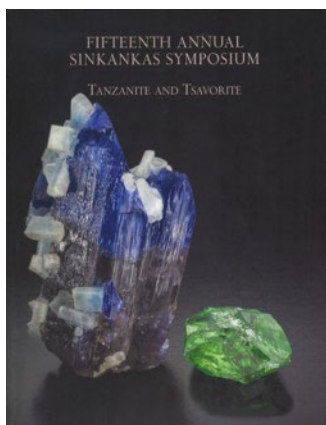
Society of Antiquaries of London,

Burlington House, London

www.societyofjewelleryhistorians.ac.uk/current_lectures

- Beth Wees—TBA
25 June 2019
- Maria Maclennan—Forensic Jewellery
24 September 2019
- Rachel Church—Brooches, Badges and Pins at the Victoria and Albert Museum
26 November 2019

New Media



Fifteenth Annual Sinkankas Symposium—Tanzanite and Tsavorite

Ed. by Stuart Overlin, 2018. Pala International, Fallbrook, California, USA, 88 pages, illus., ISBN 978-0991532032. Print on demand; price available upon request (promotional@dpidirect.com).

The Fifteenth Annual Sinkankas Symposium, featuring tanzanite and tsavorite, was held in April 2018 at the Gemological Institute of America in Carlsbad, California, and was co-hosted by the Gemological Society of San Diego (for a report on that event, see

the Conferences section of *The Journal*, Vol. 36, No. 2, pp. 162–163). Attendees received an attractive proceedings volume that provides an excellent record of some of the topics covered by the speakers.

The volume begins with a listing of the symposium programme, speaker biographies and abstracts. These are followed by speaker contributions covering a range of topics: geology and gemmology of tanzanite (Robert Gessner); inclusions in tanzanite and tsavorite (Nathan Renfro); the process of cutting a suite of fancy-colour zoisites (Meg Berry); collecting tanzanite and tsavorite crystals (Will Larson); the history of the discovery and mining of tsavorite in Kenya, and the introduction of tanzanite into the world market by Campbell Bridges (Bruce and Judith Bridges); tanzanite price trends (Stuart Robertson); and treatments and imitations of tanzanite and tsavorite (Shane McClure). The volume also includes reprints of three short publications by Campbell Bridges on tsavorite and other East African gems. It closes with extensive bibliographies covering tanzanite and tsavorite.

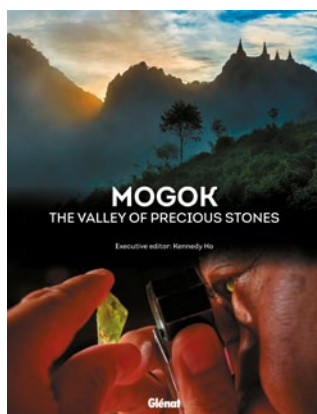
The book is printed on heavy paper stock and features many beautiful photos (mostly by photographer extraordinaire Robert Weldon) of tanzanite and tsavorite that convey their beauty as both faceted stones and mineral specimens. Gemmologists, geologists, gem and mineral collectors, and enthusiasts of tanzanite and tsavorite will appreciate this attractive and informative book.

Brendan M. Laurs FGA

Mogok: La Vallée des Pierres Précieuses/ Mogok: The Valley of Precious Stones

Ed. by Kennedy Ho and Emmanuel Fritsch, 2018. Glénat, Grenoble, France, 192 pages, illus., ISBN 978-2344029763.

EUR39.50 hardcover (separate French and English versions).



children for many years, including both Kennedy and his brother Henry. I have also known Dr Emmanuel Fritsch since his years at GIA, so this book is like family to me. That said, let us examine what they have published. There have been various books prepared on Mogok in the past couple of decades. Most all are well done. However, this one is very well done.

In the preface, Kennedy Ho captures the spirit that is felt throughout this work:

We have designed the book to appeal to the widest possible audience. A special effort has been made to present the scientific information it contains in an accessible manner that harmonises effectively with the book's content as a whole. We also wanted to convey the indescribable beauty of Mogok and its gems, which makes the heart beat faster and sets the spirit soaring. The photographs taken in the field as well as the laboratory images created using electronic microscopes reveal an array of unique mineral wonders, including rubies, spinels, peridots, sapphires....

Full disclosure before reviewing this magnificent book: I love Mogok! I have travelled to Burma/Myanmar on more than 35 occasions since my first trip in 1993 arranged by Dr Eduard Gübelin, including a dozen times to Mogok Valley itself. I also met Waing Kong Ho in 1974 and have known some of his

The following nine chapters—assembled by a team of five professionals during two years of work—stir one’s gemmological interest. ‘Blood from the Earth’ by Jean-Baptiste Rabouan introduces the reader to this team and their journeys into Mogok Valley to visit various mines and gem markets. ‘The Mythical Valley of Mogok’ by Candice Caplan delves into the mythology and the actual history of Mogok. Numerous references are quoted chronologically, so an accurate history is presented to the reader. The point is made that Mogok rubies have a history dating back to the 6th century according to Chinese documents from the Shan dynasty. This is much earlier than the usually quoted ‘fact’ that Mogok has been mined for almost a thousand years. Also included in the history are some famous personalities as well as notable ‘jewels for the crowns of the world’. A final section covers ‘miners and Buddhism’. The next chapter, ‘A Sino-Burmese Saga’ by Jean-Baptiste Rabouan, provides a fascinating account of the Ho family’s history from China to Burma, into exile, and finally welcomed by Thailand. As summed up by Kennedy Ho, ‘It all started with 30 dollars in cash, and a lot of sacrifices...’

The following chapter, ‘The Dragon with Ruby Eyes’ by Dr Emmanuel Fritsch, uncovers some of the region’s very complex geology. Highlighted are the blue and white marbles which contain spinel and ruby. There’s also a brief mention of gem-bearing pegmatites and sections on sapphires that occur mostly in syenites and on the overall diversity of gem species in the Mogok area. The chapter closes with a discussion of ‘mining operations both large and small’. ‘Rubies: The “Glowing Coal” among Burmese Gems’ by Franck Notari describes the exceptional colour of rubies from Mogok, as well as some of the other properties that set them apart. A section is devoted to the colour term ‘pigeon’s blood’ and another describes the inclusion features seen with the microscope. The chapter ends with several pages on ruby mining activities, focusing on alluvial deposits. Next,

‘The Sapphires of Mogok’ by Dr Thomas Hainschwang discusses the comparative rarity of sapphires in Mogok and describes some of their distinctive properties (e.g. inclusions). Besides blue sapphires, the chapter briefly covers other colours (including colour-change stones) as well as trapiche sapphires. The next chapter, ‘Spinel, Peridots and Other Treasures from the Valley of Wonders’ by Dr Emmanuel Fritsch and Candice Caplan, is rather short but provides an accurate discussion of spinel and peridot gems and mines, followed by other rare Mogok gems including painite, poudretteite and the recently discovered kyawthuite.

‘Hunting for Treasure’ by Jean-Baptiste Rabouan offers an in-depth look at the life of the independent miner—‘a hard life with flashes of hope’. Also described are mining companies that operate in Mogok and their efforts to balance economic interests with protecting the environment. The final chapter, ‘The Gemstone Road, from Mogok to the World’ by Jean-Baptiste Rabouan, provides a fine summary of buying gems at the source. The reader is taken from the local ‘umbrella market’ in Mogok to private negotiations for a 10 ct ‘pigeon’s blood’ ruby, ending with the book’s last words: ‘And that’s all we get to see: the rest of the negotiations take place behind closed doors. At this level, absolute discretion is always the rule.’

All recent books on Mogok are filled with wonderful photographs, as the locality is truly remarkable. This book also stuns the reader with amazing photography of this mystical locality, and presents many images of cultural and gemmological interest including mines, local dealers (past and present), and great gemstones and jewellery pieces (both historic and modern). The excellent photos and insightful text come together to make this book an integral part of your personal library.

Bill Larson FGA
Pala International
Fallbrook, California, USA

Other Book Titles

COLOURED STONES

Mineralogy of Quartz and Silica Minerals

Ed. by Jens Götze, 2018. MDPI, Basel, Switzerland, 274 pages, ISBN 978-3038973485 (softcover) or 978-3038973492 (PDF). CHF59.50 softcover or free PDF.

The Tears of Fura: An Emerald Miner’s Adventures Thru Revolution and Evolution

By Manuel J. Marcial, 2018. Self-published at Outskirts Press, Denver, Colorado, USA, 314 pages, ISBN 978-1478799030 (hardcover) or 978-1478799023 (softcover). USD49.95 (hardcover), USD29.94 (soft cover) or USD9.99 Kindle edn.

DIAMOND

Diamond Fields of Southern India

By S. Ravi, K.S. Bhaskara Rao and R. Ananda Reddy, 2018. Geological Survey of India Bulletin Series A, No. 68, 996 pages. INR3109.00.

Evolution of Magmatic and Diamond-Forming Systems of the Earth's Lower Mantle

By Anna V. Spivak and Yuriy A. Litvin, 2019. Springer International Publishing, Cham, Switzerland, 95 pages, ISBN 978-3319785172 (hardcover) or 978-3319785189 (eBook). CHF121.00 hardcover or CHF96.50 eBook.

Geology, Resources and Exploration Potential of the Ellendale Diamond Project, West Kimberley, Western Australia

By G. Boxer and G. Rockett, 2018. Geological Survey of Western Australia, Perth, Australia, 49 pages, ISBN 978-1741688153. Free PDF.

Geoscience and Exploration of the Argyle, Bunder, Diavik, and Murowa Diamond Deposits

Ed. by Andy T. Davy, Chris B. Smith, Herwart Helmstaedt, A. Lynton Jaques and John J. Gurney, 2018. Society of Economic Geologists Special Publication 20, 451 pages, ISBN 978-1629493060 (print), 978-1629493541 (flash drive) or 978-1629496399 (PDF). USD120.00 hardcover plus flash drive or USD99.00 PDF.

A Glossary of Kimberlite and Related Terms: Part 1—Glossary; Part 2—Practical Guide; Part 3—Abundance and Size Descriptors

By Barbara H. Scott Smith, Tom E. Nowicki, J. Kelly Russell, Kimberley J. Webb, Roger H. Mitchell, Casey M. Hetman and Jock V. Robey, 2018. Scott-Smith Petrology Inc., Vancouver, British Columbia, Canada, 144 pages (Part 1), 59 pages (Part 2), 56 pages (Part 3), ISBN 978-1775280606. CAD250.00 spiral-bound softcover.

GEM LOCALITIES

The Ankarana Plateau in Madagascar: Tsingy, Caves, Volcanoes and Sapphires

By Eric Gilli, 2019. Springer Nature, Switzerland, 148 pages, ISBN 978-3319998787 (hardcover) or 978-3319998794 (eBook). EUR139.99 hardcover or EUR118.99 eBook.

GENERAL REFERENCE

Catalogue of the Collections of the Geominero Museum Mineral Collection of the Autonomous Regions and Cities: Madrid Region

By Ramón Jiménez Martínez, Ruth González Laguna, María José Torres Matilla, Rafael Pablo Lozano Fernández, Eleuterio Baeza Chico, Carmen de Prada Galende, Héctor Sánchez Molinero, Alba María Carvajal de Lago and Silvia Cervel de Arcos, 2018. Instituto Geológico y Minero de España, Madrid, Spain, 77 pages. Free eBook.

Gemstone Detective: Buying Gemstones and Jewellery in Australia

By Kim Rix, 2019. Filament Publishing, Croydon, Surrey, 160 pages, ISBN 978-1912635252. GBP14.99 softcover.

Gemstone Detective: Buying Gemstones and Jewellery in Thailand

By Kim Rix, 2019. Filament Publishing, Croydon, Surrey, 128 pages, ISBN 978-1912635214. GBP12.99 softcover.

Gemstone Detective: Buying Gemstones and Jewellery Worldwide

By Kim Rix, 2019. Filament Publishing, Croydon, Surrey, 160 pages, ISBN 978-1912635467. GBP14.99 softcover.

JEWELLERY HISTORY

Ancient Rings: An Illustrated Collector's Guide

By T.N. Pollio, 2018. McFarland, Jefferson, North Carolina, USA, 180 pages, ISBN 978-1476673851. USD55.00 softcover.

The History of Jewelry: Joseph Saidian & Sons

By Caroline Childers, 2019. Rizzoli, New York, New York, USA, 194 pages, ISBN 978-0847865383. USD35.00 hardcover.

JEWELLERY AND OBJETS D'ART

American Jewelry from New Mexico: Tradition and Innovation

By Andrew L. Connors and Hannah V. Mattson, 2018. Museum of New Mexico Press, Santa Fe, New Mexico, USA, 386 pages, ISBN 978-0890136386. USD39.95 hardcover.

Art of the Jewel

By Paula Crevoshay, 2018. Crevoshay, Albuquerque, New Mexico, USA, 232 pages, ISBN 978-0988672321. USD69.95 hardcover.

Arts and Crafts Jewelry in Boston:**Frank Gardner Hale and His Circle**

By Nonie Gadsden, Meghan Melvin and Emily Stoehrer, 2018. MFA Publications, Boston, Massachusetts, USA, 224 pages, ISBN 978-0878468577. USD50.00 hardcover.

The Cartier Collection

By François Chaille, Thierry Coudert, Pascale Lepeu, Violette Petit, Pierre Rainero, Jenny Rourke, Michael Spink and Christophe Vachaudes, 2018. Flammarion, Paris, France, 744 pages (two volumes), ISBN 978-2080203854. EUR350.00 hardcover.

Chains: Jewelry in History, Function and Ornament

By Alba Cappellieri, 2018. Silvana Editoriale, Milan, Italy, 192 pages, ISBN 978-8836638468. EUR26.00 softcover.

Coloratura: High Jewelry and Precious Objects by Cartier

By Cartier and François Chaille, 2019. Flammarion, Paris, France, 240 pages, ISBN 978-2080203854. EUR95.00 hardcover.

Contemporary Traditions in Native American Jewelry

By Katie McClain Richarme and Michael Richarme, 2019. Self-published, USA, 36 pages, ISBN 978-1791985516. USD9.95 softcover.

Corbella Milano: The First Italian Manufacturer of Jewellery and Weapons for the Theatre

Ed. by Bianca Cappello and Angelica Corbella, 2018. Silvana Editoriale, Milan, Italy, 216 pages, ISBN 978-8836640362. EUR35.00 softcover.

Creating Beauty: Jewelry and Enamels of the American Arts & Crafts Movement

By Rosalie Berberian, 2019. Schiffer Publishing, Atglen, Pennsylvania, USA, 272 pages, ISBN 978-0764357466. USD59.99 hardcover.

Gold, Silver & Brass: Jewellery of the Batak in Sumatra, Indonesia

By Achim Sibeth, 2019. 5 Continents, Milan, Italy, 192 pages, ISBN 978-8874396269. EUR45.00 hardcover.

Jewellery: From Art Nouveau to 3D Printing

By Alba Cappellieri, 2018. Skira, Milan, Italy, 256 pages, ISBN 978-8857237374. EUR60.00 hardcover.

Jewellery Illustration and Design, Vol. 1

By Brambatti Manuela and Vinci Cosimo, 2018. Promopress, Barcelona, Spain, 208 pages, ISBN 978-8416851577. EUR35.00 softcover.

Jewelry: The Body Transformed

By Melanie Holcomb, 2018. Metropolitan Museum of Art, New York, New York, USA and Yale University Press, New Haven, Connecticut, USA, 280 pages, ISBN 978-1588396501. USD50.00 hardcover.

Masters of New Jewellery Design: Eclat, 2nd edn.

By Carlos Pastor, 2019. Promopress, Barcelona, Spain, 256 pages, ISBN 978-8416851928. EUR29.00 softcover.

Resonances de Cartier: High Jewelry and Precious Objects

By François Chaille, 2018. Flammarion, Paris, France, 240 pages, ISBN 978-2080203403. EUR95.00 hardcover.

Royal Rubies

By Nina Hald, 2018. Arnoldsche Art Publishers, Stuttgart, Germany, 184 pages, ISBN 978-389790518. EUR38.00 hardcover.

Scottish Jewellery: A Victorian Passion

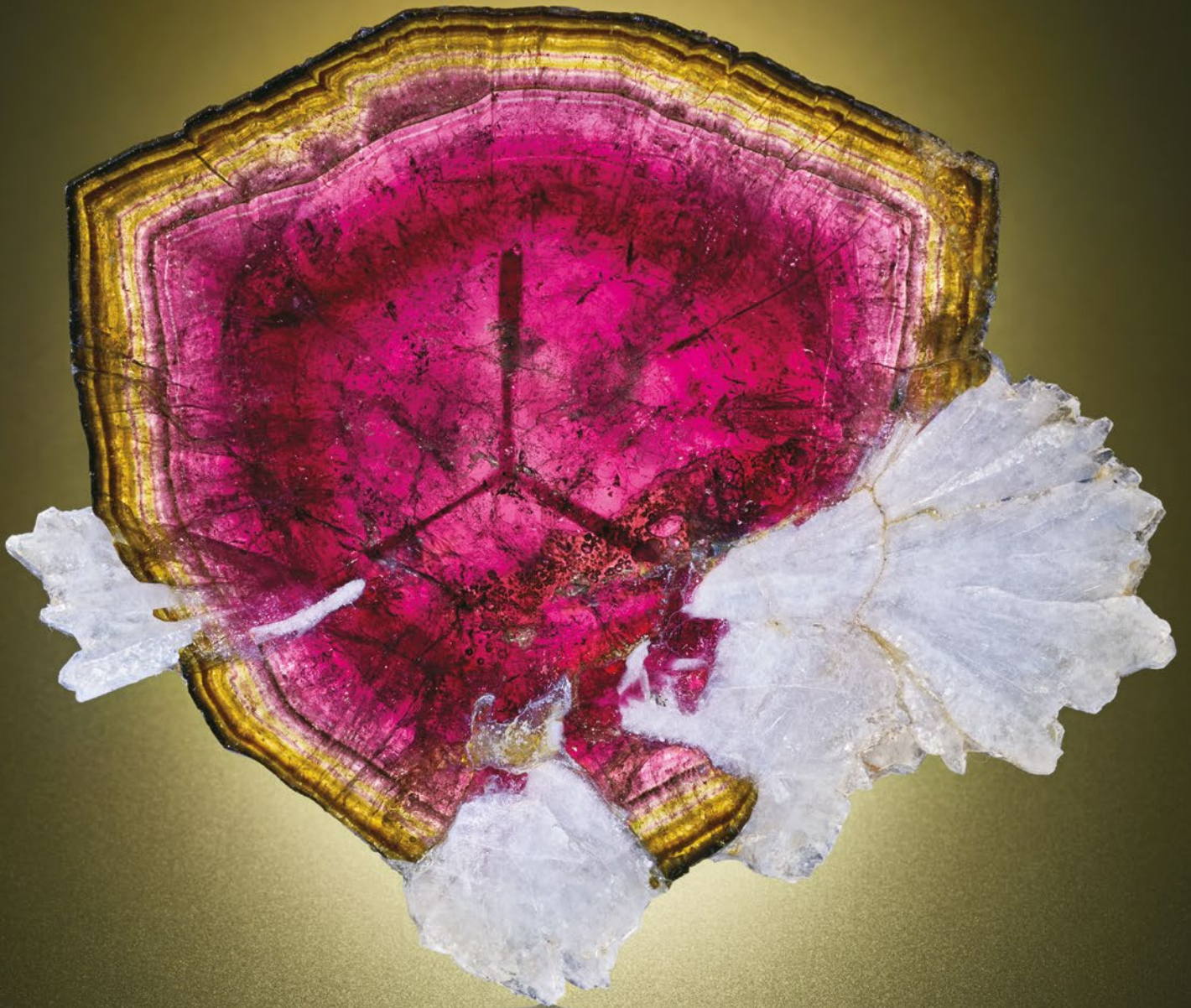
By Diana Scarisbrick, 2019. 5 Continents, Milan, Italy, 128 pages, ISBN 978-8874395248. EUR35.00 hardcover.

Simply Danish: Silver Jewellery—20th Century

By Jörg Schwandt, 2018. Arnoldsche Art Publishers, Stuttgart, Germany, 232 pages, ISBN 978-3897905269 (in English and German). EUR44.00 hardcover.

Understanding Northwest Coast Indigenous Jewelry: The Art, the Artists, the History

By Alexander Dawkins, 2019. University of Washington Press, Seattle, Washington, USA, 192 pages, ISBN 978-0295745893. USD24.95 softcover.



SGRPE
\$199.99

The Sisk Gemology Reference by Jerry Sisk Professional Edition

A comprehensive and visual gemology resource
featuring prominent and noteworthy gemstones.

jtv[®]
jewelry love
jtv.com/sgr

Literature of Interest

COLOURED STONES

Anorthite skarn with dispersed chromium-hydrogrossular from the Muslim Bagh area, Pakistan. H.A. Hänni, L. Franz and H.A.O. Wang, *Australian Gemmologist*, **26**(11–12), 2018, 286–290.

Beyond ‘horse tails’ in demantoid garnet. Z. Lewis, *Gems&Jewellery*, **27**(4), 2018, 32–35.

The color origin of gem diaspore: Correlation to corundum. C. Shen and R. Lu, *Gems & Gemology*, **54**(4), 2018, 394–403, <http://doi.org/10.5741/GEMS.54.2.394>.*

Corundum with spinel corona from the Tan Huong–Truc Lau area in northern Vietnam. N.N. Khoi, C.A. Hauzenberger, C. Sutthirat, D.A. Tuan, T. Häger and N.V. Nam, *Gems & Gemology*, **54**(4), 2018, 404–417, <http://doi.org/10.5741/GEMS.54.4.404>.*

Diversity in ruby geochemistry and its inclusions: Intra- and inter-continental comparisons from Myanmar and eastern Australia. F. Sutherland, K. Zaw, S. Meffre, J. Thompson, K. Goemann, K. Thu, T. Nu, M. Zin and S. Harris, *Minerals*, **9**(1), 2019, article 28, 28 pp., <http://doi.org/10.3390/min9010028>.*

Emerald deposits in the 21st century: Then, now and beyond. G. Giuliani, L.A. Groat and D.D. Marshall, *InColor*, No. 40, 2018, 22–32, www.gemstone.org/incolor/40.*

Emerald deposits: A review and enhanced classification. G. Giuliani, L.A. Groat, D. Marshall, A.E. Fallick and Y. Branquet, *Minerals*, **9**(2), 2019, article 105, 63 pp., <http://doi.org/10.3390/min9020105>.*

Emeralds and the Chinese market. X. Zhao, *InColor*, No. 40, 2018, 128–129, www.gemstone.org/incolor/40.*

A gemological description of Ethiopian emeralds. W. Vertriest and P. Wongrawang, *InColor*, No. 40, 2018, 73–75, www.gemstone.org/incolor/40.*

Inclusions of [sic] spinel from Burma. J. Zhu and X. Yu, *Journal of Gems & Gemmology*, **20**(Supp.), 2018, 18–23 (in Chinese with English abstract).

Iris agate revisited: Electron microscopy inspection. G. Pearson and R. Seal, *Australian Gemmologist*, **26**(11–12), 2018, 280–283.

The lavender jadeite teapot. R. Bauer, *Australian Gemmologist*, **26**(11–12), 2018, 306–307.

Magnificent old mine emeralds. I. Alexandris, *InColor*, No. 40, 2018, 136–142, www.gemstone.org/incolor/40.*

Mastering opal with the innovative reference sets. C. Unninar, *InColor*, No. 41, 2019, 82–84, www.gemstone.org/incolor/41.*

The mineral companions of Colombian emerald. G.C. Parodi, *InColor*, No. 40, 2018, 44–46, www.gemstone.org/incolor/40.*

Origine géographique des spinelles chromifères et vanadifères associés aux marbres d’Asie et d’Afrique de l’Est [Geographical origin of chromiferous and vanadiferous spinels associated with the marbles of Asia and East Africa]. G. Giuliani, A.E. Fallick, A.J. Boyce, V. Pardieu and V.L. Pham, *Revue de Gemmologie A.F.G.*, No. 203, 2018, 17–55 (in French with English abstract).

Padparadscha-like fancy sapphires with unstable colors: Coloration mechanisms and disclosure. M.S. Krzemnicki and L.E. Cartier, *InColor*, No. 41, 2019, 92–94, www.gemstone.org/incolor/41.*

A rare find [grandidierite]. B. Gobin, *Gems&Jewellery*, **28**(1), 2019, 20–21.

The Second World Emerald Symposium: Focuses on responsible sourcing. C. Unninar, *InColor*, No. 40, 2018, 6–15, www.gemstone.org/incolor/40.*

Shimmering sapphires [‘Gold Sheen’ sapphires from Kenya]. T.N. Bui, *Gems&Jewellery*, **27**(4), 2018, 36–39.

Tenebrescent zircon. J.J. Bradshaw, *GemGuide*, **38**(1), 2019, 19–20.

Under the microscope [four unusual sapphires]. G. Millington, *Gems&Jewellery*, **28**(1), 2019, 11–13.

Water in opal – What can it tell us? P. Thomas, L. Aldridge and A. Smallwood, *InColor*, No. 41, 2019, 62–69, www.gemstone.org/incolor/41.*

CULTURAL HERITAGE

Ancient Sri Lankan intaglios: Some preliminary observations. M.D.P.L. Francis and S. Wijewardane, *Australian Gemmologist*, **26**(11–12), 2018, 270–279.

Edwardian elements [jewellery]. S. Turner, *Gems&Jewellery*, **28**(1), 2019, 30–31.

Gemstone conversations: Garnet [in antique jewellery]. J. Benjamin, *Gems&Jewellery*, **28**(1), 2019, 40–41.

Held aloft the ring [Ashmolean Museum]. B. West, *Gems&Jewellery*, **27**(4), 2018, 30–31.

The history and reconstruction of the Amber Room. R. Shor, *Gems & Gemology*, **54**(4), 2018, 378–393, <http://doi.org/10.5741/GEMS.54.4.393>.*

Mazarin's passion for diamonds. C. Pittel, *Gems&Jewellery*, **28**(1), 2019, 32–35.

DIAMONDS

Diamond exploration and regional prospectivity of Western Australia. M.T. Hutchison, *Mineralogy and Petrology*, **112**(Supp. 2), 2018, 737–753, <http://doi.org/10.1007/s00710-018-0579-6>.

Diamonds from the deep: How do diamonds form in the deep earth? K.V. Smit and S.B. Shirey, *Gems & Gemology*, **54**(4), 2018, 440–445, www.gia.edu/gg-issue-search?ggissueid=1495274782005&article_subtype=diamondsfromthedeep.*

Formation of unusual yellow Orapa diamonds. S. Timmerman, I.L. Chinn, D. Fisher and G.R. Davies, *Mineralogy and Petrology*, **112**(Supp.), 2018, 209–218, <http://doi.org/10.1007/s00710-018-0592-9>.

Inclusions in natural, synthetic, and treated diamond [chart]. N.D. Renfro, J.I. Koivula, J. Muyal, S.F. McClure, K. Schumacher and J.E. Shigley, *Gems & Gemology*, **54**(4), 2018, 428–429 plus chart, <http://doi.org/10.5741/GEMS.54.4.428>.*

Natural-color pink, purple, red, and brown diamonds: Band of many colors. S. Eaton-Magaña, T. Ardon, K.V. Smit, C.M. Breeding and J.E. Shigley, *Gems & Gemology*, **54**(4), 2018, 352–377, <http://doi.org/10.5741/GEMS.54.2.352>.*

The pursuit of colour. Part 2. The relationship between light and cut in fancy coloured diamonds. C. Green, *Australian Gemmologist*, **26**(11–12), 2018, 291–302.

'The rock star that got stage fright at auction': The political economy of marketing the historic Lesedi La Rona diamond. C.J. Makgala and M. Bolaane, *Botswana Notes and Records*, **50**, 2018, 199–213, <http://journals.ub.bw/index.php/bnr/article/view/1391>.*

FAIR TRADE

Applying the OECD due diligence guidance for responsible mineral supply chains to the emerald industry. L. Maiotti, *InColor*, No. 40, 2018, 108–109, www.gemstone.org/incolor/40.*

Australian opal mining: A model for responsible mining. D. Cody, L. Cartier and J. Winch, *InColor*, No. 41, 2019, 26–32, www.gemstone.org/incolor/41.*

Bringing the Shakiso story to market: The application of traceability technology in a small-scale mining environment. D. Nyfeler and K. Link, *InColor*, No. 40, 2018, 104–107, www.gemstone.org/incolor/40.*

The gemstones and sustainable development knowledge hub. L.E. Cartier and S.H. Ali, *InColor*, No. 40, 2018, 118–119, www.gemstone.org/incolor/40.*

The Leap-Frog opportunity: The colored gemstone industry and the future of a world wide ledger. C. Teo, *InColor*, No. 40, 2018, 110–113, www.gemstone.org/incolor/40.*

Sourcing colored gemstones responsibly: Challenges and opportunities for creating sustainable value together. C. Klomp, *InColor*, No. 40, 2018, 114–115, www.gemstone.org/incolor/40.*

GEM LOCALITIES

Afghanistan's emeralds: Hidden treasures. M. Sultan and T. Aria, *InColor*, No. 40, 2018, 85–88, www.gemstone.org/incolor/40.*

Belmont emeralds – Uncompromisingly green [Brazil]. D.S. Zimmerman, *InColor*, No. 40, 2018, 76–78, www.gemstone.org/incolor/40.*

Emerald occurrences [sic] in Pakistan. B. Khan, *InColor*, No. 40, 2018, 80–84, www.gemstone.org/incolor/40.*

Emerald occurrences and exploration in northwestern Canada. L.A. Groat, *InColor*, No. 40, 2018, 34–42, www.gemstone.org/incolor/40.*

Emerald deposits near Mananjary, Madagascar: Overview by a field gemologist. V. Pardieu, *InColor*, No. 40, 2018, 95–97, www.gemstone.org/incolor/40.*

Emeralds of the Urals [Russia]. A. Burlakov and E. Burlakov, *InColor*, No. 40, 2018, 88–94, www.gemstone.org/incolor/40.*

The Ethiopian Halo-Shakiso emerald. A. Mekonnen, *InColor*, No. 40, 2018, 68–72, www.gemstone.org/incolor/40.*

Frozen opal fluids and colloidal crystal fire: Gem opal deposits in the heart of Australia. S.R. Pecover, *InColor*, No. 41, 2019, 34–60, www.gemstone.org/incolor/41.*

Green andradite from Bor open pit, Dalnegorsk, Russia. B.Z. Kantor, *Mineralogical Almanac*, 24(1), 2019, 6–7.

The Muzo companies' 10th anniversary: A decade of change [Colombian emerald]. A. Saldarriaga and J. Jiménez, *InColor*, No. 40, 2018, 48–51, www.gemstone.org/incolor/40.*

New discoveries [Ammolite]. D. Nini, *Gems&Jewellery*, 27(4), 2018, 18–19.

A new era for the historic Coscuez mine [Colombian emerald]. R. Perkins and M.A. Castilla, *InColor*, No. 40, 2018, 52–55, www.gemstone.org/incolor/40.*

Overview of Brazil's emerald production. *InColor*, No. 40, 2018, 79, www.gemstone.org/incolor/40.*

Rediscovery and history of the Chivor emerald mines: Between legends and reality (1880–1970). G. Martayan, K. Schmetzer, J.G. Ortiz and A.R. Blake, *InColor*, No. 40, 2018, 58–63, www.gemstone.org/incolor/40.*

Remarkably uniform oxygen isotope systematics for co-existing pairs of gem-spinel and calcite in marble, with special reference to Vietnamese deposits. A.E. Fallick, G. Giuliani, T. Rigaudier, A.J. Boyce, V.L. Pham and V. Pardieu, *Comptes Rendus Geoscience*, 351(1), 2019, 27–36, <http://doi.org/10.1016/j.crte.2018.11.008>.*

Les rubis de Vatmandry [The rubies of Vatmandry (Madagascar)]. J.-M. Arlabosse, A. Delaunay and N. Lenne, *Revue de Gemmologie A.F.G.*, No. 203, 2018, 6–15 (in French with English abstract).

Traversing the Swat Valley [Pakistan emeralds]. C. Evans, *Gems&Jewellery*, 27(4), 2018, 12–15.

A visit to Colombia's "green" emerald mines. C. Unninayar, *InColor*, No. 40, 2018, 143–146, www.gemstone.org/incolor/40.*

Zambia – A world emerald power. R.G. Sikri, *InColor*, No. 40, 2018, 64–67, www.gemstone.org/incolor/40.*

INSTRUMENTATION

A database of Raman spectra of precious gemstones and minerals used as cut gems obtained using portable sequentially shifted excitation Raman spectrometer. A. Culka and J. Jehlička, *Journal of Raman Spectroscopy*, 2018, 50(2), 262–280, <http://doi.org/10.1002/jrs.5504>.

On the development of an effective image acquisition system for diamond quality grading. W. Wang and L. Cai, *Applied Optics*, 57(33), 2018, 9887–9897, <http://doi.org/10.1364/ao.57.009887>.

MISCELLANEOUS

The Australian Opal Centre: An institution dedicated to opal. J. Brammall, *InColor*, No. 41, 2019, 70–80, www.gemstone.org/incolor/41.*

Chinese national standard of <emerald grading> GB/T 34545 2017 and testing procedures. R. Wei, T. Lu, J. Su, H. Chen and J. Ke, *InColor*, No. 40, 2018, 130–133, www.gemstone.org/incolor/40.*

Education – Gateway to the China [gemstone] market. A. Lucas, R. Liu and M. Ng, *InColor*, No. 40, 2018, 120–126, www.gemstone.org/incolor/40.*

NEWS PRESS

De Beers dangles synthetic carat in front of consumers. H. Sanderson, *Financial Times*, 3 January 2019, www.ft.com/content/8b502874-fee1-11e8-ac00-57a2a826423e.

Mozambique, la fièvre du rubis [Mozambique, ruby fever]. D. Giard, *Le Figaro*, 18 January 2019, www.lefigaro.fr/international/2019/01/18/01003-20190118ARTFIG00003-mozambique-la-fievre-du-rubis.php (in French).*

Rubies have never been more expensive—or ubiquitous. M. Ellwood, Bloomberg, 19 November 2018, www.bloomberg.com/news/features/2018-11-20/rubies-have-never-been-more-expensive-as-ubiquitous-in-jewelry.*

Strange fossil may be rare insect preserved in gemstone. J. Pickrell, *National Geographic*, 30 January 2019, www.nationalgeographic.com/science/2019/01/strange-fossil-may-be-insect-in-opal-gemstone-java-paleontology.*

ORGANIC/BIOGENIC GEMS

Jurassic jet of Asturias, Spain. A. Martínez-Calvo, *Gems&Jewellery*, **28**(1), 2019, 14–16.

Living coral [precious coral in the jewellery industry]. R. Galopim de Carvalho, *Gems&Jewellery*, **28**(1), 2019, 42–44.

A pocket full of shungite. S. Steele, *Gems&Jewellery*, **27**(4), 2018, 41–42.

Precious coral. L. Fan, in C.D. Beltran and E.T. Camacho, Eds., *Corals in a Changing World*. IntechOpen, London, Chapter 4, 2018, 51–72, <http://doi.org/10.5772/intechopen.73149>.*

Structural characteristic of *Tridacna* and its similar shell. X. Ou, L. Li, B. Yan and Q. Zhang, *Journal of Gems & Gemmology*, **20**(5), 2018, 15–26 (in Chinese with English abstract).

Treasure from ancient oceans [fossilised giant clam shells from Kenya]. V. Bassen, *Gems&Jewellery*, **28**(1), 2019, 26–29.

PEARLS

Comprehensive identification on golden pearl. B. Fang, X. Yan and J. Wang, *Journal of Gems & Gemmology*, **20**(Supp.), 2018, 129–132 (in Chinese with English abstract).

The gemological characteristics of pipi pearls reportedly from *Pinctada maculata*. N. Nilpetploy, K. Lawanwong and P. Kessrapong, *Gems & Gemmology*, **54**(4), 2018, 418–427, <http://doi.org/10.5741/GEMS.54.4.418>.*

Linnaeus and the pearls. J. Asplund, *Gems&Jewellery*, **27**(4), 2018, 28–29.

Mini Ming [cultured] pearls ahead - Will Akoyas become an endangered species? H.A. Hänni, *Australian Gemmologist*, **26**(11–12), 2018, 303–305.

A royal romance [pearls in 16th century Sweden]. J. Asplund, *Gems&Jewellery*, **28**(1), 2019, 22–24.

SIMULANTS

Absent ‘amber’ [identifying plastic imitations]. K. Gregory, *Gems&Jewellery*, **28**(1), 2019, 36–38.

The micro mid-infrared spectral study on quench of natural and synthetic ametrine. T. Shao, Z. Luo, T. Chen and A.H. Shen, *Spectroscopy and Spectral Analysis*, **38**(9), 2018, 2749–2756 (in Chinese with English abstract).

Spectroscopy characteristic of rhodochrosite and its imitation. H. Xu and X. Yu, *Journal of Gems & Gemmology*, **20**(Supp.), 2018, 97–104 (in Chinese with English abstract).

SYNTHETICS

Characteristic of hydrothermal synthetic beryl. L. He, C. Long, Z. Ying and N. Chen, *Journal of Gems & Gemmology*, **20**(3), 2018, 9–17 (in Chinese with English abstract).

Photoluminescence studies on nitrogen doped diamond synthesized by high temperature and high pressure method. K. Wang, W. Zhang, Y. Zhang, S. Ding, S. Chang and H. Wang, *Journal of Synthetic Crystals*, **47**(11), 2018, 2334–2337 (in Chinese with English abstract).

Synthesis and characterization of NaAlSi₂O₆ jadeite under 6.0 GPa. F. Wang, L. Wang, Z. Zhou, G. Zuo, H. Huang and Y. Zheng, *Journal of Synthetic Crystals*, **47**(11), 2018, 2403–2407 (in Chinese with English abstract).

TREATMENTS

Effect of heat treatment on spectroscopic properties of tanzanite. P. Thongnopkun and P. Chanwanitsakun, *Journal of Physics: Conference Series*, **1144**, 2018, article 012183, 4 pp., <http://doi.org/10.1088/1742-6596/1144/1/012183>.*

Emerald: Resin-filled fissures with “oil-like” films—Concerns and challenges. G. Choudhary, *InColor*, No. 40, 2018, 100–103, www.gemstone.org/incolor/40.*

Gemological identification of natural turquoise and treatment turquoise in Hubei. Y. Xu and J. Di, *Acta Mineralogica Sinica*, **38**(4), 2018, 646–654 (in Chinese with English abstract).

Luminescence characteristic and fluorescence spectrum of HPHT-treated and irradiated diamond. Q. Jia and M. Chen, *Journal of Gems & Gemmology*, **20**(3), 2018, 1–8 (in Chinese with English abstract).

Natural vs. enhanced lapidary materials: The drusy craze. H. Serras-Herman, *GemGuide*, **38**(1), 2019, 4–12.

Naturalys® – A new natural filler for emeralds. L.G. Angarita, *InColor*, No. 40, 2018, 98–99, www.gemstone.org/incolor/40.*

Progress in the technology of heat treatment and the quantitative inspection of ruby from main origins. Q. Wang and J. Di, *Superhard Material Engineering*, **30**(4), 2018, 60–64 (in Chinese with English abstract).

Visible-light excited red-emitting vacancies at carbon interstitials as indicators of irradiated and annealed type Ia diamonds. R. Lorenzi, A. Zullino, L. Prospero and A. Paleari, *Diamond and Related Materials*, **90**, 2018, 188–193, <http://doi.org/10.1016/j.diamond.2018.10.014>.

COMPILATIONS

G&G Micro-World. ‘Flower’ in demantoid • Lepidocrocite in boulder opal • Prismatic rutile in quartz • Heated Burmese pink sapphire • Sillimanite in ruby • Gilson cat’s-eye synthetic emerald • Zircon cluster in Ethiopian sapphire • Bubble in fluorite. *Gems & Gemmology*, **54**(4), 2018, 446–451, www.gia.edu/gg-issue-search?ggissueid=1495274782005&articlesubtype=microworld.*

Gem News International. Emerald with inclusions along three directions • Type IaB diamond with boron • ‘Guizhou jade’ from Qinglong, China • HPHT-grown diamond in a ring with melee • Blue sapphires treated with heat and pressure • DiamondView observation of epoxy resin filling in emeralds • Coated synthetic moissanite, rough and cut • Conference reports • Crowningshieldite. *Gems & Gemmology*, **54**(4), 2018, 452–469, www.gia.edu/gg-issue-search?ggissueid=1495274782005&articlesubtype=gni.*

Lab Notes. Natural diamond mistaken as HPHT-grown diamond • Manufactured gold-in-quartz • Freshwater pearls with host shells • Montana ruby • Pargasite inclusions in Kashmir sapphire • Irradiated melee-sized CVD-grown diamond • Lightbox CVD-grown colourless synthetic diamonds • Cat’s-eye Paraíba tourmaline. *Gems & Gemmology*, **54**(4), 2018, 430–439, www.gia.edu/gg-issue-search?ggissueid=1495274782005&articlesubtype=labnotes.*

CONFERENCE PROCEEDINGS

46th Annual Yellowknife Geoscience Forum [includes Canadian diamonds]. D. Irwin, S.D. Gervais and V. Terlaky, Northwest Territories Geological Survey, Yellowknife, Canada, 20–22 November 2018, www.nwtgeoscience.ca/sites/ntgs/files/resources/2018_geoscience_forum_abstract_and_summary_volume_1.pdf.*

*Article freely available for download, as of press time

SAVE THE DATE!

Gem-A Conference 2019

November 2-3



etc.venues
County Hall
London, UK





Pala International

PalaGems.com / PalaMinerals.com

+1 800 854 1598 / +1 760 728 9121

Tanzanites from Tanzania • 14.74 ct • 15.74 ct
Berries from Pala International Grounds • Photo: Mia Dixon